FACULTEIT
BIO-INGENIEURSWETENSCHAPPEN

UNDERSTANDING AND TACKLING JELLIFICATION: FROM POLYP TO BLOOM

Michiel De Cooman
Student number: 01608950

Promotor: Prof. dr. ir. Jana Asselman
Dr. Ilias Semmouri

Tutor: Dr. Ilias Semmouri

Master's Dissertation submitted to Ghent University in partial fulfilment of the requirements for the degree of master in bioscience engineering.

Academic year: 2022-2023

UNIVERSITEIT
GENT

Gent, 9 juni 2023

The promotors,

.....

Prof. Dr. ir. Jana Asselman

.....

Dr. Ilias Semmouri

The author,

.....

Michiel De Cooman

Acknowledgements

This thesis was established by the help of numerous people, which I want to thank briefly in the following paragraphs.
First of all, I would like to thank my tutor Dr. Ilias Semmouri for being there whenever I had doubts/ questions and for introducing me into the world of molecular biology (which was very new to me). The feedback I received was always very informative and clear, which made it possible to progress quickly. It was a great pleasure working together in the lab, calling for multiple hours and spending time together on the research vessel Simon Stevin. Secondly, I want to thank my promotor Prof. Dr. Ir. Jana Asselman for providing clear feedback on the literature study and during the presentation moments we had. It was very valuable to share ideas on the further development of the thesis and mutually work towards a clearly defined end result.

Without sampling no thesis, so thank you Jonas and VLIZ for saving a spot on the Simon Stevin research vessel every month. Also here a big thanks to Ilias for taking samples during summer, as well as to Jolien and Jonas for taking (part of) the samples in November, December and January. I should also not forget to mention Vicky who provided us with samples from the Spuikom in Ostend.

This thesis involved a lot of lab work, which was all relatively new to me. Thank you Lisa for explaining the CTAB protocol to me in the very beginning of the semester and demonstrating the use of the pipettes. I could also always count on Ilias and Jolien whenever I was unsure or had a question about something. Jolien explained the PCR protocol to me and learned me how to use all the necessary equipment. Also a big shout out to Pieter for assisting me in preparing some of the PCR samples and loading them onto the gel, this saved me a lot of precious time. Lastly, the presence of Arthur, Emmie and Sophie also boosted the atmosphere in the lab and made it a great pleasure to work there during the (often long and intense) days.

Finally, I would also like to thank my parents and girlfriend for listening to all my ideas and findings on jellyfish even though they often probably did not (want to) know what I was talking about. Your enthusiasm is one of the main drivers that kept me going. It was also always nice to talk about how jellyfish have no brain and heart to my friends while consuming a fresh, cold beer and playing a round of cards.

Michiel De Cooman, 09/06/2023

Table of contents

Abstract

In the last decades, blooms of jellyfish have been increasingly reported in both scientific literature and media. Despite the increasing research, robust evidence explaining the causes of these blooms is absent. As blooms occur very sudden and are unevenly distributed in the water, traditional morphological sampling may run into limits. The aim of this study was to determine whether jellyfish blooms in the Belgian Part of the North Sea (BPNS) can be predicted on the basis of eDNA metabarcoding, which is seen as a non-invasive, cost-effective and powerful tool for detecting certain target species. We identified Cnidaria and Ctenophora over the course of six months using both a traditional morphological method and eDNA metabarcoding of a 500 – 1000 bp fragment of the 18S rDNA gene using nanopore sequencing. Using both sampling methods, we compared spatial and temporal trends in jellyfish abundance. Our results showed that seven different species were detected based on eDNA metabarcoding and no significant spatial or temporal patterns were discovered. With traditional morphology however, temporal trends were obvious: bloom concentrations were significantly higher in summer for both phyla. Comparing both sampling techniques, no significant correlations were found between morphological counts and eDNA metabarcoding reads. Overall, we conclude that eDNA metabarcoding allows for jellyfish detection, but does not suffice for bloom prediction.

1 Introduction

1.1 The gelatinous fraction of the zooplankton: jellyfish

Plankton is a group of organisms that drift freely in the water column. They range in size from 0.02 µm (Femtoplankton) to 20 mm and more (Megaplankton) (Santhanam et al., 2019). They include both phytoplankton and zooplankton (Lumini & Nanni, 2019). Phytoplankton literally means "the plants of the sea" (MarineBio, 2019), while zooplankton is derived from the Greek words *planktos* and *zoion*, meaning "wanderer" and "animal", respectively (Kennedy, 2019; Santhanam et al., 2019). Based on etymology, one could think plankton only consist of plants and animals. However, the group also comprises bacteria and viruses, next to several protozoans, dinoflagellates and diatoms among others (Brierley, 2017). Plankton is classified according to their metabolism (autotrophic vs. heterotrophic), size (from macro to pico), life history (mero- and holoplankton) and taxonomy (e.g., gelatinous vs. crustaceous zooplankton) (Lumini & Nanni, 2019).

Energy provisioning in phytoplankton is done via photosynthesis (Kennedy, 2019). Zooplankton rely on phytoplankton, bacterioplankton, marine snow (detritus) and some smaller zooplankton as primary food sources. Based on their lifecycle, zooplankton are divided into mero- and holoplankton. Meroplankton only act part of their life as plankton and eventually transform into e.g., eggs and fish larvae, while holoplankton remain plankton for their entire life (e.g., radiolarians) (Santhanam et al., 2019). According to Santhanam et al. (2019), all aquatic organisms that are consumed by humans require zooplankton in a certain stage of their development. They thus play a vital role in the aquatic food web.

Plankton's intrinsic movements are feeble, which leads to them being at the mercy of water currents. They are dependent upon water movement for their maintenance and transport (Santhanam et al., 2019). To survive, they must be well adapted to their environment. Zooplankton are often transparent, which is used as camouflage to predators. UV-protective pigments can be present to avoid UV-light damage. However, more pigments means less transparency, increasing their visibility to predators (Johnsen & Widder, 2000). Potential predators also send out chemical signals which are intercepted by zooplankton. These info chemicals are called kairomones (major component of fish kairomones: trimethylamine). Besides fish (e.g., *Gambusia affinis*), kairomones are also emitted by e.g., the amphibian *Notophthalmus viridescens* and the aquatic bugs *Notonecta irrorata* and *Notonecta maculata* (Eveland et al., 2016). Kairomones can evoke changes in morphology, biochemistry and behavior of the receiver, zooplankton in this case (Samanta et al., 2011). Morphologic changes are e.g., the formation of a lateral spine and colonies. Changes in biochemistry include the production of toxins and/or repellents (Samanta et al., 2011). An important behavioral change is diel vertical migration (DVM), where zooplankton move up and down the water column in order to feed and seek shelter against predators (Bandara et al., 2021; Diel et al., 2020). The major chemical component of the kairomone that induces DVM of *Daphnia* is 5α-cyprinol sulfate (Pohnert, 2019).

To make the connection with jellyfish, gelatinous zooplankton (GZ) have to be considered. This is a diverse group of marine organisms including ctenophores, cnidarians and pelagic tunicates. GZ range in size from less than one millimeter up to over two meters (e.g., *Cyanea capillata*, which is the biggest jellyfish species, can measure up to 36.5 m between top and bottom of its tentacles (Smithsonian Ocean, n.d.)) and consist of a transparent, soft body (exoskeleton is lacking) with a water percentage of 95% or more (Clarke et al., 1992; Jaspers et al., 2015). Condon et al. (2012) state that gelatinous zooplankton are key members of ocean ecosystems and fulfill ecological roles that are grossly oversimplified and misunderstood. They occupy key positions in food webs, both as predator and prey: the jelly web, which is the appearance of GZ in planktonic oceanic food webs, ranges over more than three trophic levels, going from herbivores (e.g., tunicates) to higher predators (e.g., comb jellies and jellyfish) (Chi et al., 2021).

If not stressed, fish cope well with gelatinous zooplankton: they recover fast, have a longer life span and are able to escape medusa jellyfish. Not only does the latter predate on fish eggs and larvae, they also compete with larvae and juveniles by feeding on the same food source: other zooplankton (Falkenhaug, 2014). Another aspect is the predation of fish on jellyfish: many fish species (e.g., chum salmon, butterfish and spiny dogfish) predate on gelatinous species. Besides fish, also turtles

(e.g., Leatherback turtles) and sea birds (e.g., albatrosses) feed on jellyfish (Motivans, 2017; Purcell et al., 2007). Jellyfish may also aid indirectly in the feeding of sea birds by concentrating forage fish on their tentacles, which are then consumed by e.g., the thick-billed murre (Sato et al., 2015). They however also influence human activities (e.g., tourism), economies (e.g., fisheries) and ecosystem processes (GZ taking away energy from higher trophic levels) (Condon et al., 2012).

1.1.1 Taxonomy of Coelenterata

The phylum Coelenterata was introduced in 1847 and was used for all species that looked like jellyfish (D. Cairns & Gail Fautin, 2009). In dated literature, it is thus considered that jellyfish belong to the phylum Coelenterata (Anderson & Schwab, 1981; Hori et al., 1982; Hsieh & Rudloe, 1994; Miura & Kimura, 1985). Nowadays, when considering jellyfish, the term Coelenterata is replaced by the term Cnidaria (D. Cairns & Gail Fautin, 2009). Coelenterata can be seen as an (outdated) taxonomic group which is found in the kingdom Animalia and contains the phyla Ctenophora and Cnidaria (Fahlke et al., 2016; Lakna, 2017; Pisani et al., 2015).

Ctenophores and cnidarians are usually referred to as jellies. However, not both phyla are actual jellyfish (AMNH, 2017). Only the jellies belonging to the phylum Cnidaria are considered real jellyfish, while jellies from the phylum Ctenophora are referred to as comb jellies (AMNH, 2017; Çinar et al., 2014; Lakna, 2017). The general consensus is that the term "jellyfish" is only used for species that belong to the phylum Cnidaria (AMNH, 2017; Çinar et al., 2014; Lakna, 2017; Montgomery et al., 2016).

In sections 1.1.1.1 and 1.1.1.2, both phyla are discussed. **Figure 1-1** gives an overview of the genealogy of Coelenterata, which aids in understanding these following sections. For each class, the most common species that occur in both the Atlantic Ocean and the North Sea are briefly mentioned. In **Table 1**, this information is summarized.

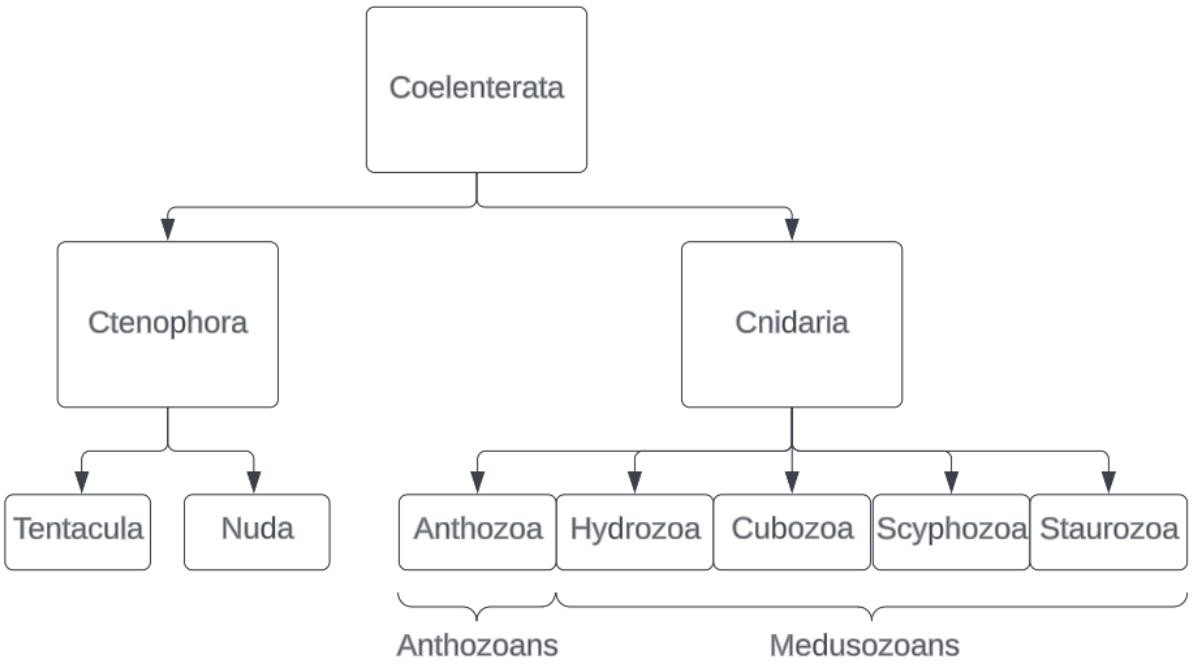

Figure 1-1 Conceptual diagram of the genealogy of Coelenterata (D'Ambra & Lauritano, 2020; Fahlke et al., 2016; Goffredo & Dubinsky, 2016; Ortman, 2008; Pisani et al., 2015).

Table 1 *Common gelatinous zooplankton species in the Atlantic Ocean and the North Sea that are discussed in this thesis. Non-native species are indicated in red (Bennett et al., 2011; Capel et al., 2017; Collins & Daly, 2005; Dawson & Martin, 2001; Gadelha et al., 2012; Gambill et al., 2018; Govindarajan et al., 2017; Grohmann et al., 1999; Holland et al., 2004; Holst et al., 2019; Holst & Laakmann, 2019; Hosia & Titelman, 2011; Krone et al., 2013; Lewis et al., 2013; Mapstone, 2014; Miller et al., 2012; Pagès et al., 1992; Schiariti et al., 2021; Van Ginderdeuren, 2013; Van Ginderdeuren, Fiers, et al., 2012; van Walraven et al., 2016; Waller et al., 2005).*

Phylum	**Ctenophora**		**Cnidaria**				
Class	**Tentacula**	**Nuda**	**Anthozoa**	**Hydrozoa**	**Cubozoa**	**Scyphozoa**	**Staurozoa**
Atlantic Ocean	*Mnemiopsis leidyi;* *Pleurobrachia pileus;* *Callianira antarctica;* *Lampea pancerina;* *Mertensia ovum*	*Beroe ovata;* *Beroe cucumis*	*Tubastraea coccinea;* *Tubastraea tagusensis;* *Caryophyllia ambrosia;* *Caryophyllia sequenzae;* *Caryophyllia cornuformis*	*Apolemia uvaria;* *Nanomia cara;* *Rhodalia miranda;* *Muggiaea atlantica;* *Muggiaea kochii;* *Gonionemus vertens*	*Copula sivickisi;* *Alatina alata;* *Carybdea marsupialis;* *Chiropsalmus quadrumanus;* *Tamoya ohboya;* *Tripedalia cystophora;* *Chirodropus gorilla;* *Tamoya haplonema*	*Aurelia aurita;* *Cassiopea xamachana;* *Cassiopea andromeda;* *Cassiopea frondosa;* *Pelagia noctiluca*	*Haliclystus auricula;* *Haliclystus octoradiatus;* *Haliclystus salpinx;* *Kishinouyea corbini;* *Depastromorpha africana;* *Lipkea stephensoni;* *Lucemariopsis capensis;* *Haliclystus antarcticus;* *Lucernaria quadricornis*
North Sea	*Mnemiopsis leidyi;* *Pleurobrachia pileus*	*Beroe gracilis*	*Metridium senile;* *Actinia equina*	*Nemopsis bachei;* *Margelopsis haeckelii;* *Rathkea octopunctata;* *Obelia* sp.; *Lovenellidae* sp.; *Clytia hemisphaerica*	Not observed	*Aurelia aurita;* *Chrysaora hysoscella;* *Cyanea capillata;* *Cyanea lamarckii;* *Rhizostoma pulmo*	*Haliclystus tenuis;* *Haliclystus auricula;* *Craterolophus convolvulus*

1.1.1.1 Ctenophora

Ctenophora are commonly referred to as "comb jellies" and are divided into two classes: Tentacula and Nuda (see **Figure 1-1**), based on whether or not they possess tentacles. The term "comb jellies" comes from "comb bearer", referring to the eight rows of comb plates that Ctenophora possess along its body (Ortman, 2008). Ctenophores contain a complex bi-radial body symmetry: radial and bilateral symmetry are combined (Fahlke et al., 2016). Comb plates, rows and symmetry are visualized in **Figure 1-2**. Comb jellies have a complete digestive system (Ortman, 2008), employ muscles and possess the most divergent nervous system in the animal kingdom (Fahlke et al., 2016). Their thick jelly-like mesoglea (a mucopolysaccharide gel reinforced with fibers (Megill et al., 2005), consisting mainly out of collagen (Chen & Wang, 2015)) is sandwiched by two epithelial layers: the outer epidermis or ectoderm and the inner gastrodermis or endoderm. Besides fibers and collagen, the mesoglea also includes a combination of muscle cells, nerves and stem cells (Tamm, 2014).

The rows of comb plates allow comb jellies to move in the water column (Ortman, 2008) and mediate their swimming performance (Heimbichner Goebel et al., 2020). The plates can beat in two directions: oral-aboral and aboral-oral. When swimming forward, the plates beat in the oral-aboral direction. When swimming reverse or performing rotations, aboral-oral beating is performed (Fahlke et al., 2016). The end where the mouth is, is called the oral side, while the other side is called aboral (Slobodkin & Bossert, 2010). This is also seen in **Figure 1-2**. The geotactic control of comb row beating is taken care of by signal transduction from the statocyst, which is a gravitometric organ, to each comb row via ciliated grooves (Fahlke et al., 2016) (**Figure 1-2**). In this way, ctenophores are able to orient their gravitational direction (Tamm, 2014).

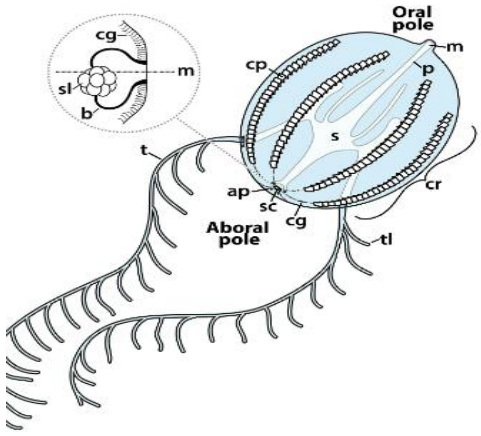

Figure 1-2 *Morphology of Ctenophora. Cr = comb row, cp = comb plate, m = mouth, p = pharynx, s = stomach, ap = anal pore, sc = statocyst, cg = ciliated groove, t = tentacle, tl = tentilla, sl = statolith, b = balancer (Fahlke et al., 2016).*

Next to forward and reverse swimming, comb jellies can also move vertically in the water column. Their propensity to move up or down is referred to as their "mood". To coordinate this, comb jellies contain various sensory modalities (e.g., to water disturbances and hydrostatic pressure), which consist of balancer cells (**Figure 1-2**). The regulation of neural inputs to these cells can change their "mood". Ctenophores are thus able to exhibit different kinds of swimming, overriding geotactic behavior. The exact mechanisms behind this need further studying (Fahlke et al., 2016).

Comb jellies employ muscles and make use of specialized adhesive cells, called colloblasts, for prey capture (Fahlke et al., 2016; Ortman, 2008). These are found both on tentacles and tentilla (specialized repeating side branches of tentacles, see **Figure 1-2**). Once the prey is caught, it enters the pharynx via the mouth and eventually ends up in the stomach (Fahlke et al., 2016). According to their morphology, ctenophores use different feeding modes (Haddock, 2007).

If the species possesses tentacles (class Tentacula), these are used for feeding. i.e., planktonic organisms can get stuck in the sticky tentillar net. The tentacles are then retracted and the comb jelly swims towards the prey (Haddock, 2007). Unilateral ciliary reverse is done (the comb jelly turns around) in order to bring the prey to the mouth (Tamm, 2014). Usage of tentacles for feeding is mainly a sit and wait strategy (Haddock, 2007).

If tentacles are absent (class Nuda), feeding can be done using lobes or engulfing. The lobes, which can be seen as extensions of the body, contain rows of oral tentacles along either side of the mouth (Haddock, 2007), also seen in **Figure 1-3A**. The prey passes between the lobes and is disturbed by the sinuous beating of the auricles (appendages on the base of the lobes which help in feeding and locomotion (L. Gershwin et al., 2014)). While trying to escape, they often touch the lobes and become trapped in the oral tentacles. Some (sub)species, e.g., *Ocyropsis maculata immaculata*, do not have functional tentacles and rely on their muscular lobes for direct prey capture (Haddock, 2007).

When feeding by engulfing, the mouths of the ctenophores are equipped with tooth-like macro cilia with which they are able to advance their lips over the prey while consuming it (Haddock, 2007). Cilia are organelles which are supported by a basal body and are involved in e.g., mechano- and gravity sensation (Alberto Bezares-Calderón et al., 2019). i.e., *Beroe cucumis* can either "bite" pieces of their prey or engulf them completely (Haddock, 2007). Reversible tissue adhesion is used in order to keep their mouth closed while swimming (Tamm, 2014). **Figure 1-3B** shows an image of *Beroe cucumis*, order Beroida, class Nuda. The comb rows, which are typical for ctenophores, are clearly visible (Welch et al., 2006).

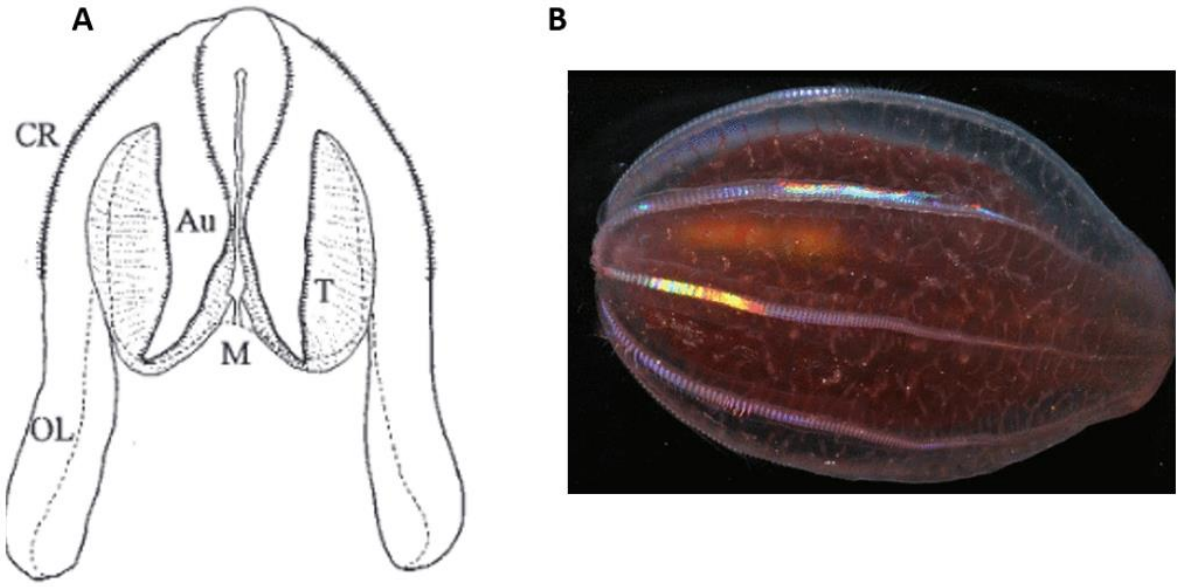

***Figure 1-3** (**A**) Morphology of the lobate ctenophore Mnemiopsis leidyi. CR = ctene row (= comb row (Ortman, 2008)), Au = auricle, T = tentillae, M = mouth, OL = oral lobe (Waggett & Costello, 1999). (**B**) Typical comb rows seen in the species Beroe Cucumis (Welch et al., 2006).*

The orders Beroida, Lobata and Cydippida are found in the Belgian part of the North Sea (BPNS). Three species occur: *Beroe gracilis*, *Mnemiopsis leidyi* and *Pleurobrachia pileus* (Van Ginderdeuren, 2013). *Mnemiopsis leidyi* is an invasive species that was first detected in 2007. After only four years, the species was observed along the whole Belgian coastline as well as in harbors. Adult individuals have been seen in the coldest winter months, implying that the species is able to survive Belgian winters (Van Ginderdeuren, Fiers, et al., 2012). Since high densities of *Mnemiopsis leidyi* were found back in ports, it is likely that they entered the Belgian marine waters via the ballast water of ships (Van Ginderdeuren, Hostens, et al., 2012).

In the South-Western Atlantic and sub Antarctic region, *Mnemiopsis leidyi* and *Pleurobrachia pileus* are the most frequently observed ctenophores. *Beroe ovata* and *Beroe cucumis* are also frequently seen. *Callianira antarctica*, *Lampea pancerina* and *Mertensia ovum* were reported a few times in low quantities (Schiariti et al., 2021). **Figure 1-4** illustrates the relative composition of Ctenophora orders at different locations in the Atlantic Ocean (Gueroun et al., 2021). In Macaronesia (island group including the Azores, Madeira, Cape Verde and the Canary Islands), 18 species of Ctenophora are recorded, belonging to four different orders.

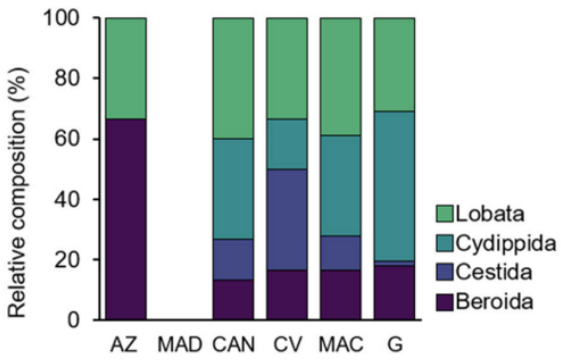

Figure 1-4 Composition of ctenophore orders at different locations. MAC = Macaronesia, AZ = Azores, MAD = Madeira, CAN = Canary Islands, CV = Cape Verde, G = Global data (Gueroun et al., 2021).

1.1.1.2 Cnidaria

When talking about jellyfish, only species belonging to the phylum Cnidaria are considered. Although Ctenophora and Cnidaria may look similar, there are clear differences in e.g., body symmetry, muscles and tentacles (Fahlke et al., 2016). In contrast to Ctenophora, which have a bi-radial body symmetry, Cnidaria have a radial body symmetry. Both phyla may use tentacles for feeding, but also these differ. Ctenophora contain so-called colloblasts (a.k.a glue cells) on their tentacles, while Cnidaria are equipped with stinging cells (cnidocytes). Cnidaria are thus able to sting. A third main difference is that Ctenophores only possess smooth muscle cells in their main body, while Cnidaria possess striated (striped) and smooth muscle cells (Seipel & Schmid, 2005).

Cnidocytes are also referred to as nematocysts and aid in feeding and repelling predators (Beckmann & Özbek, 2012). Nematocysts (also called cnidia) are produced by ectodermal cells, called cnidoblasts. They consist of a long thread with a capsule at its base, see **Figure 1-5A** (Slobodkin & Bossert, 2010). Nematocysts are stinging organelles (L. A. Gershwin, 2006) that are usually laying on the tentacles and may look like a hypodermic syringe with a long needle after firing (**Figure 1-5B**). Some produce neurotoxins to paralyze their prey. This type of nematocysts are called stenoteles. Other types eject sticky threads which immobilize prey by wrapping themselves around them (these nematocysts are called desmonemes or volvonts). Some volvonts remain attached to the tentacles after firing, making it look as if the prey is fastened to the tentacles via tiny ropes and grappling hooks. After the catch, the tentacles move the prey towards the mouth and coelenteron (the central interior cavity, also called digestive cavity). Preys are often still alive and active until the gastric cells, which are lining the coelenteron, secrete digestive juices (Slobodkin & Bossert, 2010).

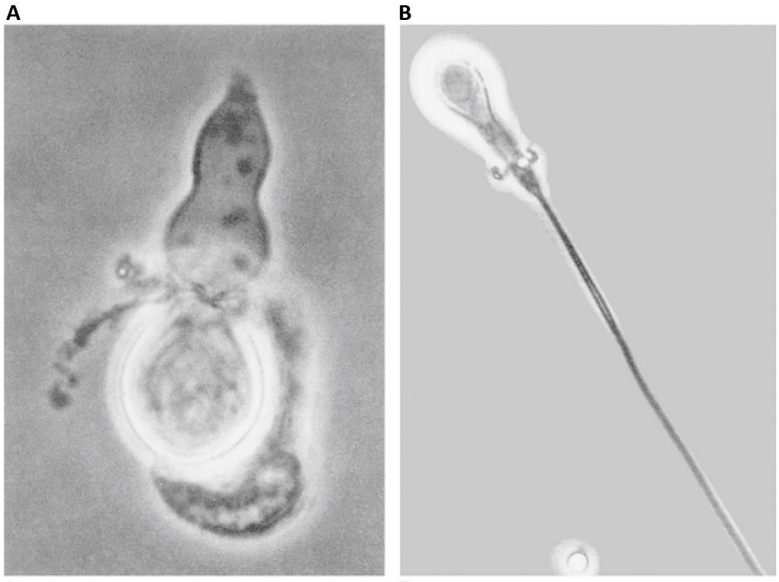

Figure 1-5 Close up of a nematocyst. (A) before firing, (B) after firing (Slobodkin & Bossert, 2010).

The phylum Cnidaria consists of five classes: Anthozoa, Hydrozoa, Cubozoa, Scyphozoa and Staurozoa (**Figure 1-1**) (D'Ambra & Lauritano, 2020; Goffredo & Dubinsky, 2016). Since the life-cycle of Hydrozoa, Cubozoa, Scyphozoa and Staurozoa mostly includes a benthic (polyp) and a free-living planktonic (medusa) stage, these classes belong to the subphylum Medusozoa (Amy Williams et al., 2019; Goffredo & Dubinsky, 2016).

Medusozoa typically undergo a three-phase life cycle (**Figure 1-6A**): planula (usually considered as a larva) – polyp – pelagic medusa (Goffredo & Dubinsky, 2016). The polyps typically reproduce asexual, while the medusa is the sexual form (Frazão et al., 2012). Depending on the class, the transition from polyp to medusa can happen via strobilation, metamorphosis or lateral budding (Laffoley & Baxter, 2016). These terms will be discussed in more detail in the sections covering the according classes.

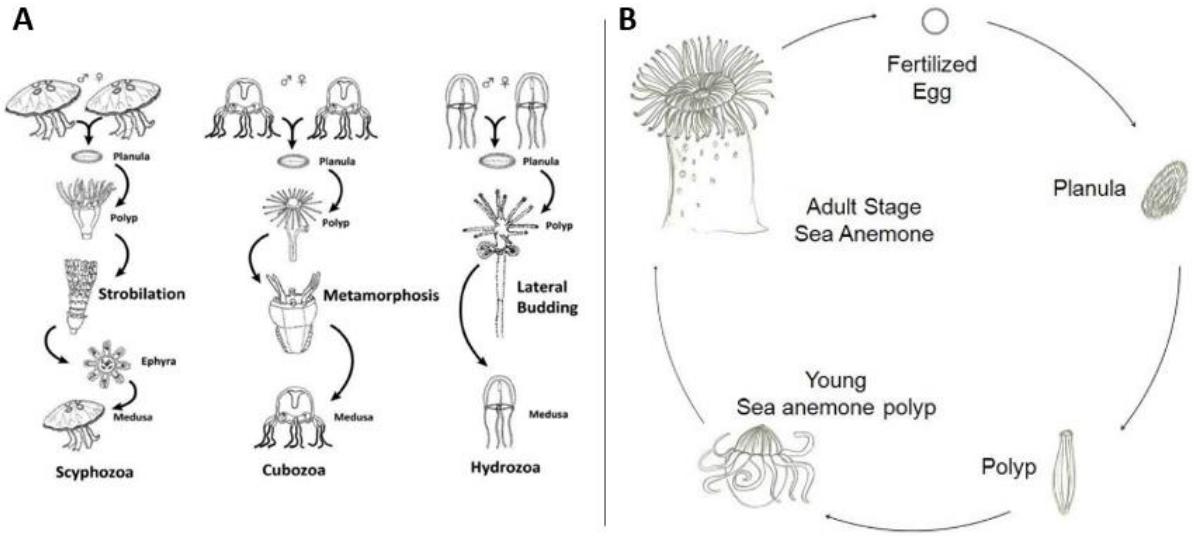

Figure 1-6 (A) Life cycle of different Medusozoa: Scyphozoa, Cubozoa and Hydrozoa (Laffoley & Baxter, 2016). (B) Typical life cycle of Anthozoa (Frazão et al., 2012).

Figure 1-6B illustrates the life cycle of Anthozoa, which consists of embryo – larva – polyp (Frazão et al., 2012) and does not have a medusa stage (Bocharova & Kozevich, 2011; Helm, 2018). The planula larvae are microphagous feeders which then develop into polyps, where organs such as the mouth, tentacles and stomach are formed (Goffredo & Dubinsky, 2016). Both sexual and asexual reproduction is realized by these polyps (Bocharova & Kozevich, 2011). The polyps then form calcareous skeletons and grow out into e.g., sea anemones (Goffredo & Dubinsky, 2016).

1.1.1.2.1 Anthozoa

Anthozoa are the largest class of Cnidaria and include sea anemones, corals and sea pens (Goffredo & Dubinsky, 2016; Shearer et al., 2002). They are defined by three main morphological/anatomical characteristics (**Figure 1-7**). Firstly, they contain an actinopharynx, which is a primordial stomach (Work & Meteyer, 2014) located at the gastrovascular cavity, formed by epidermal tissue. Within the corner of the actinopharynx, a ciliated area is found: the siphonoglyph, which aids in creating hydrostatic pressure (Swain et al., 2015). Thirdly, sheet-like partitions of the body wall, containing specialized filaments, are found. These are called mesenteries and extend to the gastrovascular cavity (Goffredo & Dubinsky, 2016). These three main characteristics (actinopharynx, siphonoglyphs and mesenteries) play an important role in expansion and retraction of the columns and tentacles of Anthozoan species (Swain et al., 2015).

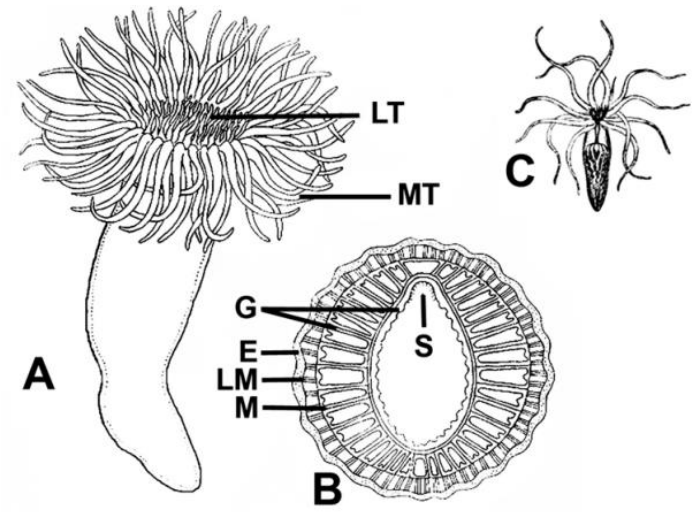

Figure 1-7 Morphology of Anthozoa. (A) benthic specimen, (B) cross-section at pharynx, (C) planktonic specimen. LT = Labial Tentacles, ML = Marginal Tentacles, G = Gastrodermis, E = Epidermis, LM = Longitudinal muscles, M = Mesentery, S = Siphonoglyph (Goffredo & Dubinsky, 2016).

Expansion assists, among other things, in prey capture, fending-off of predators and competitors, sediment removal, increase of oxygen and waste product diffusion. In order to expand, cilia lines the siphonoglyph(s) of the actinopharynx. These then pump water into the coelenteron (central cavity) and tentacles, creating hydrostatic pressure. By closing the actinopharynx' opening and additional ciliary action, the created pressure is maintained (Swain et al., 2015). Retraction of columns and tentacles is done to e.g., avoid predator detection and thus escape predation, reduce metabolic rates, generate low internal oxygen tension and prevent desiccation (= drying out (Hunt & Denny, 2008)). Contraction of the mesenteries' muscles allow water to escape the coelenteron, resulting in a pressure drop and thus retraction (Swain et al., 2015).

According to Won et al. (2001), the phylum Anthozoa is divided into three sub-classes: Alcyonaria, Zoantharia and Ceriantipatharia. The term Alcyonaria is outdated and can only be found in old literature. It was used when referring to soft corals (Babcock, 1990; Drew, 1972; Ne'eman et al., 1974). In present, Anthozoa is divided into two main groups: Octocorallia (containing soft corals, gorgonians and sea pens) and Hexacorallia (containing anemones, black corals and stony corals) (McFadden et al., 2021).

In the North Sea, research is performed on Anthozoa in Dutch wind farms. It is seen that until a depth of ten meter, the construction surface of the wind turbines is dominated by mussels. In deeper sections, Anthozoa and Hydrozoa dominate. Considering Anthozoa, the species *Metridium senile* is the most frequently observed (Krone et al., 2013). Another species that is widely distributed in the North Sea, Mediterranean- and Aegean Sea is *Actinia equina* (Gadelha et al., 2012).

Anthozoan species are also found in the Atlantic Ocean. An important example are the azooxanthellate corals *Tubastraea coccinea* and *T. tagusensis*. Both are invasive species which spread quickly and are outcompeting native species (Capel et al., 2017). Some examples of native species in the NE Atlantic Ocean include *Caryophyllia ambrosia* and *C. cornuformis*. These are deep-sea species, occurring in depths ranging from 435 m to 3000 m (Waller et al., 2005).

1.1.1.2.2 Hydrozoa

Hydrozoa is the most diverse group of cnidarians and comprises 3,800 nominal species (Goffredo & Dubinsky, 2016). They are found in all marine environments, from polar to tropical waters and from intertidal zones to ocean trenches. A small percentage is found in fresh waters (R. Calder & D. Cairns, 2009), e.g., the genus *Hydra*, which is considered the best known hydrozoan (Goffredo & Dubinsky, 2016). Hydrozoa possess a simple gastrovascular system, are deprived of an (actino)pharynx, contain septa or gastric tentacles, acellular mesoglea and generally have separated sexes (Bouillon et al., 2004).

Hydrozoans are known for their complex and diverse life cycles. This cycle often consists of three stages (see **Figure 1-6A**). A free-living planula larva, which transforms into polyps, which then bud pelagic medusae that form gametes (reproductive cells) and spawn into the water column (Cartwright & Nawrocki, 2010). Budding can be seen as an asexual way of reproduction, where organisms develop as a bud (outgrowth) from the parent (Bouillon et al., 2004). In Hydrozoans, the life-cycle varies greatly, which is reflected by a wide diversity of polyps, colonies and medusa morphologies. Some species even lack a polyp or medusa stage (Cartwright & Nawrocki, 2010).

Hydrozoans are important carnivores which predate on both plankton (when in medusa stage) and benthos (when in polyp stage). They feed on e.g., fish larvae, crustaceans, phytoplankton, bacteria, protozoans and dissolved organic matter. Others harbor symbiotic intracellular algae, which can reach very high abundances when environmental conditions are favorable, leading to seasonal blooms in planktonic communities (Bouillon et al., 2004; Goffredo & Dubinsky, 2016). Hydromedusae (the pelagic stage of hydrozoans (Goffredo & Dubinsky, 2016)) are used as biological indicators to predict oceanic water movements and several species are known as indicators of upwelling systems (Bouillon et al., 2004).

There is currently still a lack of consensus considering the classification of Hydrozoa. There have been proposals to classify them based on embryological, developmental and morphological features, which resulted in three classes: Automedusa, Hydroidomedusa and Polypodiozoa. Another possibility is to consider the cnidarian phylogenetic relationships, which resulted in subclasses Trachylina and Hydroidolina (Goffredo & Dubinsky, 2016). In Bouillon et al. (2004), the first option is followed: Hydrozoa are devided into Automedusa, Hydroidomedusa and Polypodiozoa.

In the BPNS, two orders of Hydrozoa are observed: Anthoathecata (containing e.g., *Nemopsis bachei*, *Margelopsis haeckelii* and *Rathkea octopunctata*) and Leptothecata (containing e.g., *Obelia* sp., *Lovenellidae* sp. And *Clytia hemispaerica*). In total, eleven different species are found. The most common species are *Clytia hemisphaerica*, *Margelopsis haeckelii* and *Rathkea octopunctata*. An example of an invasive species is *Nemopsis bachei* (just like the ctenophore *Mnemiopsis leidyi*, see section 1.1.1.1) (Van Ginderdeuren, 2013).

Hydrozoa are also observed in the Atlantic ocean. *Apolemia uvaria* and *Nanomia cara* are two deep-sea species, typically found in the North Atlantic. *Rhodalia miranda* is found in the SW Atlantic, while *Muggiaea atlantica* and *M. kochii* are observed in the whole Atlantic Ocean (Mapstone, 2014). The Hydrozoan *Gonionemus vertens* is native to the Pacific Ocean, but has since 1894 also been observed in the NW Atlantic (Govindarajan et al., 2017). Migrations are thus possible between different oceans.

1.1.1.2.3 Cubozoa

Cubozoa are known under the name "box jellyfish" (Goffredo & Dubinsky, 2016), since they possess a box-shaped exumbrella (Coates, 2003), which is the outer surface layer of the bell (Bouillon et al., 2004). Cubozoa is the smallest class within the phylum Cnidaria, containing around 20 species. A clear difference with other Cnidarian classes is the possession of highly developed, lens-shaped eyes (Coates, 2003).

From all Cnidarians, cubozoan medusae have the best developed eyes. They are capable of detecting specific features for navigation and hunting (Goffredo & Dubinsky, 2016). The eyes can be found on the rhopalia: marginal sense organs hanging from the bell (Coates, 2003), which is the main body of the medusa (tentacles not included) (Bouillon et al., 2004). The rhopalia are weighted down by a statolith, which functions as both a gravity-sensing organ and a weight, keeping the eyes in the same orientation independent of the body orientation. The exact function of the statolith however, needs further studying. The reason that cubozoans developed such good eyes may be because they are found in near-shore habitats. Since medusae are very soft and fragile, they easily get damaged by obstacles. In order to survive in the obstacle-rich near-shore zones, a good sight is crucial, hence the well-developed eyes. Vision is also important to detect objects at a distance and to allow for orientation to luminescent prey at night. A counter argument is that jellyfish (and thus also box jellyfish)

lack a brain, so one might ask what use it is to have a good image when there is no nervous ability to interpret it (Coates, 2003).

Cubozoans are excellent swimmers and have a highly developed orientation behavior (Kingsford & Mooney, 2014). They are found in tropical and temperate waters (L. Gershwin, 2005) and can be extremely poisonous to humans (e.g., the species *Chironex fleckeri* and *Chiropsalmus quadrigatus*). When stung by one of these species, death may result after a few minutes. Cubozoans thus form a medical challenge and public health threat. Their stings may cause mild site pain, cramping muscle pain, nausea and eventually become fatal due to cardiac failure or intracranial bleeding. No validated standards are currently in operation to deal with life threatening stings (Goffredo & Dubinsky, 2016).

The life cycle of Cubozoa differs slightly from the one of Hydrozoa and Scyphozoa. As can be seen in **Figure 1-6A**, Cubozoa are able to undergo complete metamorphosis from polyp to medusa (Coates, 2003). The polyp, which is sessile and benthic, reproduces asexually, while the medusa is motile and reproduces sexually. Metamorphosis is initiated by external factors such as temperature or light (Courtney & Seymour, 2013).

Classification of Cubozoa, as was also the case with Hydrozoa, lacks consensus. According to Gershwin (2005), 17 species are currently recognized in Australia, which is about half of the total number of historically described species. However, this is a gross underestimation of the actual morphological biodiversity (L. Gershwin, 2005). Coates (2003) states that Cubozoa only consist of one order (Cubomedusae), containing around 20 species in total.

To this day, cubozoan species have not been observed in the North Sea. Van Ginderdeuren, Fiers, et al. (2012) performed research on the different zooplankton species in the BPNS and Cubozoa was not found. This was also the case with observations of the BPNS in the period 2009-2010 (Van Ginderdeuren, 2013). When browsing through literature, no papers can be found which cover Cubozoa in the North Sea, indicating that the class is not observed in this area.

In contrast to the North Sea, Cubozoa are frequently found in the Atlantic Ocean. In the tropical Western Atlantic Ocean, species such as *Copula sivickisi* (Bahamas) and *Alatina alata* (Bonaire – Caribbean islands) are spotted (Bennett et al., 2011; Lewis et al., 2013). *Copula sivickisi* was usually only observed in the Indo-West-Pacific ocean. They might have migrated into the Atlantic via anthropogenic activities (e.g., ballast water of ships). Other species occurring in these tropical Atlantic regions are *Carybdea marsupialis*, *Chiropsalmus quadrumanus*, *Tamoya ohboya*, and *Tripedalia cystophora* (Bennett et al., 2011). Looking at the East Atlantic, *Chirodropus gorilla* and *Tamoya haplonema* are observed at the West coast of Africa (Pagès et al., 1992).

1.1.1.2.4 Scyphozoa

Scyphozoa are known as true jellyfish (Goffredo & Dubinsky, 2016) and the majority of species live in shallow coastal waters: when people get stung by jellyfish at the beach, these are mostly scyphozoans (Hale, 1999). They are exclusively marine, which distinguishes them from Hydrozoa, as these appearing in both marine and fresh waters (Arai, 1996).

Scyphozoa possess a tetra-radial symmetry: they have many structures in multiples of four. In contrast to Anthozoa, they lack a clear pharynx. Scyphozoa contain large medusae and have similar feeding and nervous systems as Cubozoa (Arai, 1996). Besides that, both classes possess statoliths, used for gravity sensing (Goffredo & Dubinsky, 2016). True jellyfish possess an elementary nervous system with which they detect light (ocelli), odor and other stimuli. Their sensory receptors are very efficient and their muscular mesoglea is used for swimming (Hale, 1999). Scyphozoa undergo strobilation (see **Figure 1-6A**) in their life-cycle: benthic polyps reproduce asexually and release free-swimming ephyrae (these are the youngest medusa stages (Holst, 2012b)), which then develop into the sexually mature medusa. More polyps means more ephyrae release, which may result in a medusae bloom (Avian et al., 2021).

Scyphozoan jellyfish are divided into four orders: Coronatae, Rhizostomeae, Stauromedusae and Semaestomeae (Abato et al., 2017; Hale, 1999). However, this division is contradicted by Kuijlen (2014), where the class is divided in only three orders: Rhizostomae, Coronatae and Semaeostomeae.

In Dutch coastal waters, medusae of five species belonging to Scyphozoa are commonly found: *Aurelia aurita*, *Chrysaora hysoscella*, *Cyanea capillata*, *Cyanea lamarckii* and *Rhizostoma octopus* (van Walraven et al., 2016). Most of these species were also observed by Van Ginderdeuren (2013). *Rhizostoma pulmo* is an additional species that was observed in the latter study. Van Ginderdeuren, Fiers, et al. (2012) indicated that *Cyanea lamarckii* is the most frequently observed scyphozoan. This is confirmed by Gambill et al. (2018) and Hosia & Titelman (2011), who state that *Cyanea lamarckii*, *Chrysaora hysoscella and Cyanea capillata* are common species in the North Sea. Moreover, *C. capillata* controls the population of *Aurelia aurita* via predation (Hosia & Titelman, 2011).

In the Atlantic Ocean, Scyphozoa are abundantly present. *Aurelia aurita* is one of the most widely distributed and studied scyphozoan species and is found all over the world (Dawson & Martin, 2001). In the western Atlantic, e.g., *Cassiopea xamachana*, *C. andromeda* and *C. frondosa* are observed. These species originate from the Indo-Pacific and dispersed into the Atlantic Ocean (Holland et al., 2004). In the North-East Atlantic, e.g., *Pelagia noctiluca* is observed (Miller et al., 2012).

1.1.1.2.5 Staurozoa

Staurozoa, known as "stalked jellyfish", can be found in temperate and boreal marine waters and are probably the least known class among Cnidaria (Miranda et al., 2017). This might be because they do not have lots of external characteristics useful for taxonomy (Miranda et al., 2016) and most species are only a couple of centimeters big (Faasse & Waajen, 2011). One of the few characteristics of Staurozoa is their funnel-shaped body (Miranda et al., 2017).

As is the case with other medusozoans (Hydrozoa, Cubozoa, Scyphozoa), the life cycle of Staurozoa consists of two main stages: polyp and medusa. The differences between these stages is however not as big in Staurozoa as it is in the other medusozoan classes. Important to note is that the medusa stage remains attached to its substrate and is thus benthic. Stalked jellyfish are unable to swim, which is in sharp contrast with the other medusozoan classes. Due to their benthic lifestyle, they often appear in intertidal and subtidal pools, attached to algae or rocks. Seagrass, shell, mud, sand and coral are other substrates that are frequently used (Miranda et al., 2017)

In the past, Staurozoa were considered as an order (Stauromedusae) within the class Scyphozoa. Due to clear differences in ovaria between Staurozoa and Scyphozoa, these were later classified as two separate classes (Faasse & Waajen, 2011). Stalked jellyfish are organized in eleven genera, six families and 2 suborders: Amyostaurida and Myostaurida (Miranda et al., 2017).

Staurozoa often live in areas camouflaged by e.g., sea weed. Due to their specific life cycle (e.g., benthic medusa) and the limited number of specialists, scientific knowledge and records are limited. Three staurozoan species are observed in front of the coast of the island Helgoland (North Sea): *Haliclystus tenuis*, *H. auricula* and *Craterolophus convolvulus* (Holst et al., 2019). In the study of Van Ginderdeuren (2013), staurozoan species were not included and/or observed in the BPNS. There is no literature available on Staurozoa in this region.

Around 80% of staurozoan species is found in the northern hemisphere (Miranda et al., 2009). In North Atlantic waters, *Haliclystus auricula*, *H. octoradiatus* and *H. salpinx* are studied (Holst & Laakmann, 2019). Around Santa Cruz, Puerto Rico and South-Eastern Brazil, *Kishinouyea corbini* is recorded. In South-African waters, *Depastromorpha africana*, *Lipkea stephensoni* and *Lucemariopsis capensis* are observed. *Haliclystus antarcticus* is a species found around South Georgia and Antarctica (Grohmann et al., 1999). *Lucernaria* sp. (e.g., *Lucernaria quadricornis*) are also typically found in the Atlantic Ocean (Collins & Daly, 2005).

1.2 Jellyfish blooms

An aggregation of mature medusae can be defined as a jellyfish bloom, depending on its density. According to Mcilwaine & Rivas Casado (2021), a density of one *Aurelia* species per m³ already causes major disruption to coastal operators and, when the total number of individuals surpasses 1,000, is seen as a jellyfish bloom. Hamner & Dawson (2009) define a bloom qualitatively as a temporary increase in the local population density of jellyfish due to a local re-distribution and re-dispersion in the population. This is caused by physical and chemical factors as well as by the swimming behavior of the medusae. *Pelagia noctiluca* is an example of a swarming species, observed to occur in densities exceeding 100 medusae per m³ and up to 600 medusae per m³ closer to shore. The interaction of wind, tides, swimming behavior and topography play an important role (Hamner & Dawson, 2009). *Poralia rufescens* can be found in densities of 250 medusae per 1,000 m³ (Hamner & Dawson, 2009), while in Eil Malk Jellyfish Lake, a marine lake situated in Palau, extreme densities of *Mastigias* species exceeding 1,000 medusae per m³ were observed (Graham et al., 2001). In the North Sea, *Muggiaea atlantica* has been observed in densities of up to 500 individuals per m³ in the waters of the German island Helgoland (Mills, 2001).

A significant increase in jellyfish blooms is seen over the last decade around the globe (Dong et al., 2010). Jellyfish aggregation is a natural phenomenon, but their increasing frequency is likely due to anthropogenic disturbances and climate change (Dong et al., 2010). In the Bering Sea for example, the combined biomass of *Chrysaora* sp., *Cyanea* sp. and *Aequorea* sp. increased more than tenfold between 1975 and 1999 (**Figure 1-8**). Similarly, in the Gulf of Maine (Atlantic Ocean), maximum medusae densities went up from one to eight siphonophores (Hydrozoa) per m³ in 1975 - 1976 to 50 - 100 individuals per m³ in 1992 - 1993 (Mills, 2001). In the Sea of Japan, a poll of 1,152 fishermen with more than 20 years' experience was performed. 65% of the participants claimed to observe that *Aurelia aurita* populations have increased over this time period (Purcell, 2005; Uye & Ueta, 2004).

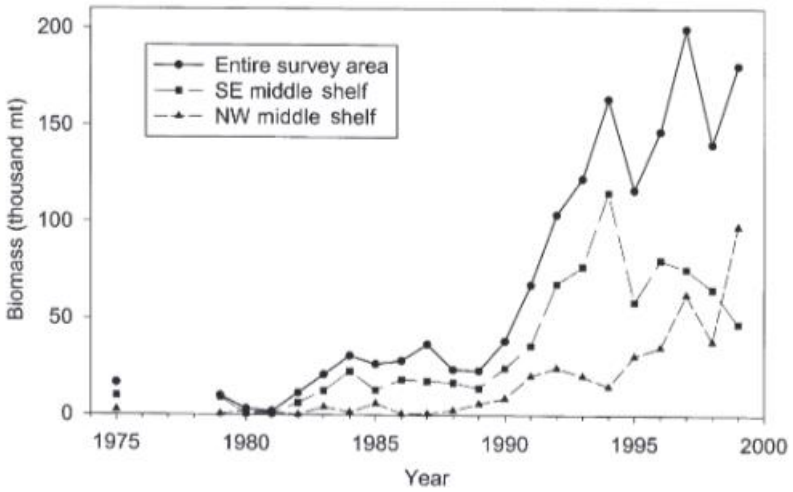

Figure 1-8 *Biomass of Chrysaora sp., Cyanea sp. and Aequorea sp. collected in the Bering Sea, expressed in metric tons (Brodeur et al., 2002).*

Jellyfish blooms have different causes and impacts, which are discussed together with the evolution of blooms in the following sections.

1.2.1 Formation and possible causes of blooms

The outbreak of jellyfish is known to be highly variable and unpredictable: individuals suddenly appear in large numbers and are later absent from the ecosystem again (Schnedler-Meyer et al., 2018). These fluctuations are seasonally dependent. Classically, at mid-latitude, phytoplankton blooms in spring, followed by a zooplankton bloom during summer. With most bloom-forming jellyfish being zooplanktivorous, jellyfish blooms are thus often seen in summer (Schnedler-Meyer et al., 2018). In the Kagoshima bay in Japan, strobilation of *Aurelia aurita* occurred between the end of December and March, when water temperatures reached 16 - 17°C. Ephyrae were then observed in early spring (Miyake et al., 2002). In the Irish

Sea, most cnidarians are observed between May and August, which is known as the typical scyphozoan jellyfish period (Lynam et al., 2011). Blooms can form under different circumstances and are influenced by several anthropogenic activities, of which the most important ones are discussed in the following sections.

1.2.1.1 Overfishing

Our oceans are currently overexploited, leading to a depletion in large fish stocks (also known as fishing down the food web: caught fish get smaller over time) (Pauly & Palomares, 2005). By fishing out predatory fish (**Figure 1-9-A**), pelagic food webs switch from mainly four trophic levels (phytoplankton - zooplankton – zooplanktivorous fish - carnivorous fish) to three trophic levels (phytoplankton – zooplankton - zooplanktivorous fish). In this new system, zooplanktivores are more abundantly present (absence of predatory control, see **Figure 1-9B**), resulting in lower zooplankton (**Figure 1-9D**) and higher phytoplankton densities (**Figure 1-9E**). These systems can result in phytoplankton blooms, increased turbidity, marine snow and hypoxia (**Figure 1-9F**) (Daskalov et al., 2007). However, besides carnivorous fish, zooplantivorous fish are currently also overexploited (drop in planktivorous fish biomass starting around 1990, see **Figure 1-9B**).

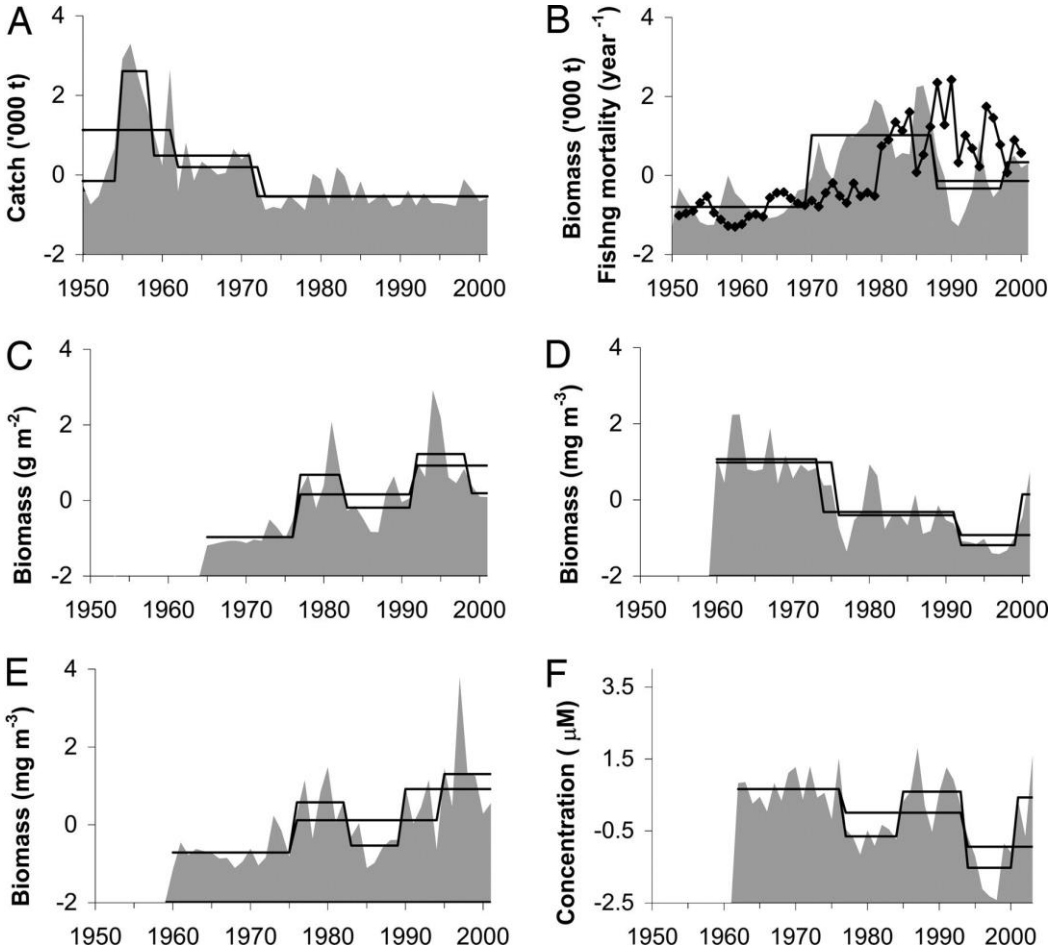

Figure 1-9 *Shifts of the four trophic levels in the pelagic ecosystem between 1950 and 2000 (data standardized to zero mean, unit variance). (**A**) Pelagic predatory fish, (**B**) Small planktivorous fish; line with diamonds represents fishing mortality, (**C**) Gelatinous zooplankton, (**D**) other zooplankton, (**E**) Phytoplankton, (**F**) Oxygen. Shifts in mean are indicated by the black lines using cut-off lengths of 15 and 7 years (Daskalov et al., 2007).*

The effect of overfishing and fishing down the food web is visualized in **Figure 1-10**. Less carnivorous fish lead to a reduction in predation on jellyfish by e.g., chum salmon, butterfish and spiny dogfish, positively affecting jellyfish populations (Purcell et al., 2007). On the other hand, overexploitation of zooplanktivorous fish removes potential competitors of gelatinous predators, as both predate on (other) zooplankton (Falkenhaug, 2014). This is e.g., seen in the Gulf of Maine (Atlantic Ocean – East coast of North America), where the abundancy of the hydrozoan species *Nanomia cara* increases due to a reduction in zooplanktivorous fish species (Purcell et al., 2007). Overexploitation of fish leads to a surplus in

zooplankton activity that can again be consumed by gelatinous species (e.g., *Mnemiopsis leidyi* in the Black Sea) (Daskalov et al., 2007). Eventually, high densities of jellyfish, which can result from overfishing (**Figure 1-9C**), eliminate the zooplankton-grazing impact on the phytoplankton bloom, leading to oxygen depletion, marine snow and increased turbidity (see green arrows on **Figure 1-10**) (Møller & Riisgård, 2007a). These blooming algae are not effectively grazed upon anymore and settle to the bottom where they decompose, leading to more hypoxia and nutrient release. Due to their higher tolerance to hypoxia, jellyfish have a strategic advantage over fish (Schnedler-Meyer et al., 2018).

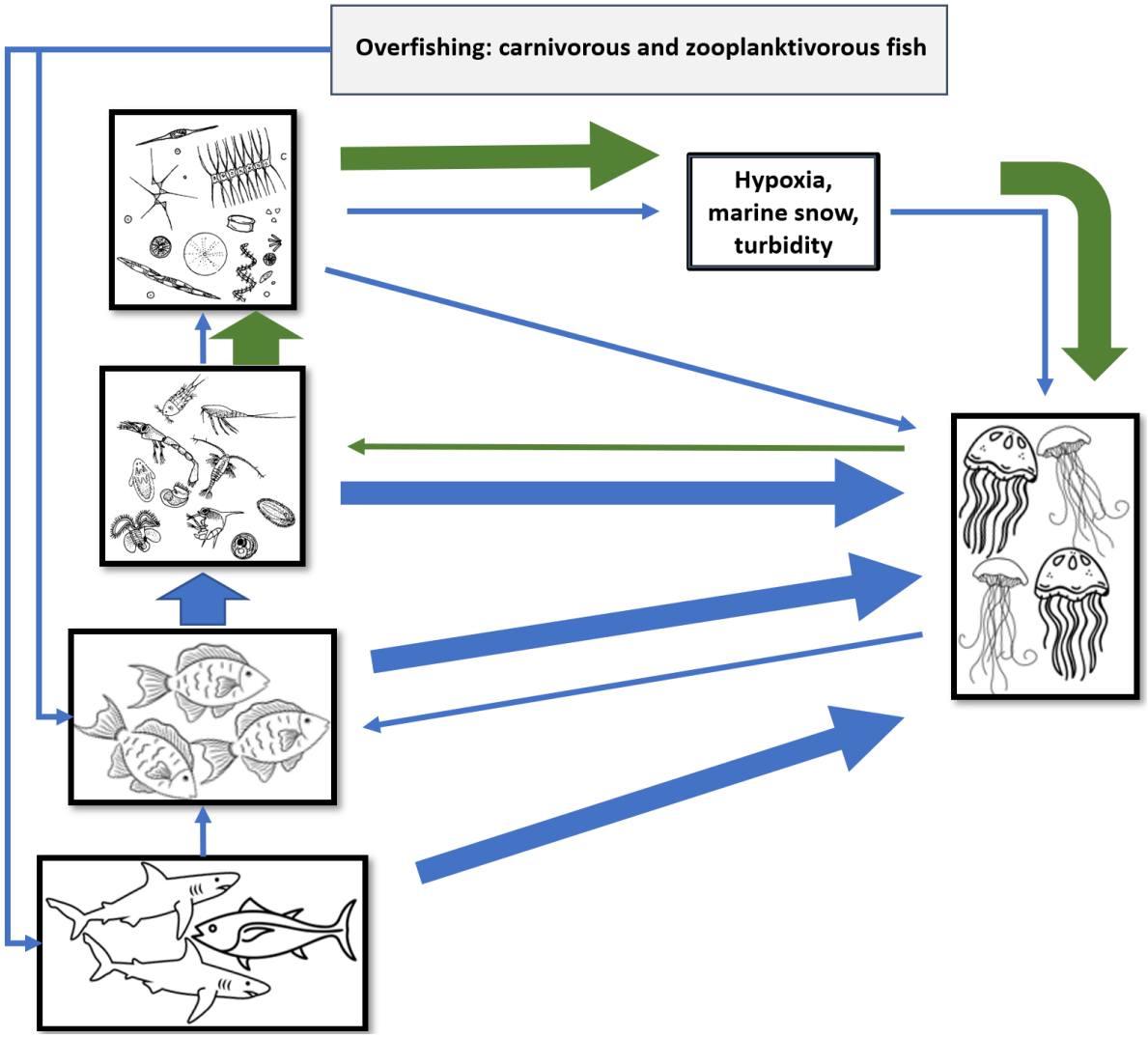

Figure 1-10 *Conceptual figure of the effect of overfishing on the aquatic food web considering phytoplankton, zooplankton, zooplanktivorous fish and carnivorous fish and the corresponding effect on jellyfish abundance. The thickness of the arrows corresponds to how strong a species is stimulated: e.g., overfishing leads to less stimulation of carnivorous fish, which leads to a big stimulation of jellyfish. Blue arrows are the initial effects of overfishing, while green arrows indicate the resulting impact of an increase in jellyfish abundance. The frames on the left side correspond to (up – down): phytoplankton, zooplankton, zooplanktivorous fish and carnivorous fish.*

In Skive Fjord, a bay in Denmark, jellyfish blooms are particularly pronounced in July and August. In the Gullmar Fjord in Sweden, heavy phytoplankton blooms were observed in 1978 and 1981 during spring and fall, along with low zooplankton and high medusae abundances (Møller & Riisgård, 2007a). The interactions discussed above are also visualized in **Figure 1-11**.

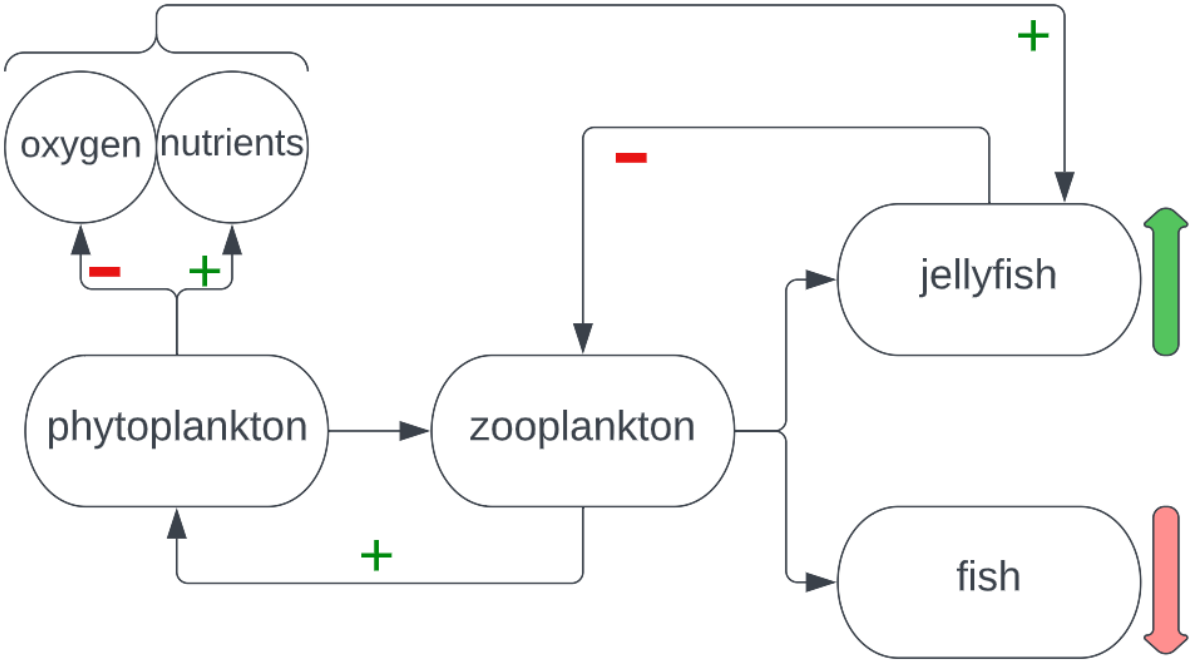

Figure 1-11 *Conceptual diagram illustrating the coherence between fish, jellyfish and other plankton (Daskalov et al., 2007; Dong et al., 2010; Møller & Riisgård, 2007a; Schnedler-Meyer et al., 2018).*

1.2.1.2 Eutrophication

Excessive nutrients lead to a high biomass of phytoplankton, which can support both polyp and medusa jellyfish. Due to all the biological activity, eutrophicated waters usually contain a lower amount of DO (Dissolved Oxygen), favoring jellyfish (see above) (Dong et al., 2010). Oxygen concentrations ≤ 2-3 mg/L are lethal to fish, while many jellyfish species (e.g., *Aurelia* sp.) can survive concentrations ≤ 1 mg O_2/L (Purcell et al., 2007). Xu et al. (2013) state that eutrophication is necessary but not sufficient for jellyfish outbreaks: an increase in phytoplankton because of eutrophication combined with higher water temperatures probably leads to long-term increases of jellyfish blooms. Additionally, some evidence is found that jellyfish directly consume autotrophs (phytoplankton): chlorophyll was found in the gut of small medusa species, *Obelia* sp. are known to consume phytoplankton and ephyrae have been found to consume protists and phytoplankton due to their smaller size (Wright et al., 2021).

In the Skive Fjord in Denmark, nitrate accumulates in the water during winter due to run-off from surrounding agriculture and pig farming. This nitrate is used up by the phytoplankton during spring, leading to algal biomass which eventually dies off and sinks to the bottom. When temperatures rise in summer, the water column gets stratified (no mixing of water layers) and re-aeration is prevented. Due to zoobenthic respiration, oxygen depletion can occur, resulting in the release of large amounts of nutrients (e.g., phosphate and ammonium) from the anoxic sediment. This results in an increase in algal biomass (phytoplankton) (Møller & Riisgård, 2007a). Besides increased nutrients, eutrophication is also associated with higher turbidity (Purcell et al., 2007).

In Mar Menor, a lagune in Spain, nitrate levels increased tenfold due to agriculture and development, while phosphate levels decreased by 10% due to wastewater treatment. These changes were associated with annual blooms of *Cotylorhiza tuberculata* and *Rhizostoma pulmo*. A high N:P ratio leads to a shift of the phytoplankton community towards flagellates and jellyfish, away from diatoms (Purcell et al., 2007). Additionally, a reduction in zooplankton size is associated with eutrophication: there may be a change towards a microplankton-based food web. Since epipelagic fish species are visual predators, both a higher turbidity and a smaller zooplankton size are detrimental. This is in contrast to jellyfish, which are not visual (exception: Cubozoa, see section 1.1.1.2.3) and consume both small and large zooplankton prey. An important

example of a jellyfish species that benefits on eutrophication by utilizing microplanktonic food is *Aurelia aurita* (Purcell et al., 2007).

1.2.1.3 Aquaculture

Falkenhaug (2014) states that cage aquaculture enhances eutrophication by increasing the availability of hard substrate on which benthic polyps may proliferate. These cages, together with other artificial structures such as ships, piers, docks, wind turbines, buoys and garbage may be an important driver for jellyfish blooms. In the Western Baltic Sea for example, the installation of 830 wind turbines with a diameter of six meter can potentially lead to a release of 4.64 billion *Aurelia aurita* ephyrae per year in the upper ten meter of the water column, which confirms that offshore wind farms have a potential to significantly increase the abundance of (scyphozoan) polyps (Janßen et al., 2013). In the Kagoshima Bay (Japan), *Aurelia aurita* polyps were found in patches on the undersurface of buoys and floating piers, but not on the bottom of ships, indicating that there may be substratum selection by the polyps. On the polystyrene piers, densities of up to 18.5 polyps/cm² were found (Miyake et al., 2002). Polyps prefer dark, sheltered areas (**Figure 1-12A**). Artificial substrates in harbors can act as nurseries, releasing great amounts of ephyrae which eventually grow into adult medusae (Duarte et al., 2013). Studies confirm that medusa densities decline when artificial substrate is removed (Duarte et al., 2013). Purcell et al. (2007) studied the effects of aquaculture on an *Aurelia aurita* population in the Tapong Bay in Taiwan. The jellyfish were abundantly present between 1999 and 2002 but completely vanished when the culture rafts (which contained fish and oysters) were removed in 2003 (**Figure 1-12B**).

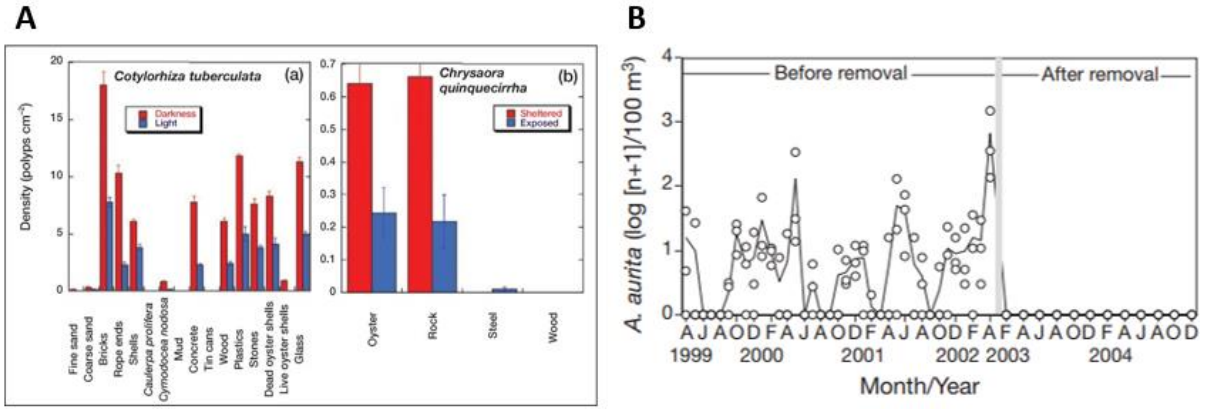

***Figure 1-12** (**A**) Jellyfish planula settlement on different kinds of substrate for two species: (a) Cotylorhiza tuberculata from the Mediterranean Sea and (b) Chrysaora quinquecirrha from Chesapeake Bay (USA) (Duarte et al, 2013). (**B**) Abundance of Aurelia aurita before and after removal of the aquaculture cages in the Tapong Bay in Taiwan (Purcell et al, 2007).*

In addition to acting as substrate for polyps, aquaculture also provides additional feed, which can lead to eutrophication (see section 1.2.1.2). Additionally, forage fish (e.g., anchovies, sardines and menhaden) are harvested for fish meal and used as aquaculture feed, leading to a reduction of zooplanktivorous fish (see section 1.2.1.1). Finally, in Asian countries, edible jellyfish (e.g., *Rhopilema esculentum*) are introduced into the ocean in high quantities: one hundred million per year in China, with similar programs running in Malaysia. These introductions undoubtedly come with unstudied ecological repercussions (Purcell et al., 2007).

1.2.1.4 Global warming

Global warming affects the distribution and growth of medusea (Dong et al., 2010). Due to warmer waters, species of warm water affinity (e.g., *Rhopilema nomadica*) and temperate affinity (e.g., *Mnemiopsis leidyi*) increase in abundance and expand their natural ranges (Falkenhaug, 2014). This is also confirmed by Purcell et al. (2007), who state that densities of 18 out of 24 studied moderate-temperature species increase with higher temperatures and that the distribution of GZ may also expand polewards (e.g., *Mnemiopsis leidyi*). A selection of species occurring in the North Sea and Mediterranean Sea is visualized in **Table 2**.

Table 2 Analysis of long-term records of Cnidaria and Ctenophora and their responses to ocean warming in the Mediterranean and North Sea. Early/ long: change in seasonal timing and duration, respectively; More/Less: increase/decrease in abundance (Purcell et al., 2007).

Species	Location	Response to warming	Source
Cnidaria			
Pelagia noctiluca	Mediterranean Sea	More	Goy et al. (1989)
Aurelia aurita	North Sea	Less	Lynam et al. (2004)
Cyanea capillata			
Cyanea lamarckii			
Liriope tetraphylla	Mediterranean Sea	More	Buecher et al. (1997); Molinero et al. (2005)
Rhopalonema velatum	Mediterranean Sea	More	Molinero et al. (2005)
Solmundella bitentaculata	Mediterranean Sea	More	Molinero et al. (2005)
Aglantha digitale	North Sea	Early, long	Greve et al. (2001)
Bougainvillia sp.			
Leuckartiara octona			
Obelia sp.			
Clytia hemisphaerica			
Chelophyes appendiculata	Mediterranean Sea	More	Buecher (1999)
Abylopsis tetragona			
Ctenophora			
Pleurobrachia pileus	North Sea	Early, long	Greve et al. (2001)
Beroe sp.			
Pleurobrachia rhodopis	Mediterranean Sea	Less	Molinero et al. (2005)

Lynam et al. (2004) state that *A. aurita*, *C. lamarckii* and *C. capillata* are negatively correlated to ocean warming in the North Sea (**Table 2**). With the currently positive winter North Atlantic Oscillation Index (NAOI), warm western air blows towards northern Europe, resulting in warmer winters and thus relatively warmer water temperatures in the North Sea. They associate a high (positive) NAOI with stronger winds and waves on one hand, and lower water inflow from Norwegian waters on the other hand, both leading to lower ephyrae development. This implies that cooler, calmer conditions during winter and spring (negative/low NAOI) positively affect the abundance of the three species (Lynam et al., 2004). These findings are sharply contradicted by Attrill et al. (2007), who demonstrated an increasing rather than decreasing trend between NAOI and jellyfish frequency due to the positive relation between jellyfish and Atlantic inflow. An increased Atlantic inflow results in more favorable conditions for jellyfish and/or actively introduces jellyfish into the North Sea. They state that Lynam et al. (2004) removed observations from 1983 (where a high jellyfish abundance was seen together with a high NAOI) in order to produce a significant negative trend. The impact of NAOI and Atlantic inflow into the North Sea on the standardized jellyfish frequency is illustrated in **Figure 1-13a** and **Figure 1-13b**, respectively.

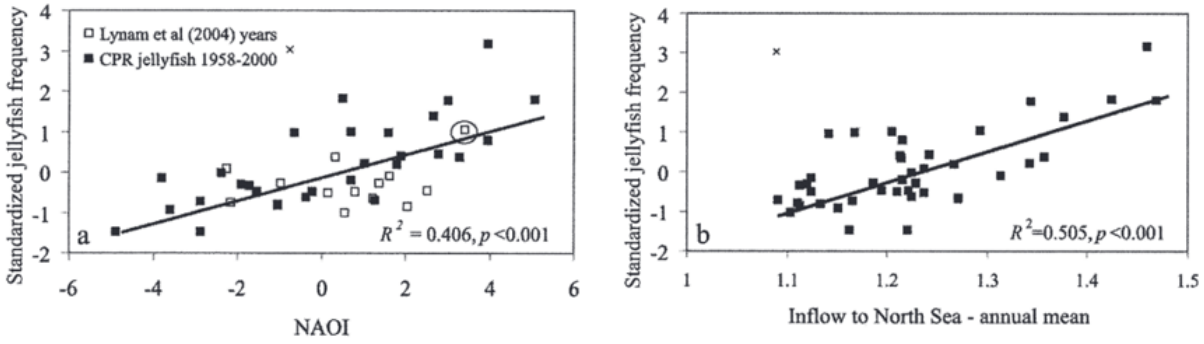

*Figure 1-13 Relationship between standardized jellyfish frequency and (**a**) NAOI, (**b**) Atlantic inflow for the west-central North Sea (Attrill et al., 2007).*

Supporting Attrill et al. (2007), Holst (2012a) examined the influence of the water temperature in winter on strobilation in the North Sea for the common species *Aurelia aurita*, *Cyanea lamarckii*, *Chrysaora hyscoscella* and *Cyanea capillata*. When the current winter temperature of 5°C is elevated to 10°C, several positive effects on strobilation are seen. For *A. aurita*, *C. lamarckii* and *C. hyscoscella*, more ephyrae per polyp are produced and/or the strobilation period extends. For *C. capillata* however, warmer winter temperatures diminish strobilation. In general, warmer winter temperatures benefit *A. aurita* and probably ensures the expansion of *C. lamarckii* and *C. hyscoscella* to the north, while negatively impacting the cold-water species *C. capillata*. (Lynam et al., 2004).

1.2.1.5 Transport of non-indigenous species (NIS)

Introduction of non-indigenous species (NIS) and the widening of their natural area forms a hazard. NIS did not co-evolve with the prey and predator of their penetrated habitat, leading to them disrupting the normal functioning of the ecosystem, taking away the resources of the indigenous fish. An important example is *Mnemiopsis leidyi*, which was introduced in the Black Sea by ballast water and resulted in a sharp decline of the fish stocks (Falkenhaug, 2014). Besides ballast water, also aquarium trades may sporadically cause the introduction of NIS (Purcell et al., 2007). Since 2007, *Mnemiopsis leidyi* is also seen in the North Sea. This introduction seems to be separate from the one in the Black Sea and is now spreading towards the Baltic Sea. Other introductions of NIS were e.g., *Rhopilema nomadica*, *Cassiopea andromeda* and *Phyllorhiza punctata* in the Mediterranean Sea (Purcell et al., 2007).

1.2.2 Ecological and societal impact of jellyfish blooms

Jellyfish blooms can have disastrous consequences for both the industry and the community. Due to their competition with fish, blooms may lead to reduced fishery production (see section 1.2.1.1). In the last decennia, a sharp increase in the amount of jellyfish-related problems considering stinging, fisheries and power stations is noticed in e.g., Japan (**Figure 1-14**).

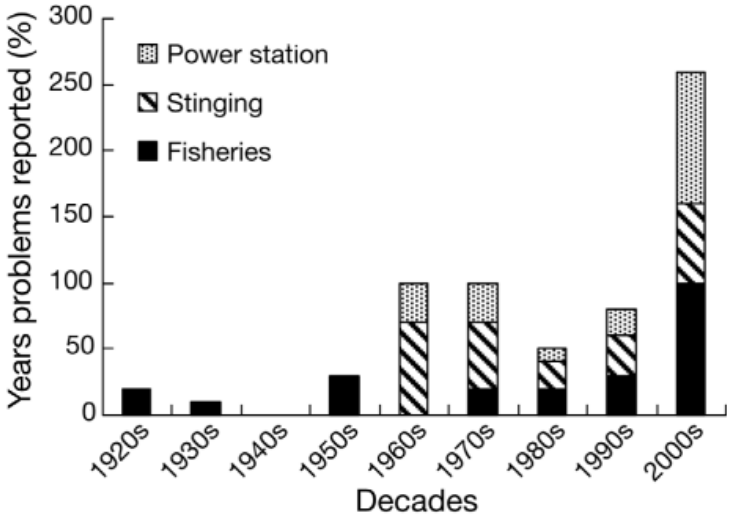

Figure 1-14 *Development of reported jellyfish-related problems throughout the decades in Japan (Purcell et al., 2007).*

1.2.2.1 Stinging

Swimmers get stung by jellyfish, resulting in a decrease in coastal tourism. Every year, an estimated 150 million jellyfish stings take place. One percent of the taxa from the phylum Cnidaria is recognized as a threat to human health (around 100 species), mainly due to stings from species belonging to the classes Scyphozoa, Cubozoa and Hydrozoa (Cegolon et al., 2013; Montgomery et al., 2016). In addition to swimmers, jellyfish also pose a stinging hazard to fishermen and divers (Purcell et al., 2007).

Reactions on stings may vary from pain and itching to more serious complications when venom enters the body. Gastrointestinal manifestations are mainly induced by *Physalia physalis* and *Pelagiidae* sp., while muscular, cardiac and

neurological manifestations are often linked to *Physalia* sp. and cubozoan species (Cegolon et al., 2013). The venoms are complex and can comprise proteinaceous cell membrane pores that form e.g., neurotoxic peptides, bioactive lipids, histamine, kinins and dermonecrotic toxins (Lakkis et al., 2015). In extreme cases, stings can be fatal (e.g., stings from *Chironex fleckeri*). Stings can also result in death if an allergic response appears or when the victim has prior health concerns (Montgomery et al., 2016). In Europe, stinging from *Cyanea capillata* and *Physalia physalis* have resulted in the death of stung victims (Montgomery et al., 2016).

Stinging is observed worldwide. In some Pacific areas, reports of up to 800 stinging events per day per beach are common (Cegolon et al., 2013). In 2003, thousands of severe stings from *Chiropsalmus quadrumanus* were reported at the Atlantic coastline of Florida (Fenner, 2005). Between 2010 and 2011, Surf Life Saving Australia reported 40,000 marine sting emergencies in the country, an increase of 30% compared to the year before. Between 2000 and 2010, stinging of *Chrironex fleckeri* caused more than 70 deaths in Australia (Li et al., 2013). For the BPNS, no articles considering dramatic encounters with jellyfish have been published so far (Vandendriessche et al., 2016).

With increased stinging, people cancel their reservations or reduce the length of their stay in coastal areas, resulting in less revenue from tourism (Falkenhaug, 2014). When comparing a beach with five jellyfish stranding events per week to a beach with one to two stranding events per week at the Catalonian coast, individual beach users are willing to pay 3.2 Euro extra to visit the latter one. For the whole of Catalonia, this is equivalent to 423 million Euro/year (Tomlinson et al., 2018). Similarly, in the Gulf of Lion (Mediterranean Sea), households are willing to pay 66 Euro to reduce yearly expected jellyfish outbreaks from nine years per decade to one year per decade and in Israel, fewer seaside visits due to jellyfish outbreaks could cause an annual loss of 1.8 - 6.2 million Euro (Tomlinson et al., 2018).

1.2.2.2 Coastal industry

Industrial installations (e.g., coastal power plants delivering cooling water) may get clogged with medusae during a bloom and stop functioning the way they should, resulting in financial losses (Dong et al., 2010). This leads to the plant being shut down for a long time, since the pipes need to be cleaned. Reports of power stations that are affected by jellyfish blooms come from all over the world: e.g., Japan, Philippines, Qatar and USA have to deal with this issue (Falkenhaug, 2014). In Korea for example, the clogging of the filtration systems by jellyfish can cause annual damages of up to 205 million US dollars, while a nuclear power station in Ontario (USA) can face costs of up to two million US dollars per day due to jellyfish abundance (Mcilwaine & Rivas Casado, 2021). A temporary shutdown of the Madras Atomic Power Station in the Bay of Bengal (Indian Ocean) during 1995-1996 lead to revenue losses of around 5.5 million Indian Rupees (around 63,000 Euro) per day (Baliarsingh et al., 2020).

1.2.2.3 Fisheries and aquaculture

Evidence shows that declines of fisheries are associated with the increase of jellyfish blooms. Besides the competition between both (see section 1.1), jellyfish may also clog fishing nets, leading to practical issues on fishing boats: there is no place left in the nets for actual fish, leading to a lower catch. In extreme cases, GZ may even tear and ruin the fishing nets due to the high weight of all the caught medusae. An additional problem is that fisheries refuse to receive the catch when the jellyfish by-catch exceeds 40% of the total weight (Bosch-Belmar et al., 2020).

In the Northern part of the East China Sea and the Yellow Sea, the annual fish catch declined 64% between 2000 and 2003, while the catch of the scyphozoan *Nemopilema nomurai* increased 250% in this period (Dong et al., 2010). Between 2005 and 2006, this species was responsible for an economic loss of ca. 270 million US dollars in the fishery industry of Japan, while in Korea, the annual damage caused by jellyfish in general was estimated between 68.2 and 204.6 million US dollars (Bosch-Belmar et al., 2020). In the Gulf of Mexico, economic losses caused by the interference of *Phylloriza punctata* on the shrimp industry in the year 2000 were estimated to be ten million US dollars whereas lower fish catches resulted in a loss of 9.7 million US dollars per year in the Italian Northern Adriatic Sea (Bosch-Belmar et al., 2020).

Both small and large jellyfish can kill fish in aquaculture pens by penetrating into the cages as a whole or via their tentacles, respectively. By doing so, the fish gills get irritated, resulting in hemorrhage and suffocation (Purcell et al., 2007). In Ireland, complex gill disorders are one of the most serious causes of mortality in marine farmed salmon, leading to an average annual loss of 12%. Similarly, economic losses of up to 1.3 million US dollars are observed in Irish and Scottish salmon aquaculture, which is mainly linked with invasions of *Pelagia noctiluca* (Bosch-Belmar et al., 2020).

1.2.2.4 Positive impacts of jellyfish blooms

Up to a given level, jellyfish blooms may also impose positive impacts: e.g., new products for food and medicine can be developed (Dong et al., 2010). In the Osaka Bay (Japan) for example, *Aurelia aurita* and *Chrysaora melanaster* were collected and used as fertilizer for vegetables (chingentsuai (a Chinese vegetable), green soybeans and perilla) (**Figure 1-15**). The two jellyfish species contain five principal components of fertilizers: nitrogen, phosphorus, potassium, magnesium and calcium, while also containing trace components (e.g., iron and manganese) that promote plant growth. Overall, both species were effective fertilizers for chingentsuai, while *Chrysaora melanaster* was also somewhat effective for perilla and green soybeans (Fukushi et al., 2003).

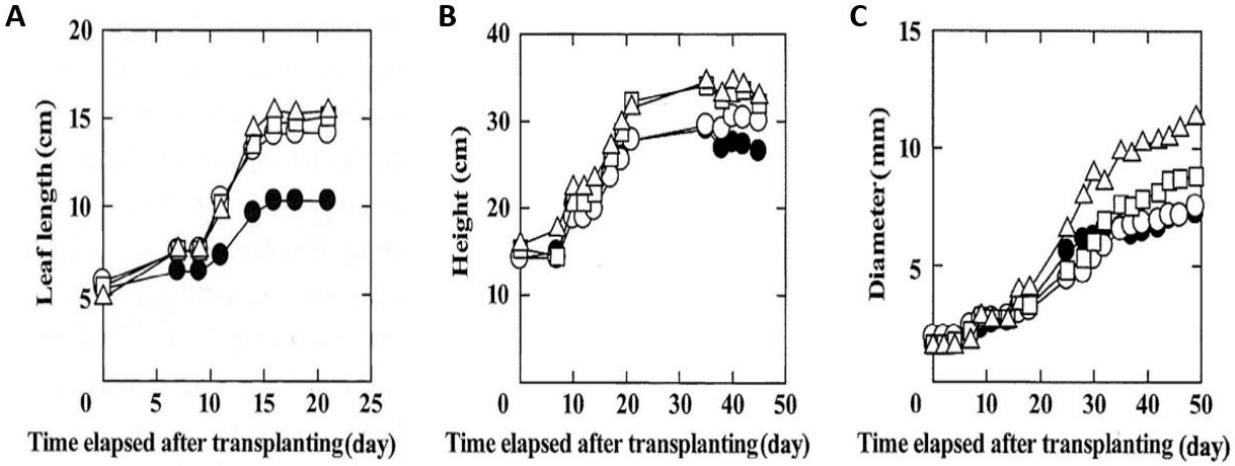

Figure 1-15 *Growth of vegetables using jellyfish as fertilizer in Japan. (**A**) chingentsuai, (**B**) green soybeans, (**C**) perilla. Open circles = Aurelia aurita fertilizer, squares = chrysaora melanaster fertilizer, triangles = chemical fertilizer, solid circles = no fertilizer (Fukushi et al., 2003).*

Jellyfish also have potential in terms of biodiscovery as they contain bioactive compounds. An important compound found in *Aequorea victoria* is the green fluorescent protein (GFP), which has led to a revolution in biotechnology (Purcell et al., 2007) and is extensively used for cellular research and medical diagnosis (Graham et al., 2014). Some jellyfish toxins contain anti-cancer compounds (e.g., the species *Chrysaora quinquecirrha*) and antioxidant nutritional supplements (e.g., the species *Rhopilema esculentum*). The collagen of jellyfish may have disease-modifying effects on osteoarthritis and box jellyfish help in understanding the neurobiology and evolution of vision (due to their complex eyes, see section 1.1.1.2.3) (Graham et al., 2014). *Physalia physalis* provided the basis for understanding anaphylaxis (a severe, life-threatening allergic reaction). This was done in the beginning of the 20th century by Charles. R. Richet, a physiology professor at the University of Paris, who studied the venom of *P. physalis* by performing animal trials. In 1913, he was awarded The Nobel Prize for Physiology or Medicine (AKlompen, 2019).

Mainly in Asia, jellyfish are used as a food source. *Rhopilema esculentum* for example, is a popular food in China and aquaculture releases millions of ephyrae into the water annually. In addition, GZ can positively influence fish populations by preventing the monopolization of overly successful fish species which come at the expense of other fish. Weak individuals are also removed by jellyfish, keeping fish stocks healthy. Some juvenile fish species seek shelter between the tentacles of large jellyfish i.e., *Rhizostoma pulmo* and *Cotylorhiza tuberculata* (Falkenhaug, 2014). This was also confirmed by Lynam & Brierley (2007), where significant positive correlations were observed between the survival of whiting (*Merlangius merlangus*) and the abundance of jellyfish (*Cyanea* sp.) in the North Sea. Considering these interactions, the economic value of jellyfish production in 2005 was estimated at 121 million US dollars worldwide (Purcell et al., 2007).

Jellyfish blooms may also induce a confined positive influence on tourism. In the Sea of Japan for example, SCUBA diving with the giant jellyfish *Nemopilema nomurai* attracted 10,000 - 15,000 divers in 2009 (Graham et al., 2014). In Palau (Micronesia), a jellyfish lake which contained swarms of up to 1.5 million *Mastigias* sp. in the mid-1980s, boosted the regional tourism with 500% between 1986 and 1997 (Dawson et al., 2001). Aquariums all over the world exhibit jellyfish and provide annual educational and recreational benefits to millions of people (Purcell et al., 2007).

As discussed above, both negative and positive impacts can be linked to jellyfish blooms. To some extent, jellyfish aggregations are a natural phenomenon (Dong et al., 2010; Falkenhaug, 2014). When jellyfish are naturally occurring, they can be linked with positive effects, which were described above. In contrast, a combination of large, long-lasting jellyfish blooms which are not coevolved with resident fish species (e.g., *Mnemiopsis leidyi*) and anthropogenic effects (e.g., overfishing) on these fish stocks induce a negative ecological impact (Falkenhaug, 2014). Overall, if jellyfish populations continue to rise in the future, their beneficial services will be outpaced by the costs that they induce (Graham et al., 2014). The question is whether this balance shifted already and if not, when it will.

1.2.2.5 Mitigation of negative impacts

In order to mitigate negative local effects of jellyfish blooms, certain measures can be taken. Coastal tourism can be maintained by installing an anti-jellyfish barrier (**Figure 1-16**). However, according to Falkenhaug (2014), when currents are relatively strong, jellyfish get smashed against this barrier and disperse as a stinging soup into the protected area. Vasslides et al. (2018) assessed the effects of a barrier net on jellyfish and other local fauna at the Brooklyn Avenue Beach (BAB) and the Windward Beach (WB) in 2011 and 2012 (both located in the USA). The anti-jellyfish barrier led to a mean daily reduction of jellyfish (expressed as catch per unit effort) within the barrier of 43.5% and 27.5% at BAB and WB, respectively. In 2012, these percentages were 57.7% and 60.4%. Fish entanglement was limited (<0.5 fish per net). Since 2014-2015, barrier nets are placed within the Mediterranean Sea (e.g., in Spain, Italy and Malta), while also Australia and the USA are starting to use them more frequently (Vasslides et al., 2018). anti-jellyfish barrier (Jelly Fish Nets, 2014).

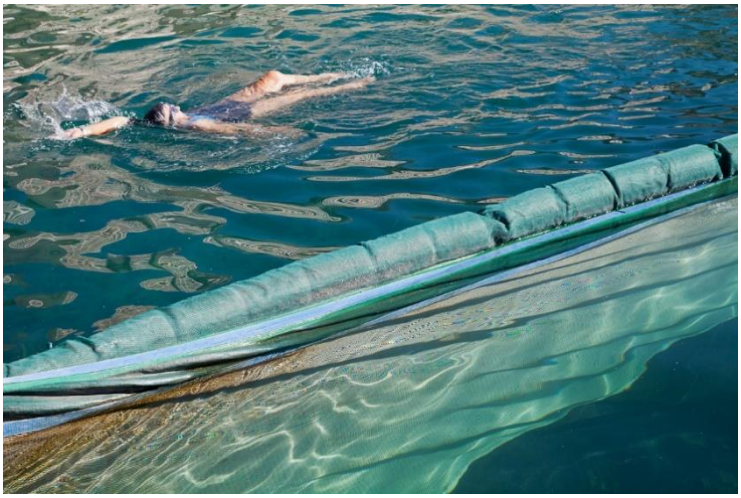

Figure 1-16 *Anti-jellyfish barrier (Jelly Fish Nets, 2014).*

Clogging of coastal plants could be managed by the use of cutting nets at the inlet op pipes: jellyfish get physically destroyed into smaller pieces and do not clog the installation anymore. It is however uncertain if this approach works: the small pieces of medusae may lead to regeneration of new jellyfish via asexual reproduction and, since the fragments maintain their stinging properties, become even more lethal to e.g., surrounding aquaculture cages (Falkenhaug, 2014). At the Japanese shore, large numbers of jellyfish are collected mechanically (around 2,850 tons per year) at some power plants to avoid a decrease in power generation or shutdown (Fukushi et al., 2003). The development of an early warning system that alerts power stations about incoming jellyfish swarms would be economically and ecologically useful (Baliarsingh et al., 2020).

To reduce the abundance of jellyfish, the usage of chemicals should not be considered, since these affect the biodiversity in a negative way. Biocontrol can be an option, e.g., *Mnemiopsis leidyi* is predated by *Beroe ovata* in the Black Sea and by *Chrysaora quinquecirrha* in the Chesapeake Bay (USA) (Falkenhaug, 2014; Purcell et al., 2007). However, care should be taken that the introduced species does not become an issue itself (Falkenhaug, 2014). Since artificial structures can act as

nurseries for polyps, changes in design and surface characteristics may be beneficial, as well as regulating garbage disposal, which can function as substrate (Duarte et al., 2013). The transport of non-indigenous species should also be limited by controlling e.g., ballast water of ships (Falkenhaug, 2014).

To diminish the frequency at which jellyfish blooms occur, changes have to be made which act directly on the causes of these blooms. Reducing nutrient pollution (eutrophication), overfishing, transport of NIS, the amount of artificial substrate and global warming are steps in the right direction. One should note that the ecosystem will respond slow towards these changes and that they come with a significant economic cost in the short-medium term (Dong et al., 2010). Besides that, a global cooperation is needed to tackle the problem of jellification which ultimately results from changes in the benthopelagic food web.

1.2.3 Evolution of jellyfish blooms

The occurrence and frequency of jellyfish blooms depends both on the geographical location and the time. Blooms are not evenly distributed around the world and seasonality plays an important role. The next two sections are focused on both temporal- and spatial patterns.

1.2.3.1 Temporal patterns

Barz & Hirche (2007) studied the abundance, distribution and prey composition of *Cyanea lamarckii*, *C. capillata*, *Aurelia aurita* and *Chrysaora hysoscella* in the Southern North Sea. Three different temporal patterns were observed (**Figure 1-17A**). Firstly, *C. lamarckii* occurs early (February-August). Secondly, *C. capillata* and *A. aurita* are seen from April-August and lastly, *C. hysoscella* only appears late throughout the year (August-September). The latter can be explained by the fact that the polyps require warm waters to initiate strobilation. As was already discussed in section 1.2.1, most cnidarians are observed between May and August in the North Sea (Lynam et al., 2011). This matches the findings of Barz & Hirche (2007).

Doyle et al. (2007) examined the stranding events of five different medusa jellyfish species across the Irish and Keltic Seas (**Figure 1-17B**). *C. hysoscella* and *C. lamarckii* have a niche period where medusae are present, while *Rhizostoma octopus* and *A. aurita* are reported in bigger time frames throughout the year. The majority of stranding events is seen between June and July. *A. aurita, C. lamarckii* and *C. hysoscella* seem to strand consecutively in April, May and June (Doyle et al., 2007). A possible explanation for the later stranding of *C. capillata* compared to *A. aurita* is that the latter is a potential food source for *C. capillata* (Barz & Hirche, 2007).

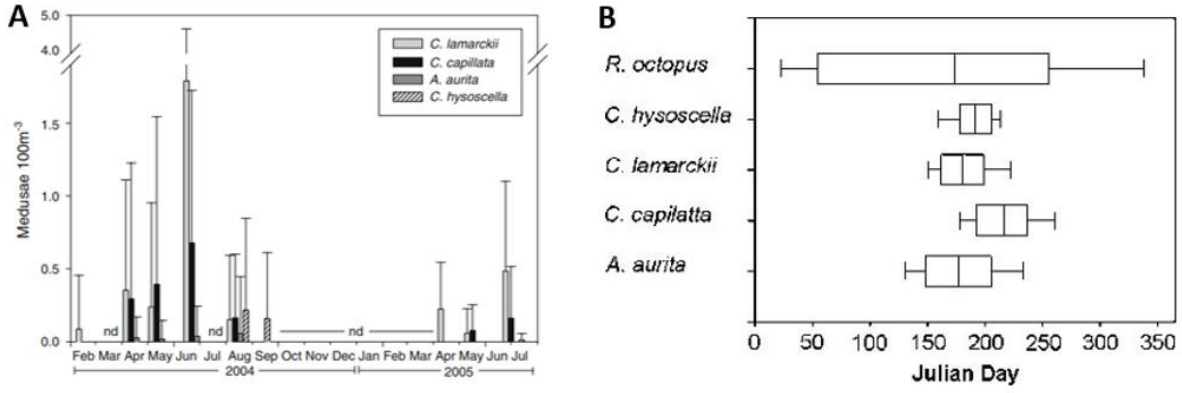

***Figure 1-17** (**A**) Abundance of Cyanea lamarckii, C. capillata, Aurelia aurita and Chrysaora hyscoscella in 2004 and 2005 in the Southern North Sea (Barz & Hirche, 2007). (**B**) Reported jellyfish stranding events throughout the year around the Irish and Keltic Seas (Doyle et al., 2007).*

The horizontal distribution of these species also differs through the seasons. *C. lamarckii* and *C. capillata* for example, showed an easterly distribution around April/May, which changed to a more western distribution by June. This is visualized for *C. capillata* in **Figure 1-18** (Barz & Hirche, 2007).

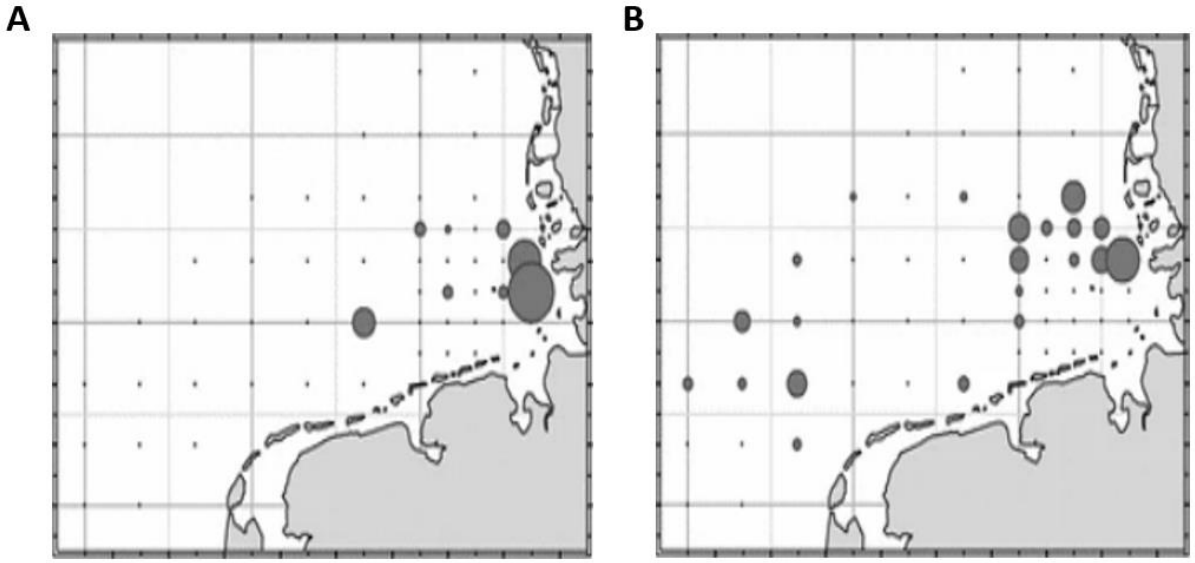

Figure 1-18 Distribution of Cyanea capillata in May (A) and June (B) in the Southern North Sea (part of the Dutch, German and Danish coast) (Barz & Hirche, 2007).

1.2.3.2 Spatial patterns

The spatial distribution differs among jellyfish species and is dependent on several water parameters. The distribution of *Chrysaora plocamia* in the Northern Humboldt Upwelling System (Pacific coast of South America) for example, is strongly temperature dependent (See **Figure 1-19**).

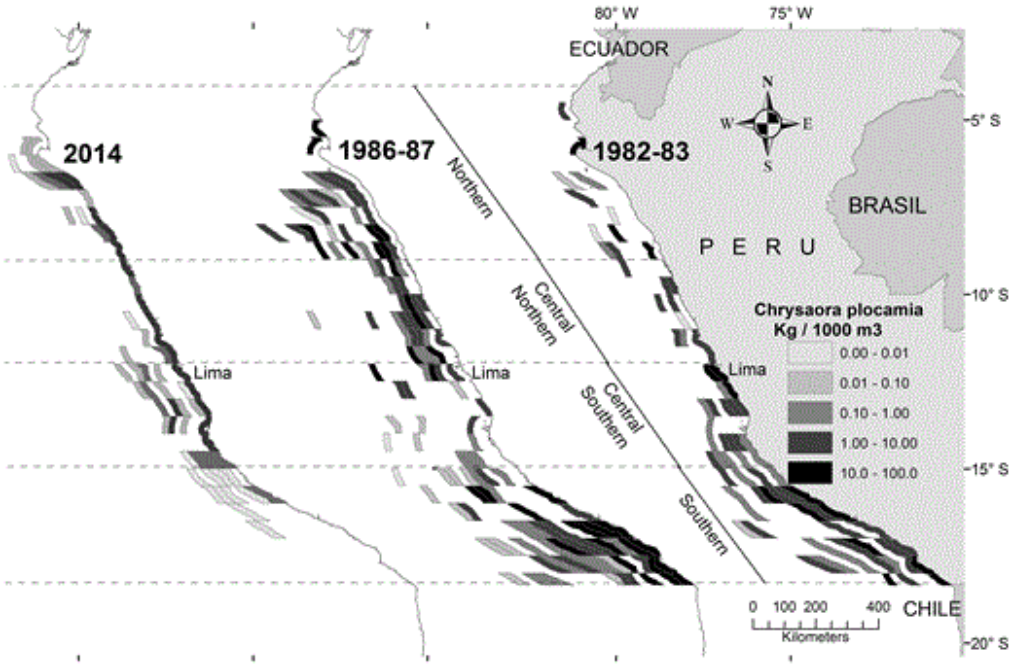

Figure 1-19 Spatial distribution of Chrysaora plocamia in the Northern Humboldt Upwelling System (Quiñones et al, 2018).

During warm El Nino years (1982 - 1983 and 1986 - 1987), the species is more widely distributed than during a neutral, colder year (2014). In 1982 - 1983, individuals were seen up to 185 km from the coast. In 1986 - 1987, this distance increased to 280 km. In a neutral, colder year (2014), the medusae were mainly distributed closely constrained to the coast. Distribution of species is temperature dependent. Besides elevating the sea surface temperature, El Nino effects also deepen the thermocline, which prevents the upwelling of cold, nutrient-rich waters. Because of this, flagellate species (which are seen as a major prey of jellyfish) increase, since they are less selective feeders than diatoms and cope better with low nutrient concentrations. This leads to a higher jellyfish abundance (Quiñones et al., 2018).

Doyle et al. (2007) conclude that not only predominant current regimes play a role, but also physical boundaries (e.g., the Celtic Sea Front) and behavioral mechanisms (e.g., swimming) maintain the individuals in a certain place. The occurrence of jellyfish in a specific area is thus not entirely passive. The temperature dependency of the spatial distribution is visualized in **Figure 1-20**. In the warm southerly waters, *Chrysaora hysoscella* and *Cyanea lamarckii* were dominant, while in the far north, *Cyanea capillata* was observed in substantial numbers. *Aurelia aurita* was found both in colder and warmer waters (which confirms the results of Holst (2012a), see section 1.2.1.4). Extensive jellyfish aggregations of *Rhizostoma octopus* were mainly located at the mouth of three large estuarine bays (A, B, C on **Figure 1-20c**) (Doyle et al., 2007).

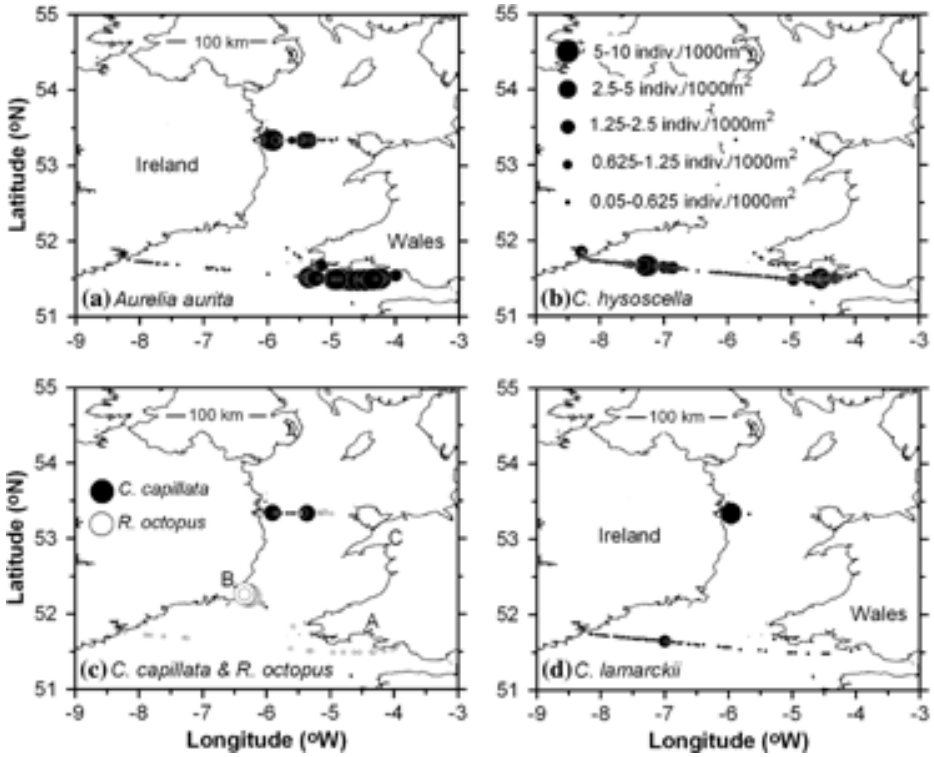

Figure 1-20 *Spatial Distribution of the five jellyfish species across the Irish and Celtic Seas. In (c), the letters A, B and C stand for three estuarine bays: (A) Carmarthen Bay, (B) Rosslare Harbor, (C) Tremadoc Bay (Doyle et al., 2007).*

1.2.3.3 Long-term projections of jellyfish blooms

With overfishing, eutrophication, aquaculture activities, global warming and the introduction of NIS increasing, jellyfish blooms are prone to become more frequent in the (near) future (Goffredo & Dubinsky, 2016). These causes are all interconnected: e.g., aquaculture provides additional feed, which enhances eutrophication. This feed is made of fish meal and thus enhances overfishing (Purcell et al., 2007). Overfishing leads to hypoxia, turbidity and nutrient release, reinforcing eutrophication and jellification (Daskalov et al., 2007; Purcell et al., 2007). Due to global warming, new species may expand increasingly polewards (e.g., *Mnemiopsis leidyi*), leading to additional introductions of NIS (Purcell et al., 2007).

In the North Sea, a more gelatinous future is expected as well (Attrill et al., 2007). The trends in jellyfish frequency between 1958 and 2000 are visualized in **Figure 1-21A**. It is important to note that not all species will benefit from warming (e.g., the cold-water species *C. capillata* will not) (Holst, 2012a). As was seen in section 1.2.1.4, Lynam et al. (2004) expects a decrease in abundance of *A. aurita*, *C. lamarckii* and *C. capillata* in the North Sea. This is contradicted by both Holst (2012a) and Attrill et al. (2007), which expect a more gelatinous future for the North Sea. Since the conclusions of Lynam et al. (2004) are based on outdated data (1971 - 1986) and data from 1983 was removed, the outcome of the other two studies is followed.

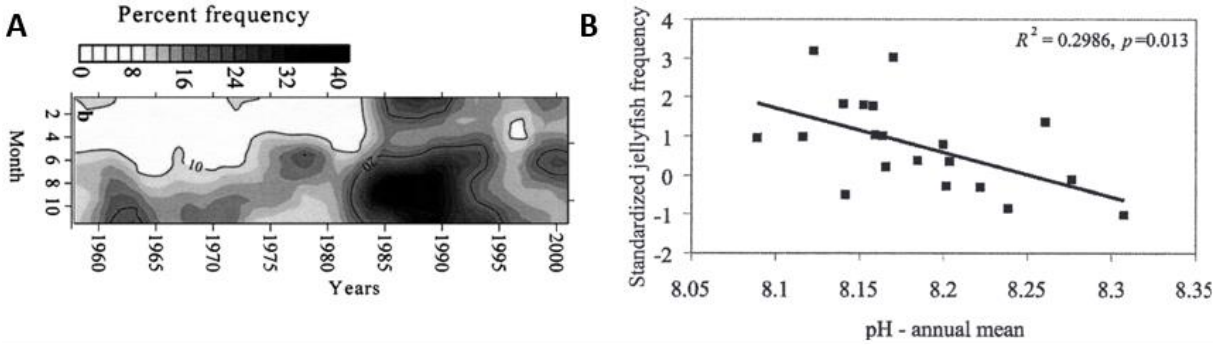

Figure 1-21 (A) Trends in jellyfish frequency, expressed in % occurrence since 1958: monthly averages for the whole North Sea region (Attrill et al., 2007). (B) Relationship between standardized jellyfish frequency and mean annual pH for the west-central North Sea (Attrill et al., 2007).

The pH is predicted to decrease in the next century due to rising CO_2 emissions. This could positively affect jellyfish abundances in the North Sea (**Figure 1-21B**): calcifying plankton is negatively impacted by (more) acidic conditions, leaving more ecological space for jellyfish to thrive (Attrill et al., 2007; Richardson et al., 2009). When analyzing a larger area than the North Sea, no significant relationship is found between acidity and jellyfish abundance. It is even stated that acidification can negatively impact jellyfish by affecting the calcium-rich statoliths which are essential for orientation. The relationship between jellyfish and pH still needs further studying in order to draw an unambiguous conclusion (Richardson et al., 2009).

1.3 Innovative ways to study jellyfish dynamics

As the abundance of jellyfish blooms is likely to increase in the future, it is of vital importance to investigate and monitor jellyfish dynamics. Innovative, pioneering methods are required to form a clear and accurate image of the future of jellyfish in the oceans.

1.3.1 Drift model

An innovative way to investigate jellyfish dynamics in the North Sea is the model created by Dulière et al. (2014), which estimates the drift of jellyfish as a function of water currents, waves and tides. It is possible to go both backward in time (starting point: stranding events, see **Figure 1-22A**) and forward in time (starting point: polyp locations, see **Figure 1-22B**). The model was applied on both *Aurelia aurita* and *Chrysaora hyscoscella* species, which stranded massively on May 25th 2013 and August 1st 2013, respectively. Based on the observed stranding events, the model simulated a four-week backtrack of the drift trajectory of *Aurelia aurita* (**Figure 1-22A**). In this figure, the green points indicate that the jellyfish came from the English Channel. Since the polyps of *Aurelia aurita* require hard substrate to colonize, the surrounding harbors in this channel are likely to be the possible locations of origin. Simulating back in time can be a useful tool to find polyp locations in the Southern North Sea.

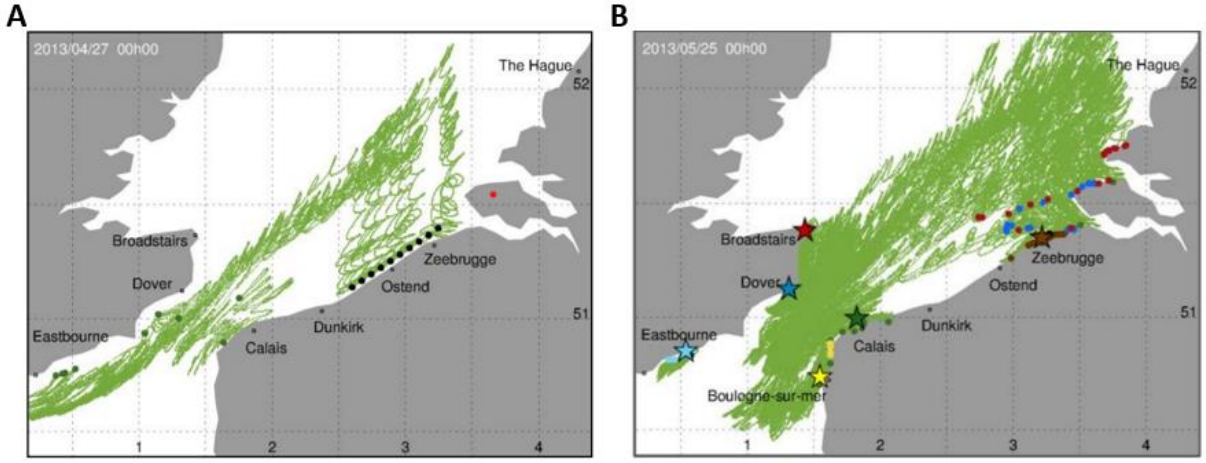

Figure 1-22 *Simulated drifting trajectory of Aurelia aurita in the North Sea. (**A**) 4-week backtrack. black dots = starting location (beaching location of jellyfish, 25/05/2013), green points = jellyfish location four weeks before stranding (27/04/2013). (**B**) 4-week forecast. Stars = harbors where jellyfish were virtually released (27/04/2013), points = jellyfish positions on 25/05/2013. The color of the points corresponds to the color of the harbor of origin. Green lines = drift trajectory (Dulière et al., 2014).*

By selecting a number of harbors (indicated as stars on **Figure 1-22B**) and virtually releasing jellyfish hourly (seen as particles in the model), their future drift can be computed. After four weeks of drifting, *Aurelia aurita* species end up in great numbers in front of the Belgian coast, which supports the stranding events and thus indicates that the model works. Simulating forward in time could help in the prediction and timing of future jellyfish blooms in the North Sea.

As with every model, assumptions have to be made. Here, it is assumed that jellyfish drift passively through the water, just below the sea surface: swimming behavior is thus neglected in **Figure 1-22**. The vertical position of jellyfish is however very important: jellyfish released at the water surface are more influenced by tides, waves and water currents than jellyfish released close to the sea bottom. Because of this, two jellyfish that were released at the same location but at a different depth can be distanced more than 100 km away from each other in less than one week time (**Figure 1-23**). Other model uncertainties rely upon the hydro-meteorological conditions (provided by operational forecast models at the UK Met Office and RBINS) and on the initial conditions.

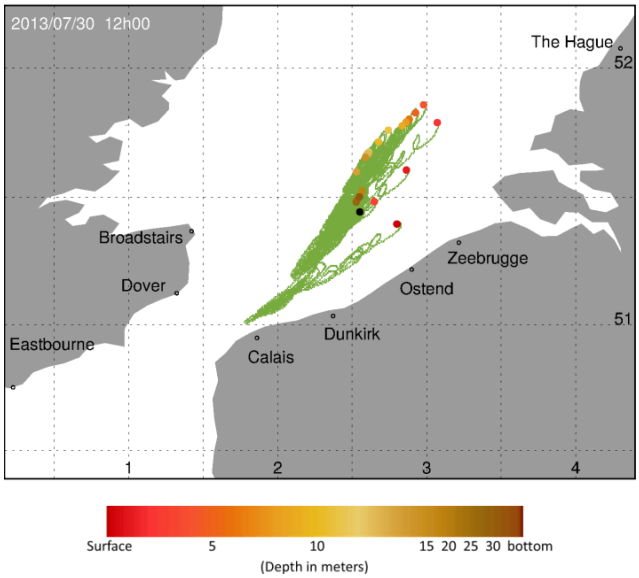

Figure 1-23 Differences in drift trajectory of Chrysaora hysoscella by releasing the species at different depths in the North Sea. black point = point of release (15/07/2013), filled circles = jellyfish positions at 15, 20, 25 and 30/07/2013, light green = simulated drift trajectory. The colors refer to different depths of release (see color bar) (Dulière et al., 2014).

Dekker et al. (2016) studied the influence of swimming behavior on the drift trajectory, based on the model created by Dulière et al. (2014). Four scenarios and their corresponding effect on swimming behavior are visualized in **Figure 1-24**. When including swimming behavior, the no-swimming behavior travel distance can be reduced by ± 25% for scenario 1 and 2, and ± 50% for scenario 3 and 4. Swimming behavior thus has a significant impact and should not be neglected.

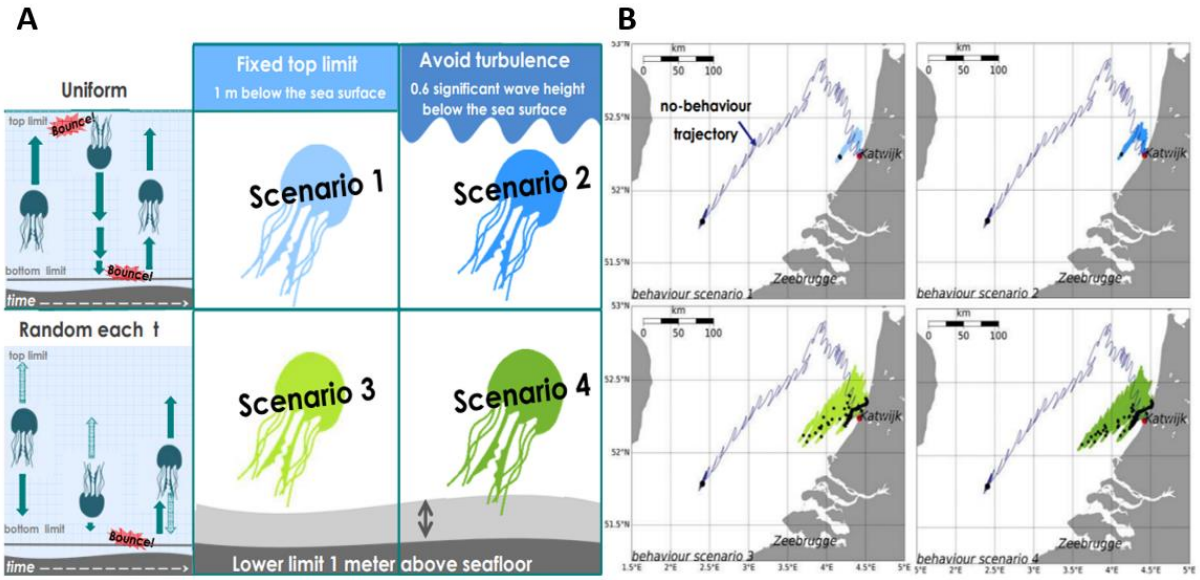

Figure 1-24 (A) four different swimming scenarios. (B) Estimated jellyfish trajectories dependent on the swimming scenario: 18 days backtrack. red point = starting point (25/05/2013), black points = simulated final position of jellyfish after 18 days backtrack (07/05/2013), dark blue point = simulated jellyfish location on 07/05/2015 if swimming behavior is neglected (Dekker et al., 2016).

1.3.2 Other monitoring techniques

Jellyfish can be monitored using different techniques. Invasive methods such as catching medusa in trawls and nets might be the most straightforward and are executed in several studies involving the North Sea (Lynam et al., 2005; Lynam & Brierley, 2007; van Walraven et al., 2016). This technique is not optimal, since GZ are very fragile and are easily damaged by any kind of net. The possibly shattered remains are often unidentifiable and can lead to wrong results (e.g., the underestimation of the effective abundance) (Båmstedt et al., 2003). Another obvious detection method are shoreline surveys, which focus on stranding data (Fleming et al., 2013).

More advanced technologies make use of e.g., satellites, light aircrafts and unmanned aerial vehicles (UAV). The use of imaging satellites however, is not suited for jellyfish monitoring due to the relative low resolution, imaging challenges considering water vapor and the time it takes to orbit and access data (Mcilwaine & Rivas Casado, 2021). Aerial surveys can be used to study gelatinous aggregations beyond the range of conventional ship-based techniques since bigger areas (e.g., thousands of square kilometers in the Irish Sea) are studied at a rapid pace and technological advances such as a LIDAR system (Light Detection And Ranging) make it possible to gather data from beneath the surface (up to a few meters deep). Nevertheless, these surveys are only suitable for relatively large medusae which are not too transparent and aggregate in the upper few meters of the water column (Houghton et al., 2006). Schaub et al. (2018) compared the percent cover estimates by UAVs with net haul densities. Data from both techniques were highly comparable for all aggregations, demonstrating the potential of UAVs as a powerful tool to study jellyfish aggregations *in situ*.

Since 1946, a Continuous Plankton Recorder (CPR) is used to collect jellyfish data in the North Atlantic and the North Sea. This device is towed monthly behind different merchant ships on regular routes at a standard depth of 6.5 m, providing consistent biological and environmental data over both months and years (Attrill et al., 2007). Until recently, underwater video observations were analyzed by human observers, resulting in a time-consuming and financially costly technique (Martin-Abadal et al., 2020). By using a deep object detection neural network, automatic detection and quantification of different jellyfish species is possible. This form of artificial intelligence, using real-time processed video sequences, correctly quantifies the number and class of jellyfish in up to 93.8% of the time. This innovative technique can provide a fast, cost-effective and efficient way to monitor jellyfish and may be used to develop e.g., a jellyfish early-warning system, reducing the impact on e.g., coastal power plants and tourism (Martin-Abadal et al., 2020). Besides a normal camera, one could also make use of sonar imagery. This acoustic technique has a higher usability in deeper areas (where light is absent) than a normal camera, but suffers from a lower resolution and/or grey-scale coloring, which may complicate the detection task (Martin-Abadal et al., 2020). Båmstedt et al. (2003) state that a Remotely Operated Vehicle (ROV), which is equipped with a scanning sonar and a video camera, provides the most accurate data on total abundance and depth distribution of large-sized medusae.

Polyps are usually detected using both visual and photographic surveys that are carried out by divers (Duarte et al., 2013; van Walraven et al., 2016). Since *in situ* species identification is impossible, polyp aggregations are collected and raised in the lab until ephyrae grow into young medusae, which can then be identified (Duarte et al., 2013).

Besides morphological processing, one could also make use of molecular tools such as metabarcoding. Bucklin et al. (2016) defines this technique as the large-scale taxonomic identification of samples by analyzing one or more DNA regions, which are called barcodes. This is done by high-throughput sequencing (HTS), yielding millions of DNA sequences and allowing large-scale analysis. The used DNA can be either intracellular (extracted from the sample) or extracellular (environmental DNA) (Bucklin et al., 2016). Metabarcoding has the significant advantage of detecting the "hidden diversity" of communities and has promising applications in e.g., detecting non-indigenous species, studying impacts of climate change and monitoring the health of ecosystems (Bucklin et al., 2016; Semmouri et al., 2021).

Environmental DNA (eDNA) are traces of DNA which can be retrieved from e.g., mucus, skin cells, feces, gametes and organelles and are sampled from sea- and freshwater, soil, air, sediment, ice or permafrost (Deiner et al., 2017). Some of the advantages of working with eDNA instead of intracellular DNA in metabarcoding is that the technique is noninvasive and cost-effective. Care should however be taken to reduce false negatives, false positives and bio-informatic errors (Miya, 2022). In Feng et al. (2022), two different barcodes are used: cytochrome oxidase I (COI) and small subunit ribosomal RNA genes (18S). A comparison between eDNA barcoding and morphological processing is illustrated in **Figure 1-25**: eDNA (both COI and 18S) reveal a higher richness at phylum, class and order level, while 18S also reveals a higher number of unique taxa at family level. The richness at genus and species level is lower when using eDNA metabarcoding. In total, compared

to visual assessment (based on net sampling), seven more orders were identified using eDNA metabarcoding and two to four times more medusae taxa were displayed (Feng et al., 2022).

Semmouri et al. (2021) studied the composition of the zooplankton community in the BPNS using both a DNA metabarcoding approach and a traditional, morphological approach. Using metabarcoding, taxa were detected with a higher resolution: 10 - 33 taxa were identified using DNA metabarcoding, compared to 8 - 14 taxa using morphological observations.

Metabarcoding can be seen as an effective, efficient tool for the study and monitoring of (gelatinous) zooplankton diversity. This was also confirmed by Deiner et al. (2017), who stated that eDNA metabarcoding can sample a greater diversity and increase the resolution of taxonomic identifications, compared to conventional methods. Additionally, this technique causes less disturbance to the marine environment and is less laborious than e.g., catching medusae in nets (Ames et al., 2021; Takasu et al., 2019). One should however note that the rate at which eDNA is produced, the transport of this eDNA and the fate in time is species dependent. In some cases, this may lead to inconsistent results relative to the species' true local abundance (Deiner et al., 2017). Semmouri et al. (2021) conclude that if the focus solely lies on identifying dominant taxa, metabarcoding is preferred over morphological techniques, while a complementary approach of metabarcoding and morphological techniques is recommended if one wants to identify as many taxa as possible at the highest resolution.

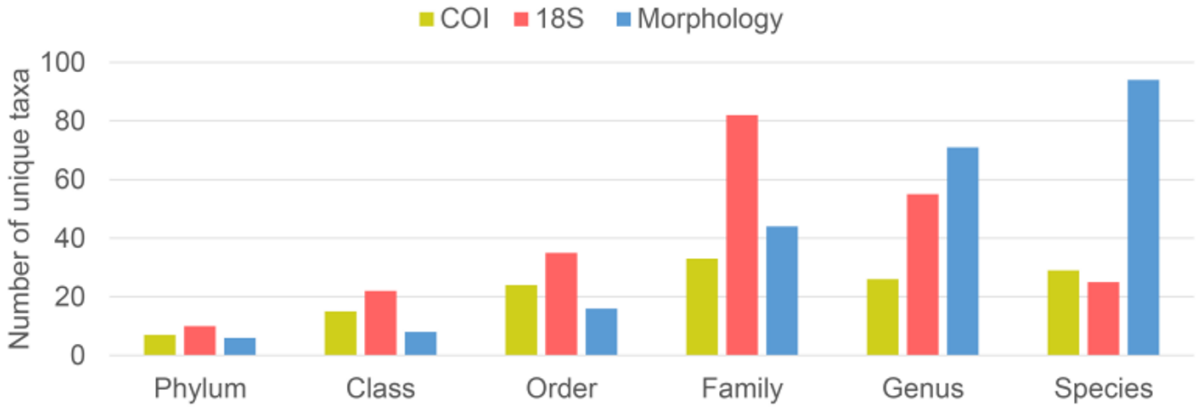

Figure 1-25 Number of mesozooplankton taxa per taxonomic level using eDNA barcoding (COI and 18S) and morphology (Feng et al., 2022).

The sequencing is usually done in the lab, leading to a significant delay between sample collection and interpretation of the results (Ames et al., 2021). To avoid this, Ames et al. (2021) developed a fieldable eDNA sequencing kit, which makes sequencing possible on site by utilizing the field-deployable, battery-powered MinION sequencing platform of Oxford Nanopore Technologies (ONT).

2 Objective of the study

Jellification is supposedly becoming a major issue in our oceans and seas. The sudden proliferation of jellyfish abundance can have disastrous consequences for the industry, tourism and the aquatic food web. Little is however known about whether these so called jellyfish blooms in the North Sea are present and if they occur regularly.

In this thesis, therefore, the presence of jellyfish at different locations and times in the Belgian Part of the North Sea (BPNS) is investigated. Additionally, by extracting eDNA from seawater samples and performing metabarcoding, we aim to get first insights in the distribution patterns of the gelatinous zooplankton in the North Sea. We will compare these observations with abiotic factors (pH, water temperature, turbidity etc.) and other biotic factors in order to try to explain the observed spatial and temporal patterns. We will assess which species can be found on the basis of eDNA and in what life stage (larvae, polyps or medusae), as well as study whether eDNA metabarcoding is an appropriate technique for jellyfish monitoring in general. Based on observed patterns, a better assessment of future jellyfish blooms in the BPNS could be made. In this study, we mainly focused on the following research questions:

- How are gelatinous plankton communities currently composed and which factors define their spatial and temporal dynamics?
- How effective is the application of eDNA metabarcoding in the detection of jellyfish?
- Is it possible to detect spatiotemporal trends in jellyfish presence and/or abundance with eDNA metabarcoding, allowing this technique to detect jellyfish blooms?

3 Methodology

3.1 Sampling and sample preparation

Seawater samples were taken monthly in the BPNS between August 2022 and January 2023 using the research vessel (RV) Simon Stevin (**Table 3**). During one-day Lifewatch campaigns (i.e., the months August, November, December and January), only the nine stations closest to shore were sampled (120, 130, 215, 230, 700, 710, 780, 330 and ZG02, see **Figure 3-1A**), while during multiple-day Lifewatch campaigns (September and October), all stations were visited. Stations 120, 130, 700, 710, 780, 215 and 230 are considered nearshore, while stations W09, W10, LW01 and LW02 are considered far-offshore. The remaining stations are in between near- and far-offshore. Additionally, more nearshore samples were taken at the Blue accelerator Platform in August and September, at the Spuikom in August, September, November and January, and at the quay (pontoon) in August, September and December (**Figure 3-1B**). The two latter stations are located in constructed harbor sections (CHS) and thus not directly in the open sea. In total, 74 seawater samples were taken throughout the sampling period. At each station (except for the CHS stations and the Blue accelerator Platform), zooplankton were also physically caught by the use of a vertical WP2 net, consisting of a 57 cm diameter steel ring, a 2.6 m long net with a 200 µm mesh size, a plastic bucket to collect the sample, a heavy weight to prevent uplifting and a mechanical flowmeter. The WP2 net was brought down to just above the sea floor before being hauled up again at a slow pace (max. speed of 1 m/s, total duration of approximately 3 min). Subsequent to this operation, the plastic bucket is removed from the net and brought to the wet laboratory of the RV, where 6% formaldehyde is added. Samples are stored in the sample library at the Marine Station Ostend (MSO) and the yielded organisms are scanned with the ZooScan device (Mortelmans et al., 2019). If Cnidaria and/or Ctenophora were scanned, this was registered. Sampling was conducted simultaneously with the long-running sampling efforts (since 2014) by Flanders Marine Institute. The resulting data from the sampling efforts was consequently merged with this dataset.

Table 3 *Sampling locations and date of sampling. NA = Not Available - not sampled in that month, BA = Blue Accelerator Platform, SP = Spuikom.*

Station	Coordinates		Month					
	Latitude N	Longitude E	August	September	October	November	December	January
120	51.19	2.70	17/08/22	28/09/22	25/10/22	NA	14/12/22	NA
130	51.27	2.91	17/08/22; 18/08/22	28/09/22	25/10/22	23/11/22	NA	19/01/23
215	51.28	2.61	17/08/22	28/09/22	25/10/22	NA	14/12/22	NA
230	51.31	2.85	17/08/22	28/09/22	25/10/22	23/11/22	02/12/22	19/01/23
700	51.38	3.22	18/08/22	28/09/22	25/10/22	22/11/22	12/12/22	19/01/23
710	51.44	3.14	18/08/22	28/09/22	25/10/22	22/11/22	12/12/22	19/01/23
780	51.47	3.06	18/08/22	28/09/22	25/10/22	22/11/22	12/12/22	19/01/23
330	51.43	2.81	18/08/22	28/09/22	25/10/22	23/11/22	12/12/22	19/01/23
ZG02	51.33	2.50	17/08/22	28/09/22	25/10/22	NA	14/12/22	NA
421	51.48	2.45	NA	28/09/22	25/10/22	NA	NA	NA
435	51.58	2.79	NA	28/09/22	25/10/22	NA	NA	NA
W07bis	51.59	3.01	NA	28/09/22	25/10/22	NA	NA	NA
W08	51.46	2.35	NA	28/09/22	25/10/22	NA	NA	NA
W09	51.75	2.70	NA	28/09/22	25/10/22	NA	NA	NA
W10	51.68	2.42	NA	28/09/22	25/10/22	NA	NA	NA
LW01	51.57	2.25	NA	28/09/22	25/10/22	NA	NA	NA
LW02	51.80	2.55	NA	28/09/22	25/10/22	NA	NA	NA
BA	51.25	2.92	17/08/22	28/09/22	NA	NA	NA	NA
SP	51.23	2.95	29/08/22	05/09/22	NA	29/11/22	NA	19/01/23
Quay	51.23	2.93	17/08/22; 18/08/22	05/09/22	NA	NA	02/12/22	NA

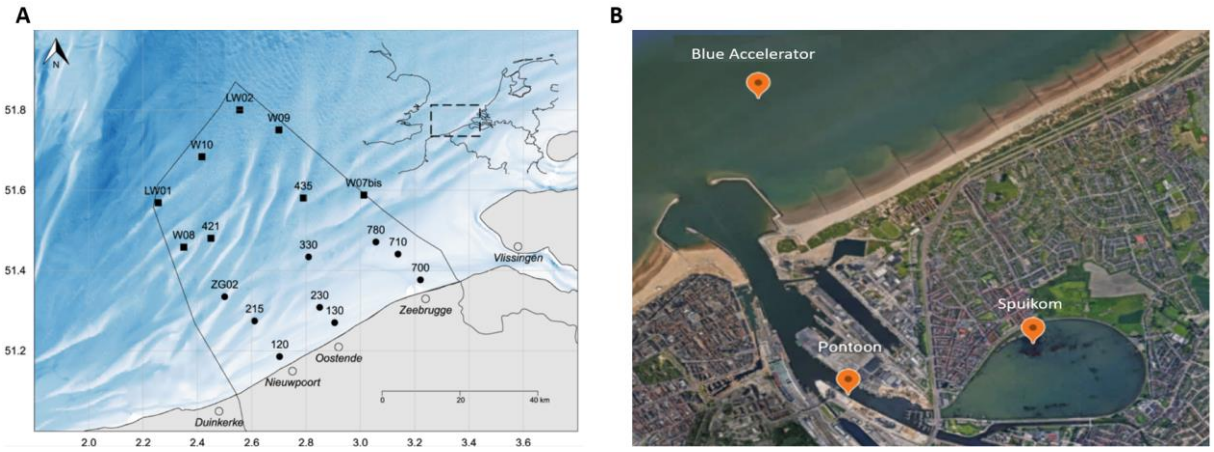

Figure 3-1 (A) Sampling locations of the RV Simon Stevin at the BPNS (Flanders Marine Institute (VLIZ), 2023). (B) Locations of the Blue accelerator Platform, Pontoon and Spuikom in Ostend.

Water samples were collected by means of a CTD (Conductivity-Temperature-Density) carousel, equipped with six Niskin bottles, of which one was filled with seawater at a depth of three meters (**Figure 3-2A**). The water samples were filtered on board of the RV, using *Pall Corporation Supor ® 0.2 µm 47 mm PES 100/pk* filters, which were afterwards folded in eight and stored in labelled 2 mL Eppendorf tubes in the freezer (-16°C) of the RV. The setup of the filtration system is visualized in **Figure 3-2B**. Three replicates were taken per station and 500 mL water was filtered per replicate. The used motor in the setup is produced by *KNF, type N816.3KT.18 Laboport*, while the rod is produced by *Pall Corporation, Product No. 15402*. In order to avoid contamination between different sampling stations, the cups were thoroughly cleaned in between sampling with tap water and subsequently with 70% ethanol (Chemlab, Ethanol denaturated with Eurodenaturant (Disolol) CL00.1807.5000). The stored filters were taken to the lab in Ghent and stored in -85°C. Additional controls were performed in the lab with deionized water following the same procedure.

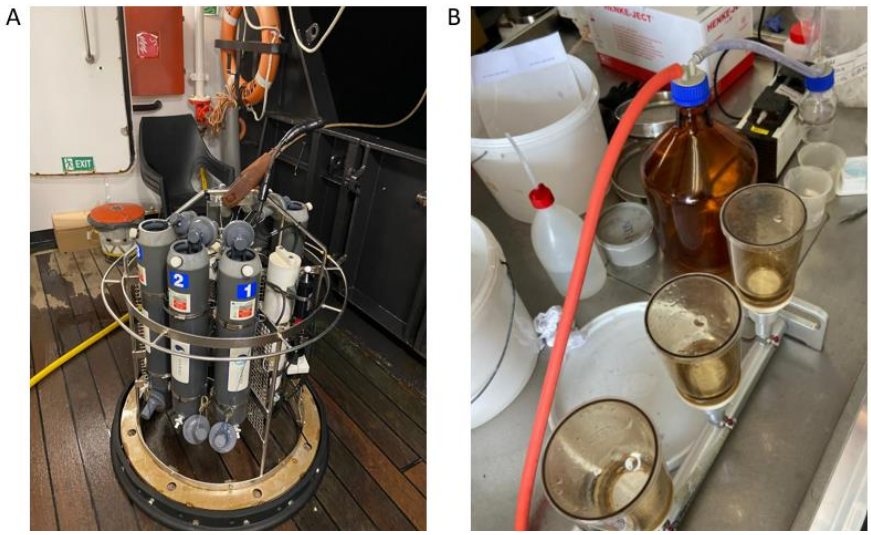

Figure 3-2 (A) CTD device on the RV Simon Stevin, (B) Sample filtration setup in the wet lab of the RV Simon Stevin.

3.2 DNA extraction and amplification

Environmental DNA (eDNA) of all samples was extracted using the DNA extraction protocol based on Djurhuus et al. (2017) with modifications. The protocol uses the QIAGEN GmbH DNeasy® Blood & Tissue Kit. The filters containing eDNA were cut in half and placed in 2 mL Eppendorf tubes, after which 165 µL ATL buffer was added twice to each tube, parted by a 30 min incubation period at 56°C. Afterwards, 20 µL Proteinase K was added and the tubes were incubated for 2 h at 56°C in a VWR Incubating Mini Shaker. The dislodged eDNA (supernatant) was then transferred into a new 2 mL Eppendorf tube, after which the tubes were centrifuged to create a pallet. Once again, the supernatant was transferred to a new tube and

mixed with 320 µL AL buffer and 320 µL ethanol (96%-100%, Sigma-Aldrich for molecular biology CAS-No: 64-17-5). This solution was then sent through the filter of a DNeasy spin column via centrifugation. The filters of the spin column were washed using 500 µL AW1 and 500 µL AW2 buffer. Finally, 30 µL AE buffer was sent through the filter to retrieve the DNA (instead of 200 µL described in the Qiagen protocol). This was performed twice, in order to have an A and a B-series. The full protocol is available in Attachment 1: DNA Extraction of Seawater Samples protocol. The quality of the DNA extractions of elution series A and B was investigated using Nanodrop (Thermo Scientific Nanodrop 2000 Spectrophotometer). The amount of DNA (ng/µL), as well as the 260/280 and 260/230 ratios were inspected. As a rule of thumb, we assumed extractions to be successful if values for DNA quantity were at least 10 - 20 ng/µL, while both ratios had to fluctuate between 1.8 and 2.2. Samples of which Nanodrop gave undesired results were extracted an additional time.

After extraction, samples of satisfying quality were amplified. For this, the primer pair F-566 [sequences (5'-3') CAG CAG CCG CGG TAA TTC C] and R-1200 [sequences (5'-3') CCC GTG TTG AGT CAA ATT AAG C] of the 18S ribosomal DNA gene was selected based on their wide taxonomic range (Hadziavdic et al., 2014). Amplifications were performed in volumes of 50 µL containing 25 µL Invitrogen Platinum Hot Start PCR 2X Master Mix, 1 µL of 20 µM forward and reverse primer stock solution and 0.5 - 5 µL template DNA (±100 ng). The solution was then diluted with DNase free water (NFW) until 50 µL. PCR amplification was carried out using the PCR thermocycler (analytikjena 846-x-070-280 Biometra TAdvanced Basiseinheit), which was set at 94°C for 2 min to activate DNA polymerase. The PCR reaction itself consisted of 35 cycles of denaturation at 94°C for 30 s, annealing at 55°C for 30 s and extension at 72°C for 1 min.

Samples that were successfully amplified, (monitored by gel electrophoresis, see section 3.3) were amplified once more with an adapted 18S forward/reverse primer pair [sequences (5'-3') TTT CTG TTG GTG CTG ATA TTG C CAG CAG CCG CGG TAA TTC C and ACT TGC CTG TCG CTC TAT CTT C CCC GTG TTG AGT CAA ATT AAG C, respectively]. Briefly, the 18S specific primers were tailed with universal sequences as recommended by ONT (2023) to allow for multiplexing of all samples in a third PCR round. Amplifications happened in the exact same way as with the F-566/R-1200 primers, except that now 1 µL template DNA (PCR product of amplification with F-566/R-1200 primers) was used for all samples.

To identify the samples during sequencing and analysis, a third (and last) PCR amplification was performed, where the samples were tagged using the SQK-LSK110 protocol of Oxford Nanopore Technologies (2023), allowing for multiplexing (through incorporating Oxford Nanopore barcode sequences into the amplicons of the second PCR round). Amplifications were performed in volumes of 50 µL containing 25 µL LongAmp Taq 2x master mix, 1 µL of PCR Barcode (Oxford Nanopore Kits, one of BC1-BC96, at 10 µM), 1 µL final PCR product and 23 µL DNase free water. After mixing by pipetting up-and-down and a brief centrifugation (short spin of 5 - 10 s, VWR Galaxy Minicentrifuge SN 0910 0713), PCR amplification was carried out using the PCR thermocycler, which was set at 95°C for 3 min for initial denaturation, followed by a PCR reaction consisting of 20 cycles of denaturation at 95°C for 15 s, annealing at 62°C for 15 s and extension at 65°C for 90 s, according to the barcoding PCR protocol of Oxford Nanopore Technologies (2023a).

3.3 Gel electrophoresis

After each amplification, 1.5% agarose gel electrophoresis was performed to evaluate if PCR was successful, with success being indicated by the presence of a band for each sample around 500 - 700 base pair amplicons on the gel. In this research, gel electrophoresis had to be performed three times (amplification with F-566/R-1200 primers, amplification with adapted 18S primers and amplification when applying tags).

0.6 g agarose (PanReac AppliChem, Agarose low EEO (Agarose Standard), CAS-No: 9012-36-6) was mixed with 60 mL 1x Tris/Borate/EDTA (TBE) buffer and heated in a microwave until a homogenous and transparent solution was obtained. After cooling down to ± 60°C, 6 µL SafeStain was added to the mixture which was, after firmly swirling, poured onto a 60 mL tray that was securely clamped into a holder. One or two combs were inserted (depending on the amount of samples). After 20 - 30 min, the solidified gel was placed in a 1x TBE buffer bath. 6 µL of Thermofisher Scientific GeneRuler 100 bp

DNA Ladder was injected in the middle well of the gel to measure amplicon length. The samples were prepared by mixing 2 µL of PCR product with 3 µL NFW (Nuclease Free Water) and 1 µL ThermoFisher Scientific DNA gel Loading Dye. After mixing by pipetting up and down and a short centrifugation, the 6 µL solution was injected in the remaining wells of the gel. An electric potential of 100V (Bio rad Powerpac 300) was applied for 30 - 45 min to separate the different lengths of DNA strands. Afterwards, the gel was transferred onto a UV-lamp (Vilber Lourmat TFX-35M, put on 75%) and success was evaluated. In some cases, when the colorization of the bands was visible but unclear, the solution was prepared an additional time with 4 µL PCR product instead of 2 µL.

3.4 Qubit assay

The eDNA quantity was measured by a Qubit® double-stranded DNA Broad Range (BR) Assay Kit (Life Technologies, Eugene, OR, USA) and read by a Qubit® 2.0 Fluorometer (Life Technologies, Eugene, OR, USA). First, a working solution was prepared: 199 µL buffer and 1 µL Qubit reagent was used per sample. For calibration of the device, two standard solutions were prepared by adding 190 µL working solution to 10 µL standard. Next, 199 µL working solution was mixed with 1 µL of the tagged samples. The working solution, as well as the prepared samples, were vortexed (VWR) for 2 - 3 seconds and incubated for 2 - 3 minutes at room temperature before quantification in the Qubit® device. To avoid degradation, samples were analyzed within 15 minutes after preparing the working solution and light penetration in the room was limited. The quantitative results were multiplied by 200 since the samples were diluted 200 times (199 µL working solution added to 1 µL sample).

3.5 Library preparation and DNA sequencing using the MinION platform

Library preparation and DNA sequencing were performed using the 1D PCR barcoding Expansion Pack 1-96 (EXP-PBC096) with the SQK-LSK110 kit (Oxford Nanopore Technologies, 2023a). All barcoded libraries were equimolarly pooled to obtain 1 µg eDNA in total in a 1.5 mL DNA LoBind Eppendorf tube. Library preparation was carried out according to the manufacturer's protocol with slight adaptations. Briefly, amplicons were end-repaired using 3 µL NEBNext Ultra II End-Repair/dA-tailing enzyme mix (E7546) at 20°C for 5 min and 65°C for 5 min, after which they were purified with 60 µL of resuspended CleanNGS beads. Next, adapter ligation was carried out with 25 µL of Ligation Buffer (LNB), 5 µL of Adapter Mix F (AMX-F), and 10 µL of NEBNext Quick T4 DNA Ligase (New England Biolabs, USA), followed by another purification step using the magnetic beads. The washing step, using 250 µL of Short Fragment Buffer (SFB), was performed twice before the DNA was eluted by incubation in 15 µL of Elution Buffer (EB) for 10 min. Each flow cell was primed with 1000 µL of priming mixture (Oxford Nanopore Technologies, 2023a). Then, 12 µL of the amplicon library was diluted in a total of 75 µL of running buffer according to protocol. Next, the pooled library was loaded onto an FAM94370 flow cell via the SpotON sample port and the DNA was sequenced on a MinION device for 72 h using standard MinIon settings. The flow cell had 1717 pores available after flow check. For base calling, the locally installed software Guppy version v6.4.6 (Oxford Nanopore Technologies, 2023b) was used with standard settings, but adapter trimming and demultiplexing (--barcode_kits EXP-PBC096) commands enabled.

3.6 Bioinformatics and data analysis

After sequencing on the MinION, the raw reads were filtered and trimmed using Nanofilt version 2.6.0 on the High Performance Computer (HPC): base pair lengths smaller than 500 bp and bigger than 1000 bp were omitted and a quality (Phred score) of ten was used. To assign taxonomy to the trimmed and filtered reads, we blasted the barcodes to compare those reads with the SILVA eukaryote database (Quast et al., 2013). To classify each sequence, the best BLAST hit against the SILVA database was used, with positive identification defined as a hit with at least 95% identity and an e-value cut-off of 1E-4. Relevant taxa were chosen by filtering on the terms “Cnidaria” and “Ctenophora” and consulting the WoRMS database to verify the found species were relevant and occurred in the BPNS or its surroundings. Names were manually checked while sub-species level identifications were set to species level and synonyms were resolved. Consequently, reads with the same taxonomic annotation were merged using R software (RStudio, version 4.1.3) to compute read abundances.

The first part of the data analysis focused on morphological data acquired from Lifewatch campaigns on the Simon Stevin. Firstly, significant temporal and spatial differences between environmental parameters were examined using the non-parametric Kruskal-Wallis test, followed by a pairwise Wilcoxon test. Temporal differences were expressed per year (examined period 2014 - 2022), month and season, while the spatial component was examined by comparing the different sampling stations independent of time. Differences were considered statistically significant if the adjusted p-value (Benjamini-Hochberg (BH) method) was smaller than 0.01 and boxplots were used for visualization. Additionally, Spearman rank correlation analysis was employed to determine correlations between the different environmental parameters. A Principal Component Analysis (PCA) including a correlation circle was plotted to visualize which parameters cluster together and correlate using the packages FactoMineR (v.2.8), ggplot2 (v.3.4.1) and corrplot (v.0.92) in R v.4.1.3.

Subsequently, correlations, spatial differences and temporal differences between environmental parameters (abiotic parameters, nutrients and pigments) and Cnidaria/Ctenophora blooms and densities were investigated in a completely analogous way as was done with the environmental parameters among themselves. During Lifewatch campaigns, Cnidaria and Ctenophora were physically caught at each sampling station using WP2 nets. Based on the volume of water in the nets, counts of both phyla were expressed as densities (#/m³) and stored together with all other environmental parameters. The term "density" is used for the complete dataset (values of zero included), while the term "blooms" refers to the datapoints where Cnidaria and/or Ctenophora were observed (and where densities were thus strictly > 0).

Two sets of generalized additive models (GAMs) were used to determine the main environmental drivers to the bloom formation of both phyla in the BPNS. GAMs were fitted using the mgcv package (v.1.8-42) in R. For each particular model, we modelled the log10(abundance/m³ + 1) as a function of a selection of environmental predictors. To assess which parameters would be selected for constructing the GAMs, we first investigated the correlation between the variables (Spearman) after outlier removal. This was done by removing datapoints that were greater than the mean value plus three times the standard deviation. To avoid collinearity, variables with a concurvity > 0.8 were removed from the analysis after evaluating their potential ecological significance in the model. Concurvity refers to the generalization of collinearity, referring to the situation where a smooth term can be approximated by some combination of the others. There is no universal criteria for concurvity, but one study on the effects of it suggests values > 0.5 start to introduce noticeable errors (He, 2004).

The variables that were selected for constructing the GAMs include water temperature, Secchi depth, salinity, chlorophyll a and nitrate for Cnidaria blooms and water temperature, Secchi depth, salinity, beta carotene and silicate for Ctenophora blooms. The best model was chosen based on acceptable concurvity values (< 0.8) and the highest deviance explained (indicating the amount of variability in the data explained by the model). The residuals of the best fitted model were used to test for underlying assumptions of normality and homogeneity (Zuur et al., 2009). When the variability of the residuals was similar across the range of fitted values, homogeneity was concluded. Graphical diagnostics were used to evaluate normality. Normality was assumed if the QQplot showed a straight line of residuals and when the histogram of the residuals showed a bell-shaped curve (Wood, 2006; Zuur et al., 2009)

The second part of the data analysis focused on eDNA metabarcoding and made use of the data that was obtained after sequencing on the MinION. Prior to downstream analyses, the sequence data were normalized using sequencing depth. This normalized dataset was subsequently used to create plots visualizing e.g., species distributions per sampling station or per month, number of reads throughout time and scatterplots comparing metabarcoding reads with morphological densities (see section 4). A GAM model was used to determine the main environmental drivers to the occurrence of *Mnemiopsis leidyi* in the BPNS using this normalized data. The log10(*Mnemiopsis leidyi*) reads were modelled as a function of temperature, Optical Back Scatter (OBS) and salinity. The procedure for model selection was completely analogous as for the GAM models of Cnidaria and Ctenophora blooms. For cluster analysis (PCA), read counts were normalized using the centered log ratio function (clr) using the compositions package (v.2.0-6) in R. Pseudo count was performed (all data + 1) to account for read values of zero.

4 Results

4.1 Investigation of environmental data

4.1.1 Cluster analysis of the environmental variables

The clustering of the samples based on environmental parameters was visualized using a PCA analysis. 28.6% and 19.8% of the variance is explained by the first and the second axis, respectively (**Figure 4-1**). All nutrient concentrations (nitrate, nitrite, phosphate and silicate) and all pigment concentrations (chlorophyll a, chlorophyll b, beta carotene, antheraxanthin, fucoxanthin, diatoxanthin, diadinoxanthin and prasinoxanthin) cluster together to some extent. Nitrate, phosphate and silicate concentrations are better represented by the PCs than nitrite concentrations. Phosphate concentrations correlate significantly with nitrate and silicate concentrations (Spearman Rho values of 0.71 and 0.81, respectively, $p < 2.2e\text{-}16$). Similarly, chlorophyll a, diadinoxanthin and beta carotene are better represented pigments than e.g., chlorophyll b, prasinoxanthin and diatoxanthin. Spearman Rho values of 0.78 and 0.89 are found between chlorophyll a versus beta carotene and diadinoxanthin, respectively ($p < 2.2e\text{-}16$). Diadinoxanthin also correlates significantly with beta carotene (0.88, $p < 2.2e\text{-}16$). Other abiotic parameters such as temperature and conductivity also correlate (Rho value of 0.95, $p < 2.2e\text{-}16$), as well as Secchi depth and salinity (0.66, $p < 2.2e\text{-}16$). OBS and Secchi depth are negatively correlated (angle of 180° between both vectors, see **Figure 4-1A)** corresponding with a Spearman Rho of -0.78 ($p < 2.2e\text{-}16$). Both densities of Cnidaria and Ctenophora are poorer represented by the PCs. The vector for Cnidaria is situated between temperature and chlorophyll while the vector of Ctenophora is in line with the vectors of the different pigments (**Figure 4-1A**).

In general, pigment concentrations (i.e., chlorophyll a, beta carotene, diadinoxanthin, fucoxanthin and diatoxanthin) contribute the most to the first dimension, while the second dimension is dominated by nutrient concentrations (i.e., nitrate, phosphate and silicate) (**Figure A- 1**).

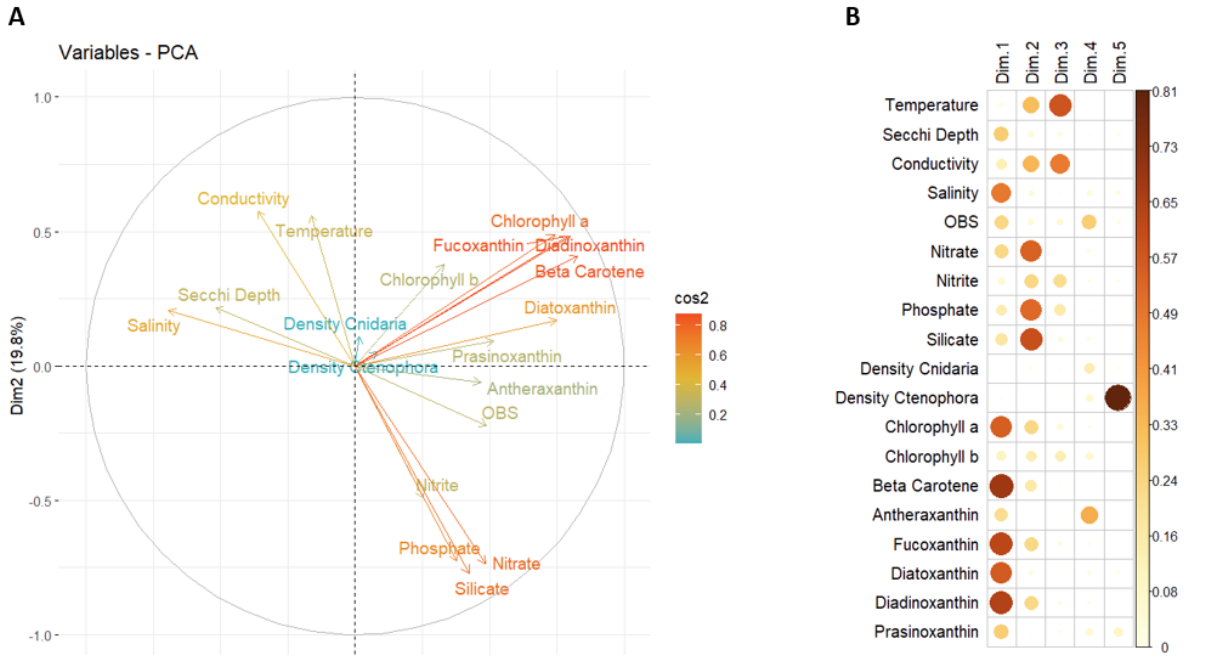

Figure 4-1 *(**A**) Correlation circle plot. Vectors are the loadings on PC1 (x-axis) and PC2 (y-axis). The quality of representation of the variables (parameters) is indicated by the squared cosine (cos2). A high cos2 value indicates a good representation of the parameter of the principal component and will be positioned close to the circumference of the correlation circle. A low cos2 indicates that the variable is not well represented by the PCs and will be positioned close to the center of the circle. The vector length indicates the strength of the relationship and the angle between two vectors gives the degree of correlation (adjacent vectors are highly correlated, orthogonal (90°) vectors are uncorrelated, opposite (180°) vectors are negatively correlated. (**B**) Correlation plot of the cos2 of variables on all the dimensions.*

4.1.2 Environmental differences between sampling stations

No clear clustering patterns can be distinguished between different sampling stations based on environmental parameters as lots of overlap is present (**Figure 4-2A**). Variation between sampling stations and environmental parameters (nutrients, pigments and other abiotic parameters) is visualized using boxplots (**Figure A- 2**, **Figure A- 3**, **Figure A- 4**).

No significant differences between sampling stations and seawater temperature are found. Secchi depth and salinity do differ between sampling stations (Kruskal-Wallis rank sum test with χ^2 (df = 16) of 423.06 and 675.22, respectively, $p < 2.2e-16$). Stations closer to the shoreline (e.g., 130, 700 and 710) have a significantly lower Secchi depth than far offshore stations (e.g., LW01, LW02 and W10), as well as a significantly lower salinity (Pairwise Wilcox test, BH adjusted, $p < 0.01$). Both Secchi depth and salinity are minimal around station 700 (**Figure A- 2**).

Nutrient concentrations differ significantly between different sampling locations: A Kruskal-Wallis rank sum test resulted in a χ^2 (df = 16) of 229.88, 208.28, 256.44 and 288.4 for nitrate, nitrite, phosphate and silicate, respectively, $p < 2.2e-16$. Near-shore stations (e.g., 130, 230, 700, 710 and 780) correspond to higher nutrient concentrations than far-offshore stations (e.g., LW01, LW02, W10) (**Figure A- 3**). These differences are significant for all studied nutrients (Pairwise Wilcox test, BH adjusted, $p < 0.01$).

Pigment concentrations significantly differ between different sampling locations. A Kruskal-Wallis rank sum test resulted in e.g., a χ^2 (df = 16) of 167.15 and 343.16 for chlorophyll a and beta carotene, respectively, $p < 2.2e-16$. Observed patterns of pigment concentrations relative to the sampling stations are similar to those of nutrient concentrations: near-shore stations (e.g., 130, 230, 700, 710 and 780) correspond to higher concentrations than stations far-offshore (e.g., LW01, LW02 and W10), independent of which pigment is looked at (**Figure A- 4**). The differences between these stations are significant for chlorophyll a, beta carotene, fucoxanthin, diadinoxanthin and diatoxanthin concentrations (Pairwise Wilcox test, BH adjusted, $p < 0.01$).

4.1.3 Temporal differences between environmental parameters

No clear clustering patterns are seen between different months and years (studied period: 2014 – 2022) due to a big overlap in data (**Figure 4-2B, C**). When comparing different seasons and adding ellipses to the PCA plot, it is noticeable that two main orientations are found, where summer (June - August) and spring (March - May) are oriented in one way and contribute mainly to the first dimension while fall (September - November) and winter (December - February) are oriented in another way and contribute mainly to the second dimension (**Figure 4-2D**). Temporal differences between environmental parameters (nutrients, pigments and other abiotic parameters) are visualized using boxplots.

Figure 4-2 PCA plots focusing on clustering patterns for (A) sampling station, (B) sampling month, (C) sampling year and (D) sampling season. Single points refer to an individual sample taken at a specific time and location, as indicated in the legend.

The seawater temperature differs significantly between different months (**Figure 4-3**) (Kruskal-Wallis rank sum test with χ^2 (df = 11) of 1039.4, p < 2.2e-16). Highest water temperatures are found in July and the water is the coldest in February. Except for January and March, the temperature of each month differs significantly from any other month (Pairwise Wilcox test, BH adjusted, p < 0.01). Similar patterns are seen for conductivity, where concentrations are the highest in summer months and the lowest in winter months (**Figure 4-3**). Values for Secchi depth and salinity differ less pronounced between different months, but the difference is still significant (Kruskal-Wallis rank sum test with χ^2 (df = 11) of 72.616, p < 3.877e-11 and 52.017, p < 2.708e-07 for Secchi depth and salinity, respectively). Secchi depth is significantly lower in winter (e.g., December, January and February) than in summer (e.g., June, July and August), while for salinity significant differences are less clear but still present between e.g., August and October (Pairwise Wilcox test, BH adjusted, p < 0.01) (**Figure 4-3**). Seasonal differences for temperature, conductivity, Secchi depth and salinity are visualized in **Figure A- 5**.

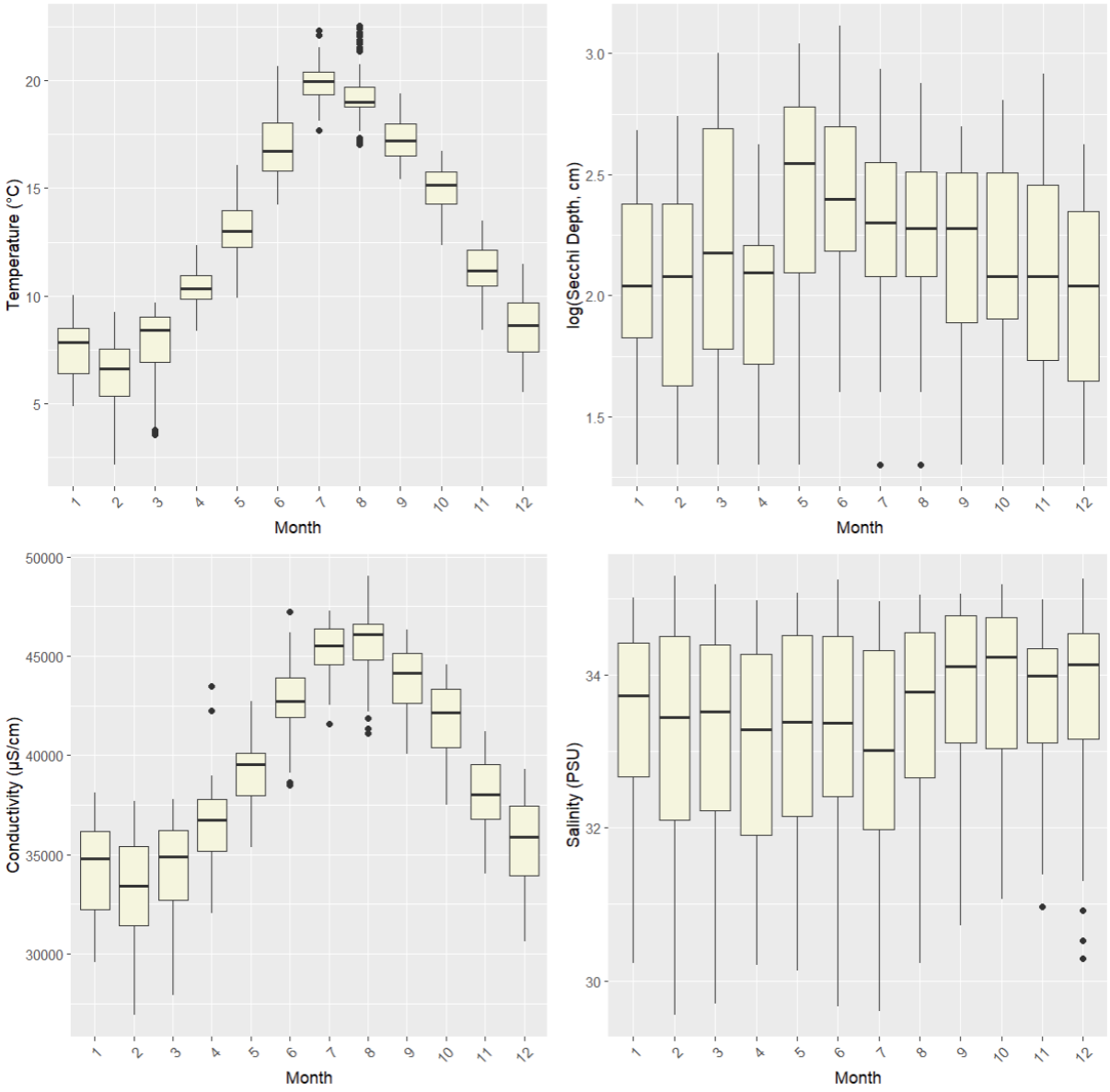

Figure 4-3 Boxplots showing temporal variation in a selection of measured environmental parameters.

When comparing different nutrient concentrations at different months, a general pattern can be observed of concentrations being the highest in the first months of the year (January and February) after which they significantly drop around March to slowly increase again towards the end of the year (**Figure A- 6**). Concentrations in summer and spring are significantly lower than concentrations in winter, independent of the observed nutrient (Pairwise Wilcox test, BH adjusted, $p < 2.2e\text{-}16$). For phosphate and silicate, concentrations in spring are significantly lower than those in summer (Pairwise Wilcox test, BH adjusted, $p < 0.01$). For nitrate and nitrite these differences are not significant (**Figure A- 7**).

Except for antheraxanthin, all pigment concentrations differ significantly per month (Kruskal-Wallis rank sum test, $df = 11$, $p < 0.01$). Pigment concentrations increase between January and April, after which a concentration drop is seen in May. Concentrations then gradually increase again through summer to eventually decrease gradually between September and December (**Figure A- 8**). Focusing on some of the most important pigments (i.e., chlorophyll a, beta carotene and diadinoxanthin, see **Figure 4-1**), concentrations in January are significantly lower than in April, while concentrations in May are significantly lower than those in April and June (Pairwise Wilcox test, BH adjusted, $p < 0.01$). In August, concentrations are significantly higher than in December ($p < 0.01$). Seasonal variation in measured pigment concentrations is visualized in **Figure A- 9**. Besides months and seasons, the temporal variation throughout the years (2014 – 2022) is visualized in **Figure A- 10**, **Figure A- 11** and **Figure A- 12**. No clear patterns were seen throughout this timeframe.

4.2 Morphological investigation of caught Cnidaria and Ctenophora

4.2.1 Temporal and spatial differences between Cnidaria and Ctenophora densities and blooms

The physical catch of both phyla and thus its density are inconsistent over time. In 2014 and 2015, no Cnidaria were caught. In the following years, densities were registered scattered throughout the year and no clear pattern could be derived (**Figure 4-4**). Similarly, no clear patterns were seen for Ctenophora densities but they were detected at each sampling year (**Figure 4-5**).

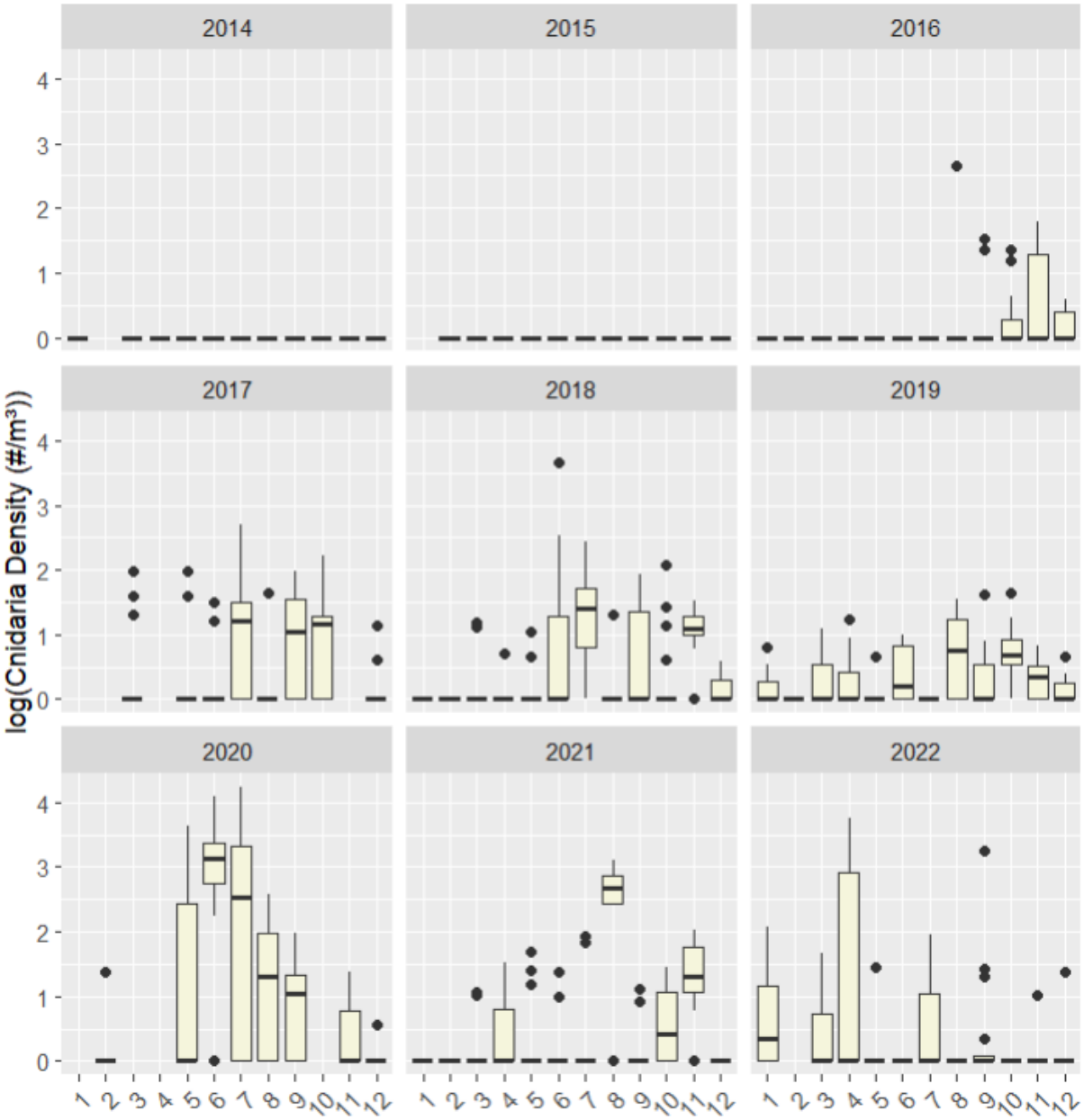

Figure 4-4 Monthly fluctuation of Cnidaria densities for the period 2014 – 2022, expressed in #/m³. Densities were log transformed to account for multiple outliers: pseudocount was performed (all data +1) in order to be able to take the logarithm of the zero counts (ln(1) = 0).

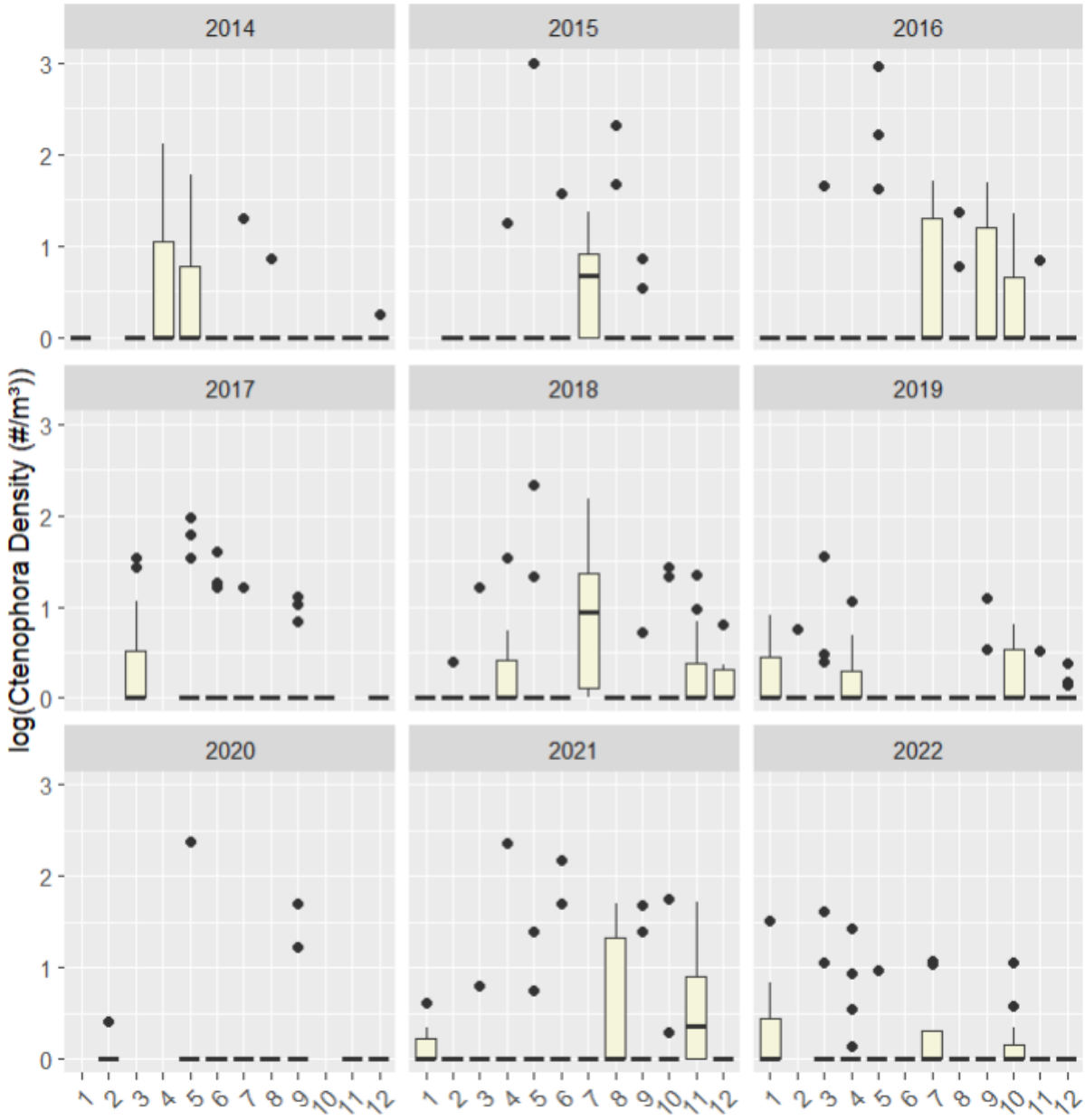

Figure 4-5 Monthly fluctuation of Ctenophora densities for the period 2014 – 2022, expressed in #/m³. Densities were log transformed to account for multiple outliers: pseudocount was performed (all data +1) in order to be able to take the logarithm of the zero counts.

Blooms of Cnidaria and Ctenophora (based on datapoints where Cnidaria and/or Ctenophora were observed and where densities were thus strictly > 0) vary significantly among different months (Kruskal-Wallis rank sum test with χ^2 (df = 11) of 80.121, p = 1.398e-12 and 62.565, p = 3.084e-09 for Cnidaria and Ctenophora, respectively), years (χ^2 (df = 6) of 99.66, p < 2.2e-16 for Cnidaria and χ^2 (df = 8) of 37.419, p = 9.636e-06 for Ctenophora) and seasons (χ^2 (df = 3) of 64.733, p = 5.722e-14 and 39.917, p = 2.944e-08 for Cnidaria and Ctenophora, respectively). For months and seasons, similar patterns are observed: blooms are less abundant in the beginning of the year (generally seen in winter) and are most pronounced in spring and summer (April – August) (**Figure 4-6**). This is confirmed by statistics: bloom concentrations in winter are significantly lower compared to the other three seasons for both phyla (Pairwise Wilcox test, BH adjusted, p < 0.01). Cnidaria concentrations are also significantly lower in spring than in summer (p < 0.01), while this discrepancy is not significant for Ctenophora. When looking at the bloom concentrations throughout the sampling years (2014 - 2022), it is visually apparent that there was a reduction in 2019, after which bloom concentrations peaked in 2020 to slowly decrease again until 2022 (**Figure 4-6**). Due to a lack of observations, a Pairwise Wilcox test could not be done to test if the differences that are visually seen are significant.

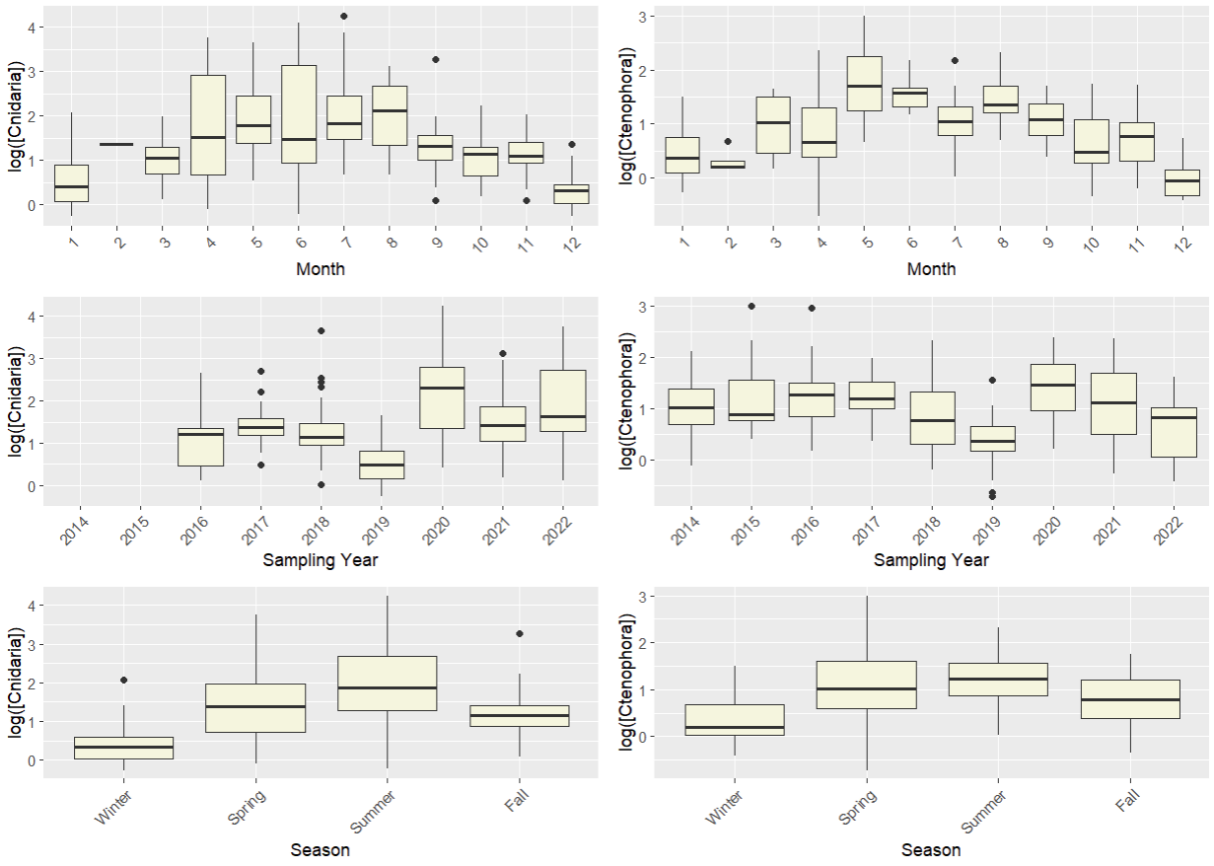

Figure 4-6 Boxplots showing temporal variation (per month, per year and per season) of Cnidaria and Ctenophora blooms. All values are log transformed to account for multiple outliers, resulting in the neglection of zero-counts. Blooms are expressed in #/m³.

No clear patterns or differences can be observed between Cnidaria and Ctenophora blooms and sampling location (**Figure 4-7**). Spatial differences are insignificant for both phyla (Kruskal-Wallis rank sum test, p > 0.01).

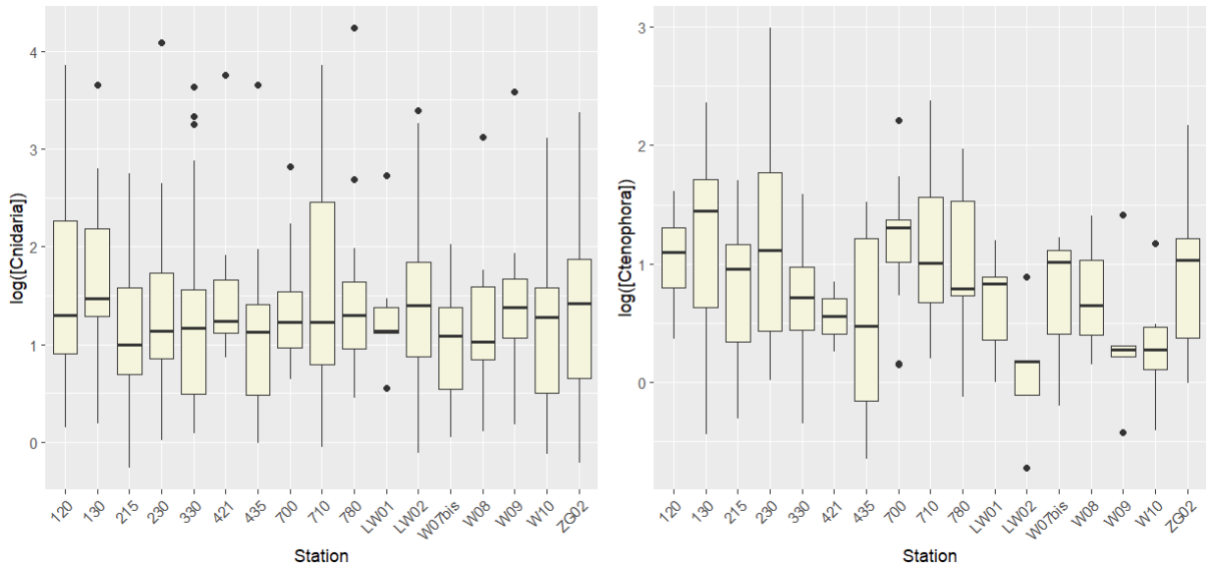

Figure 4-7 Boxplots showing spatial variation in Cnidaria and Ctenophora bloom concentrations, expressed in #/m³.

4.2.2 Effect of environmental parameters on Cnidaria and Ctenophora densities and blooms

Correlograms (correlation plots) were made to study potential links between environmental parameters on one hand and densities and blooms of Cnidaria and Ctenophora on the other hand. No significant correlations are observed between densities of Ctenophora and any environmental parameter (**Figure A- 13**, **Figure A- 14**). For densities of Cnidaria, weak but significant correlations are seen. Seawater temperature, conductivity and salinity correlate weak but significant with the density of Cnidaria (correlation coefficients of 0.14 ($p < 0.001$) for temperature and conductivity, and 0.06 ($p < 0.05$) for salinity) (**Figure A- 13A**). Considering nutrients, only nitrate, phosphate and silicate concentrations are weakly correlated with Cnidaria densities (coefficients of -0.11 ($p < 0.001$), -0.08 ($p < 0.05$) and -0.07 ($p < 0.05$), respectively) (**Figure A- 13B**). Chlorophyll b is the only pigment that correlates significantly with the density of Cnidaria (coefficient of 0.15, $p < 0.001$) (**Figure A- 14**).

When looking at blooms rather than densities, and thus neglecting densities of value zero, correlation coefficients become more pronounced. Temperature, conductivity and salinity correlate significantly with bloom concentrations of both Cnidaria and Ctenophora (**Figure 4-8A**). For temperature, clear positive correlation coefficients of 0.42 and 0.36 are observed for Cnidaria and Ctenophora, respectively ($p < 0.001$). Salinity is strongly negatively correlated with blooms of both phyla, with correlation coefficients of -0.22 and -0.44 ($p < 0.001$) for Cnidaria and Ctenophora, respectively. As was the case with Ctenophora densities, no significant correlations are found between nutrient concentrations and Ctenophora blooms ($p > 0.05$). For Cnidaria blooms, two of the same nutrient concentrations (i.e., phosphate and silicate) are significantly negatively correlated as for Cnidaria densities, with correlation coefficients being rather small and a significance of only < 0.05 (**Figure 4-8B**). There is no significant correlation between nitrate concentrations and Cnidaria blooms, while this correlation was significant for Cnidaria densities ($p < 0.001$), see **Figure A- 13B**.

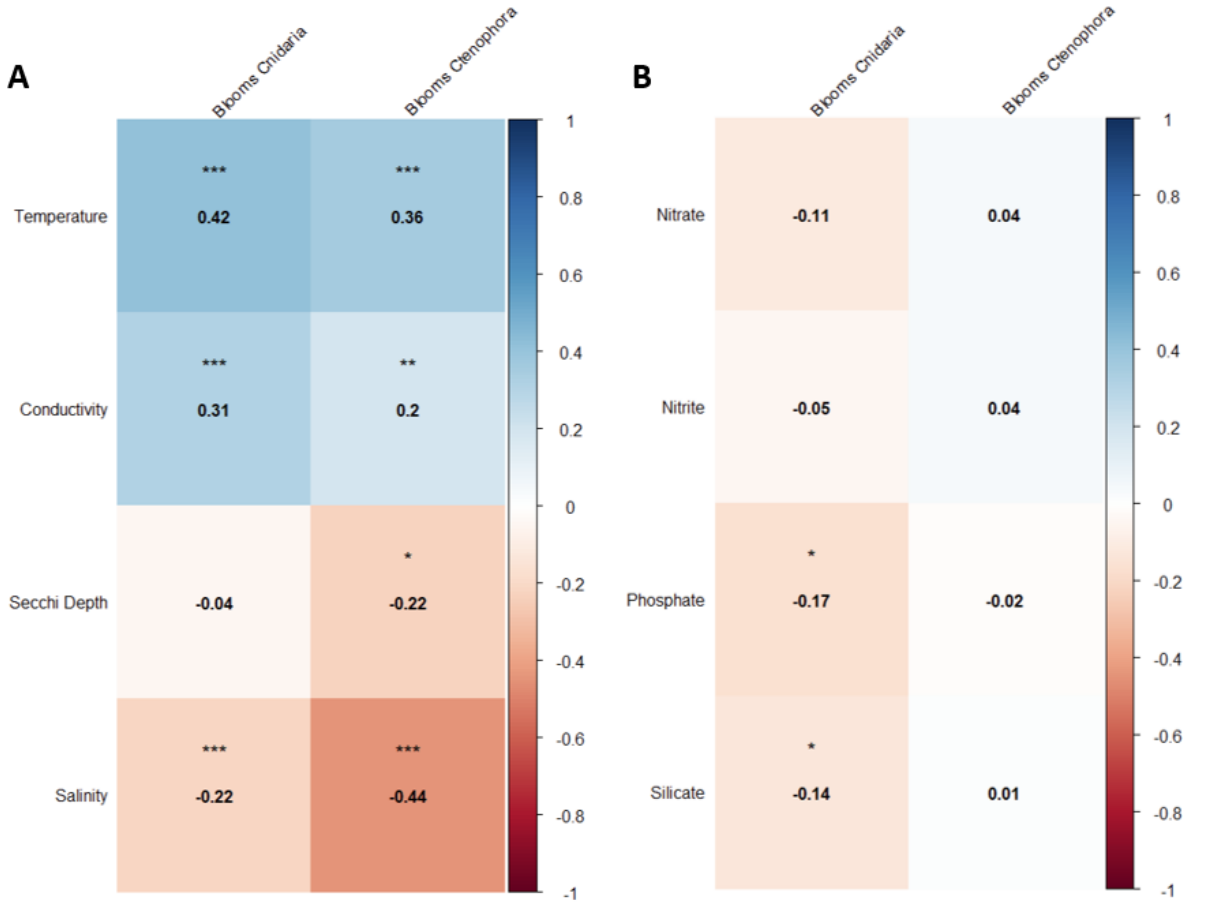

*Figure 4-8 Correlation plot depicting the correlation (Spearman rank) between Cnidaria and Ctenophora bloom concentrations (columns) and **(A)** a selection of measured environmental parameters (row) and **(B)** a selection of measured nutrients (row). The Spearman rho correlation coefficient is shown in each cell. Color of the cell indicates the strength and direction of the correlation, as depicted in the legend. Asterisks indicate correlations with a p-value smaller than 0.05 (*), 0.01 (**) and 0.001 (***).*

Except for prasinoxanthin, all pigments correlate positively and significantly (p-values between < 0.001 and < 0.05) with bloom concentrations of both phyla (**Figure 4-9**). This is in big contrast with **Figure A- 14**, where chlorophyll b was the only pigment that correlated significantly with the density of Cnidaria. Significant correlation coefficients are equally strong for all pigments and vary around 0.3 – 0.4.

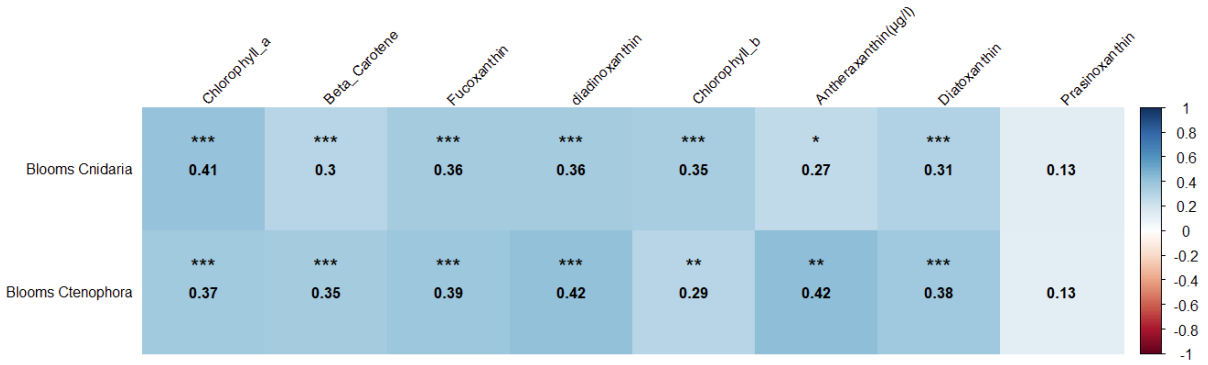

Figure 4-9 *Correlation plot depicting the correlation (Spearman rank) between Cnidaria and Ctenophora bloom densities (rows) and a selection of measured pigment concentrations (columns). The Spearman rho correlation coefficient is shown in each cell. Color of the cell indicates the strength and direction of the correlation, as depicted in the legend. Asterisks indicate correlations with a p-value smaller than 0.05 (*), 0.01 (**) and 0.001 (***).*

The impact of environmental parameters on Cnidaria and Ctenophora blooms was also evaluated by means of a GAM model. GAM modelling confirmed temperature as being one of the most important environmental predictors of Cnidaria and Ctenophora blooms (**Figure 4-10**, **Figure 4-11**). The deviance that is explained by the variables temperature, Secchi depth, salinity, chlorophyll a and nitrate in both models is 56.2% (Cnidaria blooms) and 50.9% (Ctenophora blooms). The significant correlations between Cnidaria blooms and environmental parameters derived from the correlation plots (**Figure 4-8**, **Figure 4-9**) were confirmed by the GAM model, but significance levels differed for salinity ($p < 0.01$ in GAM instead of 0.001 in the correlation plot) and chlorophyll a ($p < 0.05$ instead of 0.001). For Ctenophora blooms, the GAM model resolved significant influence of temperature ($p < 0.01$), Secchi depth ($p < 0.01$), salinity ($p < 0.01$), beta carotene ($p < 0.05$) and silicate ($p < 0.01$) on Ctenophora abundance. In the correlation plot, no significant correlation was observed between silicate and Ctenophora blooms (**Figure 4-8B**), while significance levels for temperature, Secchi depth, salinity and beta carotene were $p < 0.001$, $p < 0.05$, $p < 0.001$ and $p < 0.001$, respectively. Diagnostic plots for both models are visualized in **Figure A- 15** and **Figure A- 16**.

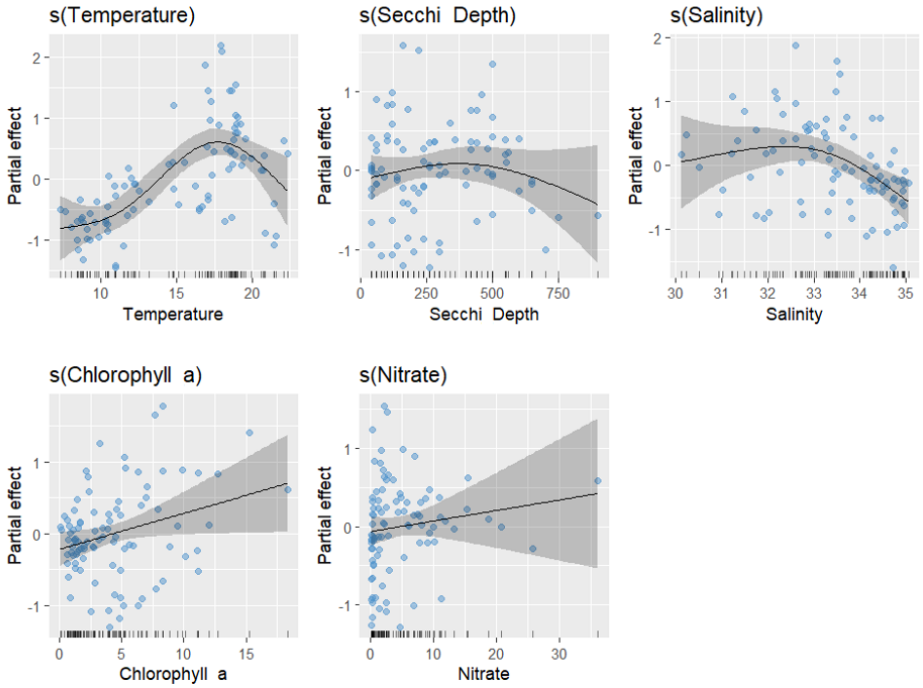

Figure 4-10 Generalized additive model (GAM) plots showing the partial effects of selected explanatory variables on the log transformed abundances of Cnidaria blooms in the survey areas of the Belgian Part of the North Sea. The tick marks on the x-axis are observed data points. The y-axis represents the partial effect of each variable. The shaded areas indicate 95% confidence intervals.

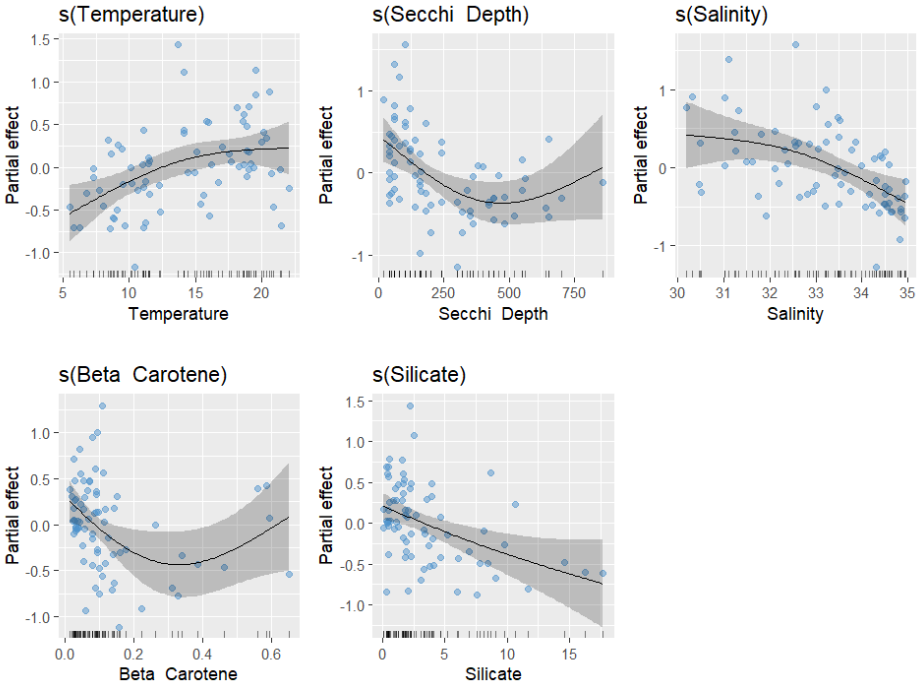

Figure 4-11 Generalized additive model (GAM) plots showing the partial effects of selected explanatory variables on the log transformed abundances of Ctenophora blooms in the survey areas of the Belgian Part of the North Sea. The tick marks on the x-axis are observed data points. The y-axis represents the partial effect of each variable. The shaded areas indicate 95% confidence intervals.

4.3 Investigation of Cnidaria and Ctenophora species based on eDNA metabarcoding

Nanopore sequencing technology is used to assess dynamics and trends in marine gelatinous zooplankton assemblages via eDNA metabarcoding at 21 locations. Except for stations 700 and 710 in December, PCR was successful for all samples. After sequencing, processing and stringent quality filtering, on average 52% of the initial reads were retained, of which around 2.7% was annotated to Cnidaria or Ctenophora (**Table A- 1**).

eDNA metabarcoding resulted in the identification of seven species, of which the invasive ctenophore *Mnemiopsis leidyi* was most commonly found: reads were reported at both nearshore (e.g., 120, 130, 230, 700) and far-offshore (e.g., W07, W08, W10, LW01) stations in all sampling months, except for December (**Figure 4-12**). *Rhizostoma pulmo* was detected in the same months but in smaller amounts and particularly at near-shore stations, except for W09 in October. Anthozoan species were observed from October until January both far- and nearshore, while *Gonothyraea loveni*, *Obelia bidentata*, *Pleurobrachia* sp. and *Sarsia tubulosa* were only detected in one specific time and place (Spuikom November, ZG02 August, 700 January and Spuikom January, respectively) (**Figure 4-12**). Species were observed in 45 out of 69 samplings.

Figure 4-12 *Stacked bar plot of major species recovered in the samples through eDNA metabarcoding, visualized as fractions.*

4.3.1 Cluster analysis

The clustering of the retrieved species was visualized using a PCA analysis. 20.5% and 18.4% of the variance is explained by the first and the second axis, respectively (**Figure 4-13A**). The different species cluster together in three clear groups: *Rhizostoma pulmo* and *Pleurobrachia* sp. correlate (Spearman Rho values of 0.39, $p < 0.01$) and contribute the most to the first dimension (**Figure 4-13B**). A second group consists of *Mnemiopsis leidyi* and *Obelia bidentata*, which contribute the most to the second dimension (no significant correlation, $p > 0.01$). The third group includes *Gonothyraea loveni*, *Sarsia tubulosa* and *Anthozoa* sp. (no significant correlations, $p > 0.01$). The first two groups are better represented by the PCs

than the third group. The vectors of *Rhizostoma pulmo* and *Pleurobrachia* sp. are positioned perpendicular on the vectors of *Mnemiopsis leidyi* and *Obelia bidentata* (**Figure 4-13A**).

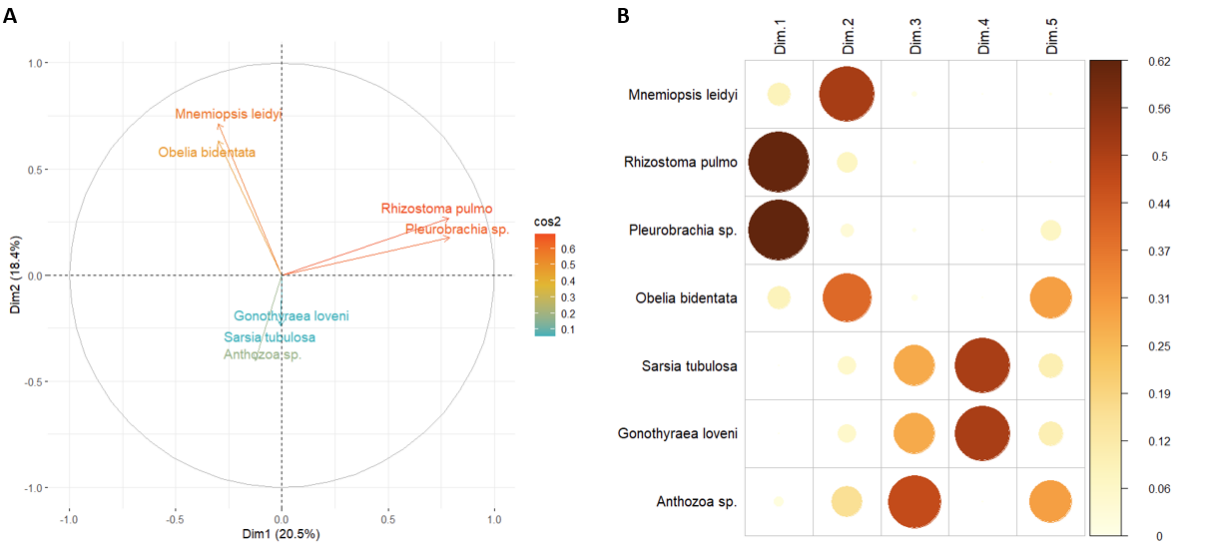

Figure 4-13 (A) *Correlation circle plot. Vectors are the loadings on PC1 (x-axis) and PC2 (y-axis). The quality of representation of the different species (parameters) is indicated by the squared cosine (cos2). A high cos2 value indicates a good representation of the parameter of the principal component and will be positioned close to the circumference of the correlation circle. A low cos2 indicates that the parameter is not well represented by the PCs and will be positioned close to the center of the circle. The vector length indicates the strength of the relationship and the angle between two vectors gives the degree of correlation (adjacent vectors are highly correlated, orthogonal (90°) vectors are uncorrelated, opposite (180°) vectors are negatively correlated. (**B**) Correlation plot of the cos2 of species on all the dimensions.*

4.3.2 Spatial distribution of species

Cnidaria/ Ctenophora reads do not differ significantly between different sampling stations (**Figure A- 18**) (Kruskal-Wallis rank sum test, $p > 0.01$). Species were identified at each sampling location (**Figure 4-14**). *Mnemiopsis leidyi* was abundantly observed in both nearshore (e.g., 120, 130, 215, 230 and 700) and far-offshore (e.g., LW01, LW02, W09 and W10) locations. *Anthozoa* species were detected in four stations: two nearshore (130 and 780), one far-offshore (LW01) and one in between (330). Similarly, *Rhizostoma pulmo* was found nearshore (230, 700, 710) and far-offshore (W09). Other species were observed at one specific sampling station only (**Figure 4-14**).

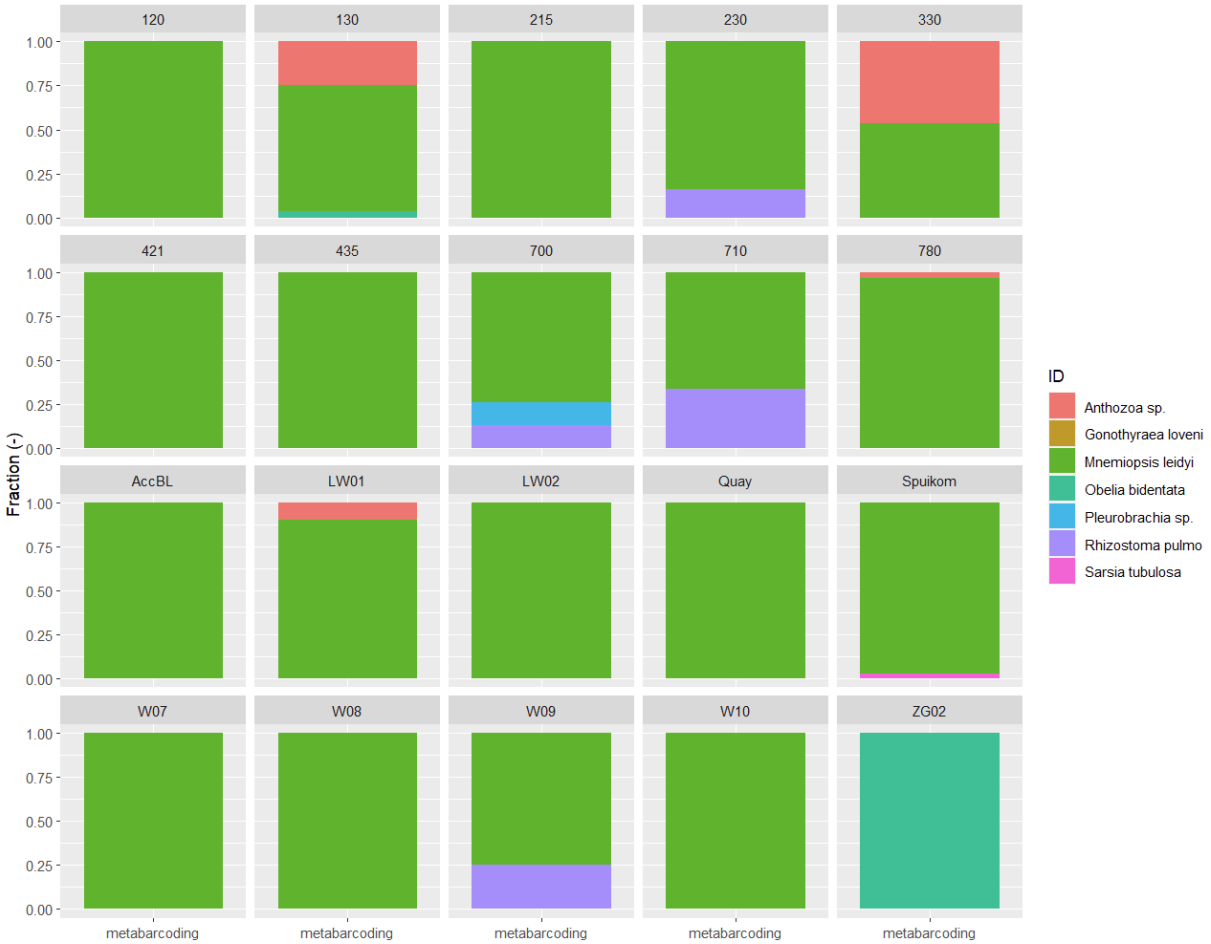

Figure 4-14 Stacked bar plot of major species recovered in the different sampling stations through eDNA metabarcoding, independent of time, visualized as fractions.

4.3.3 Temporal distribution of species

Cnidaria/Ctenophora reads do not differ significantly between sampling months (**Figure A- 19**) (Kruskal-Wallis rank sum test, $p > 0.01$). Most Cnidaria and Ctenophora reads are found in August (140.2, normalized reads) and the least are found in December (0.5, normalized reads) (**Table 4**). Numbers are clearly lower in November, December and January compared to August, September and October (**Figure 4-15A**). In August, reads are found majorly at the two constructed harbor sections Spuikom (33.5%) and quay (22.5%) and at the nearshore station 780 (38.2%). The Spuikom also represents 73.3% of the reads in September. In October, the majority of reads (61.2%) is found at nearshore stations while in November stations 215 and 230 represent 51.6% of the total reads. All reads in December are explained by station 780, while stations 330, 780 and Spuikom contribute the most to the number of reads in January (20.8%, 16.0% and 41.5%, respectively). Far-offshore stations were only sampled in September and October.

Table 4 Spatial distribution of retrieved eDNA metabarcoding reads throughout the sampling period.

Sampling month	Total annotated reads (#)	Nearshore (%)	Far-offshore (%)	Spuikom (%)	Quay (%)
August	140.2	43.7	NA	33.5	22.5
September	100.8	7.1	3.0	73.3	0
October	82.9	61.2	7.7	NA	NA
November	7.2	97.2	NA	2.8	NA
December	0.5	100	NA	NA	NA
January	7.9	58.5	NA	41.5	NA

When considering the species distribution throughout the different sampling months, it is clear that in August, September and October nearly all reads are explained by one species: *Mnemiopsis leidyi* (**Figure 4-15B**, **Figure 4-16A**). In November, the two main species are *Mnemiopsis leidyi* (60.4%) and *Anthozoa* sp. (30.3%). In December, only *Anthozoa* sp. were observed while the number of reads in January are mainly explained by *Sarsia tubulosa* (41.4%) and *Anthozoa* sp. (36.8%) (**Table 5**).

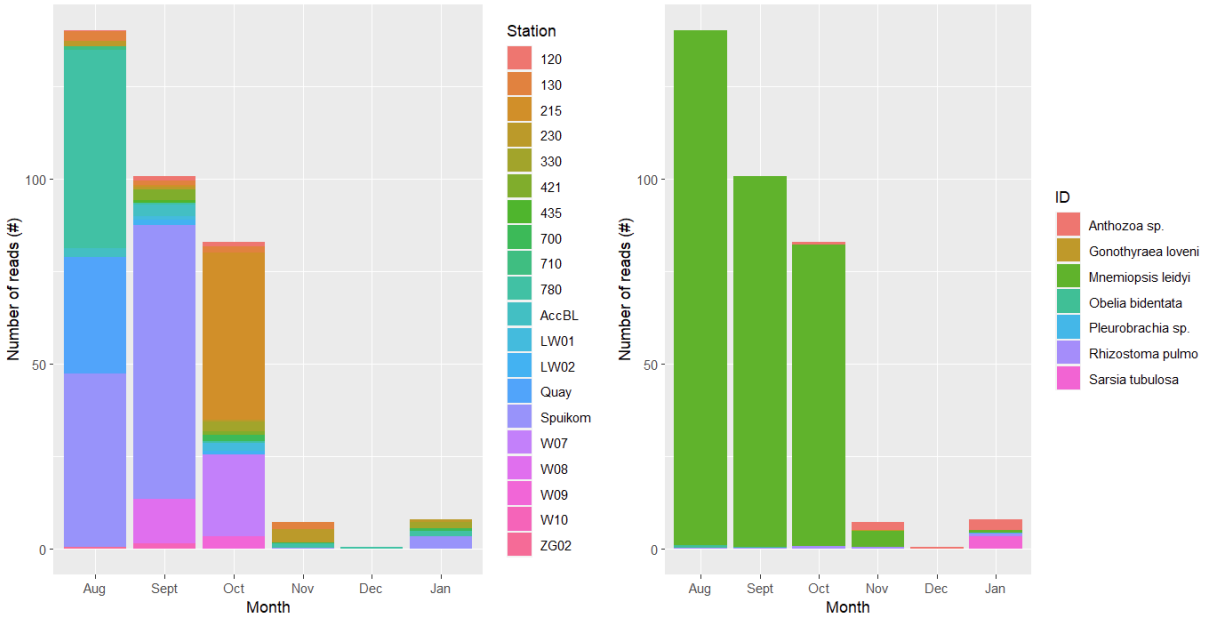

Figure 4-15 *Stacked bar plot of the number of reads (#) per sampling month that are explained by (**A**) the different sampling stations and (**B**) the different species. The number of reads is normalized.*

Table 5 *Species distribution of retrieved eDNA metabarcoding reads throughout the sampling period.*

	August (%)	September (%)	October (%)	November (%)	December (%)	January (%)
Mnemiopsis leidyi	99.2	99.5	98.2	60.4	0	8.5
Anthozoa sp.	0	0	0.8	30.3	100	36.8
Gonothyraea loveni	0	0	0	2.8	0	0
Obelia bidentata	0.5	0.2	0	0	0	0
Pleurobrachia sp.	0	0	0	0	0	4.4
Rhizostoma pulmo	0.2	0.3	1	6.5	0	8.9
Sarsia tubulosa	0	0	0	0	0	41.4

A maximum of two different species is detected per sampling station. In each sampling month, stations without any species detection, stations where one species was detected and stations where two species were detected are found (**Figure 4-16B**).

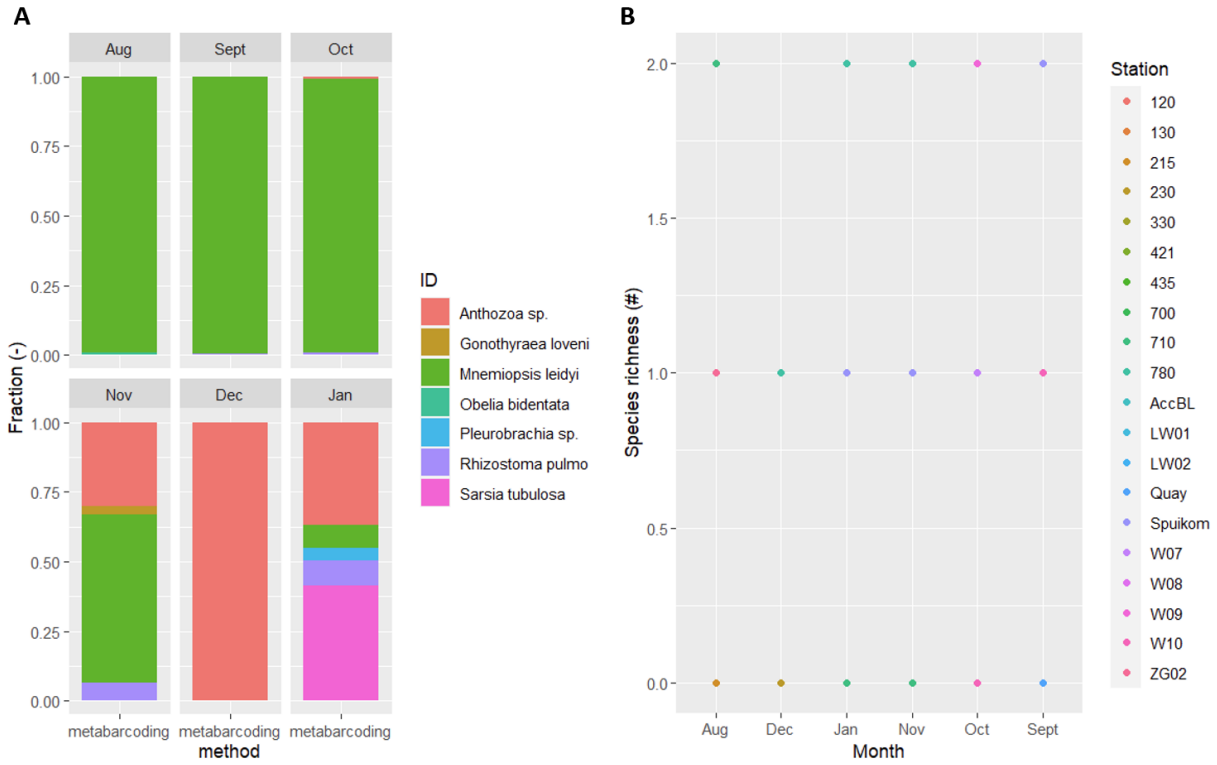

Figure 4-16 (A) Stacked bar plot of major species recovered in the different sampling months through eDNA metabarcoding, independent of location, visualized as fractions. (B) Species richness that is found at the different stations throughout the different sampling months.

4.3.4 Correlation between environmental parameters and barcoding reads

In contrast to the correlation plots made in section 4.2.2, no significant correlations are observed between Cnidaria and Ctenophora reads and environmental parameters including temperature, conductivity, salinity and OBS ($p > 0.05$) (**Figure 4-17**).

Figure 4-17 Correlation plot depicting the correlation (Spearman rank) between Cnidaria and Ctenophora reads (rows) and a selection of measured abiotic parameters (columns). Spearman rho correlation coefficient is shown in each cell. The color of the cell indicates the strength and direction of the correlation, as depicted in the legend.

Correlations between *Mnemiopsis leidyi* reads and environmental parameters (temperature, salinity and OBS) were also evaluated by means of a GAM model (**Figure 4-18**). GAM modelling hardened the absent relation between the observed

parameters and the retrieval of *Mnemiopsis* reads ($p > 0.05$), confirming the output of the correlation plot (**Figure 4-17**). The deviance that is explained in the GAM model is 15.5%. Diagnostic plots for the model are visualized in **Figure A- 17**.

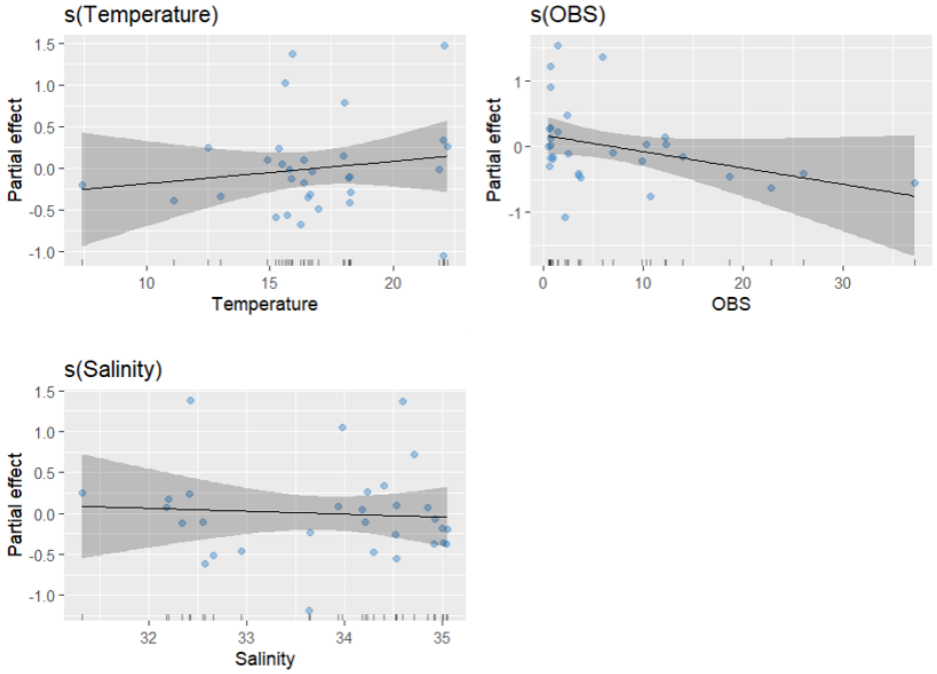

Figure 4-18 *Generalized additive model (GAM) plots showing the partial effects of selected explanatory variables on the log transformed abundances of Mnemiopsis leidyi reads in the survey areas of the Belgian Part of the North Sea. The tick marks on the x-axis are observed data points. The y-axis represents the partial effect of each variable. The shaded areas indicate the 95% confidence intervals.*

4.3.5 Comparison of morphological densities and metabarcoding reads of Cnidaria and Ctenophora

Morphological counts were compared with eDNA metabarcoding reads for 54 sampling events. In 11 samples (20.4%), Cnidaria and/or Ctenophora were physically present, while 34 samples (63.0%) contained eDNA of (one of the) two phyla. In ten of the samples (18.5%), both counts and reads were found, while in 24 samples (44.4%) reads were found but morphological counts were absent. In one sample (W10, sampled in October), Ctenophora were morphologically caught but no eDNA was found. Scatterplots are used to compare the morphological densities with the reads retrieved by eDNA metabarcoding. No significant correlation is found between the densities (counts) and reads for both phyla (**Figure 4-19**).

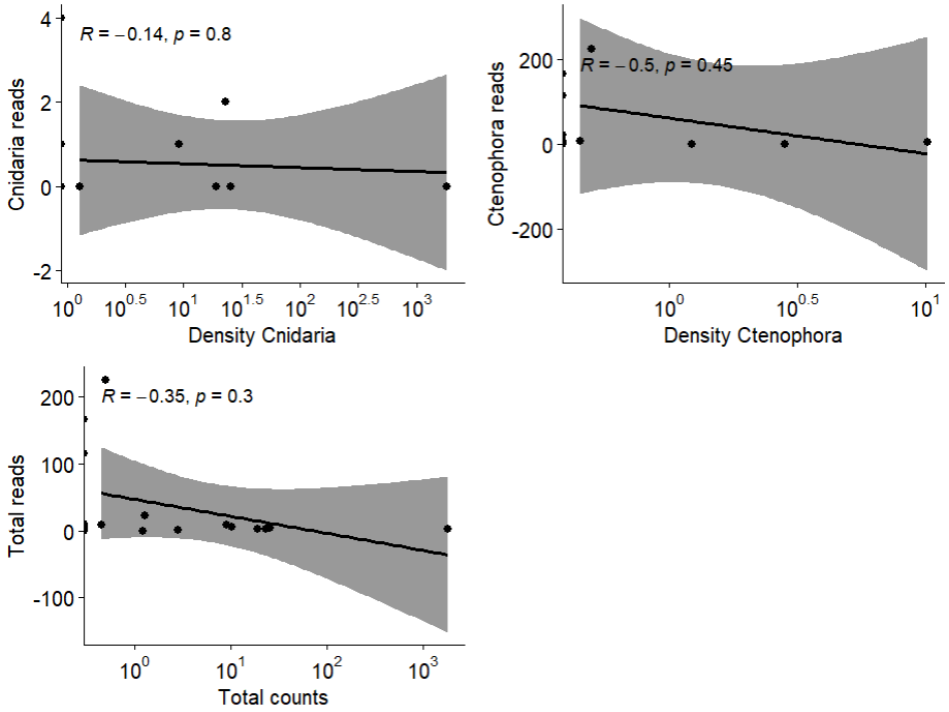

Figure 4-19 Correlation between the number of barcodes detected expressed in reads and the (log-transformed) number of individuals detected by morphology, expressed in densities (counts) for (A) Cnidaria, (B) Ctenophora and (C) the sum of both phyla. The R and p-value are indicated for the regression axis, as is the 95% confidence interval.

5 Discussion

5.1 Trends in Cnidaria and Ctenophora dynamics

5.1.1 Spatial trends

Our results based on the monitoring dataset indicate that Cnidaria and Ctenophora blooms do not differ significantly among different sampling locations (**Figure 4-7**). Blooms do not occur significantly more frequent at nearshore stations than at far-offshore stations, independent of the used sampling technique (morphology or eDNA metabarcoding). The different identified species with eDNA metabarcoding were detected at both near- and far offshore locations (**Figure 4-14**). We do have to note that for eDNA metabarcoding, more reads were found at nearshore stations compared to far-offshore stations in both September and October (7.1% nearshore versus 3.0% far-offshore in September and 61.2% versus 7.7% in October, see **Table 4**). However, in the other sampling months, far-offshore stations were not sampled and no clear comparison or significant trend can thus be observed.

In contrast to these findings, Vansteenbrugge et al. (2015) found that average densities of gelatinous zooplankton gradually declined towards open sea in the BPNS between March 2011 and February 2012. The highest densities were found in coastal and lower estuary locations. This is also confirmed by Doyle et al. (2007), who found that extensive jellyfish aggregations of *Rhizostoma pulmo* were mainly located at the mouth of three estuarine bays. Similarly, Van Ginderdeuren et al. (2012) observed *Mnemiopsis leidyi* all along the Belgian coastline up to 27 km offshore, while further offshore the ctenophore was not found anymore. A possible explanation for these observations may be that there is an increased availability of hard substrate in coastal zones on which benthic polyps can proliferate (Falkenhaug, 2014). Besides that, high nutrient inputs nearshore may eventually result in an increased food source for gelatinous zooplankton (Dong et al., 2010; Quiñones et al., 2018; Vansteenbrugge et al., 2015). An increase in phytoplankton can also lead to higher jellyfish abundances and thus blooms (Møller & Riisgård, 2007a; Wright et al., 2021).

The (insignificant) higher number of nearshore metabarcoding reads in September and October (**Table 4**), together with the fact that a substantial amount of reads is addressed to the constructed harbor section "Spuikom" in August, September and January (33.5%, 73.3% and 41.5%, respectively), could thus be linked with nutrient concentrations, phytoplankton concentrations and the availability of hard substrate. We did indeed observe significantly higher nutrient concentrations nearshore (**Figure A- 3**), as well as a positive correlation between pigment concentrations (which indicate the presence of phytoplankton) and jellyfish blooms (**Figure 4-9**).

One way to account for the fact that we did not observe any significant spatial trends for Cnidaria and Ctenophora dynamics for neither of the sampling techniques is by looking at the water temperature. Several studies declare that higher water temperatures are found closer to the coast line (Van Ginderdeuren et al., 2014; van Keeken et al., 2007; Vansteenbrugge et al., 2015). As there is a significantly strong positive correlation between water temperature and Cnidaria and Ctenophora blooms (**Figure 4-8A**, **Figure 4-10**, **Figure 4-11**), it stands to reason that greater blooms are observed closer to the shore. However, we did not find any significant differences between sampling stations and water temperature (**Figure A- 2**). This, together with the fact that correlations between blooms and nutrients were low (**Figure 4-8B**), might explain why no significant distinctions between blooms among different locations are observed. This hypothesis is in turn contradicted by the strong correlation between blooms and pigment concentrations, which are also significantly higher nearshore.

5.1.2 Temporal trends

We found that Cnidaria and Ctenophora blooms are significantly greater in spring and summer months compared to winter and fall. When visually comparing bloom concentrations with the temperature throughout the year, a clear link is observed (**Figure 4-3** and **Figure 4-6**). Correlations between water temperature and blooms of both phyla are indeed significant (**Figure 4-8A**). Aligned with this, most eDNA metabarcoding reads are found in August and September (**Table 4**, **Figure 4-15**). However, no significant correlation between temperature and Cnidaria/Ctenophora reads is found, which is probably due to a lack of data (**Figure 4-17**).

The positive link between temperature and gelatinous blooms is confirmed in multiple studies: Lynam et al. (2011) state that most cnidarians occur between May and August in the Irish Sea, while Vansteenbrugge et al. (2015) recorded the highest gelatinous zooplankton densities in the BPNS in summer and fall. Purcell et al. (2007) state that 18 out of 24 studied moderate-temperature species globally increase with higher water temperatures. Similar observations are found in other studies (Attrill et al., 2007; Dong et al., 2010; Falkenhaug, 2014; Holst, 2012a; Lynam et al., 2004).

Other environmental parameters such as salinity, nutrients and pigments also significantly differ throughout the year. Salinity is significantly lower in e.g., August compared to October, which explains the strong negative correlation with blooms (**Figure 4-8A**): high bloom densities occur at lower salinity concentrations, and as blooms are greater in spring and summer, lower salinities are to be expected in these seasons. This relationship is confirmed in literature: according to Xing et al. (2020), the optimal range of salinity for asexual reproduction of *Aurelia coerulea* polyps is 25 – 33 PSU, with higher salinities significantly reducing the number of new buds or ephyrae. For *Chrysaora quiquecirrha*, ephyrae and polyp production are the highest between 11 and 25 PSU (Purcell et al., 1999). This indicates that the effect of salinity is species-dependent.

Phosphate and silicate concentrations are negatively correlated with Cnidaria blooms (**Figure 4-8B**). Higher bloom concentrations (in summer) occur when nutrient concentrations are lower, which is indeed the case in spring and summer. This can be explained by the fact that from spring on, a lot of nutrients are used up for phytoplankton growth. This increase in phytoplankton results in higher pigment concentrations in spring and summer. Phytoplankton is consumed by zooplankton, which acts as the primary food source for Cnidaria and Ctenophora (Falkenhaug, 2014). In this way, increased bloom concentrations can be linked with higher pigment concentrations and reduced nutrient concentrations. These findings are confirmed in literature: Excessive nutrients lead to phytoplankton blooms, which increase polyp and medusa abundance and lead to oxygen depletion and higher turbidity, favoring jellyfish once again (Dong et al., 2010; Purcell et al., 2007; Wright et al., 2021). As medusae consume zooplankton, blooms can be observed along with high phytoplankton concentrations and low zooplankton abundances (Møller & Riisgård, 2007a).

5.2 Accuracy of eDNA metabarcoding

Based on eDNA metabarcoding, seven species were found, distributed between both nearshore and far-offshore stations. As far-offshore stations were only sampled in September and October, analysis of a spatial distribution (nearshore versus far-offshore) is only based on these two months. As discussed in section 5.1.1, more reads are found nearshore, indicating that Cnidaria/Ctenophora are slightly more present in these locations, which is in line with findings from literature (Doyle et al., 2007; Van Ginderdeuren, Hostens, et al., 2012; Vansteenbrugge et al., 2015). However, due to the limited amount of data, one should be careful about drawing conclusions. Two stations situated in constructed harbor sections were also sampled: Spuikom (sampled in August, September, November and January) and quay (sampled in August and December). 56.0%, 73.3%, 2.8% and 41.5% of reads originated from constructed harbor sections in August, September, November and January, respectively. This seems to confirm the findings of Doyle et al. (2007) and Vansteenbrugge et al. (2015) that high(est) densities are found in more estuarine conditions (see section 5.1.1).

It is clear that more reads are found in summer compared to fall and winter (**Figure 4-15**), which is consistent with literature (Lynam et al., 2011; Purcell et al., 2007; Vansteenbrugge et al., 2015). A comparison with spring cannot be made due to a lack of data (no samples were taken in spring). *Mnemiopsis leidyi* was the most abundant species and was found throughout the whole sampling period except for December, probably due to problems with DNA sequencing in the laboratory. Although more reads are found in August (140.22) compared to e.g., December (0.51), no significant correlation is found between Cnidaria/Ctenophora reads and temperature or salinity (**Figure 4-17**). This may again be explained by the lack of data on which the correlation plot is based.

At first glance, in this thesis, the spatial trends in Cnidaria/Ctenophora dynamics based on eDNA metabarcoding do not correspond well with the morphological observations for the BPNS, but, since a higher number of reads is seen at nearshore samples and constructed harbor sections (**Table 4**), do correspond well with findings from literature. However, no significant differences between near- and far-offshore locations could be proven, resulting in the same conclusion considering spatial trends as with morphological data (blooms). Temporal trends based on morphological data and eDNA metabarcoding correspond at first sight: bloom concentrations and metabarcoding reads are higher in summer compared to e.g., fall and winter. For metabarcoding however, these differences could not be explained statistically (no significant differences, $p > 0.01$).

The discrepancy between both sampling techniques becomes clear when comparing morphological densities with eDNA metabarcoding reads: no significant correlations can be derived (**Figure 4-19**). This is in sharp contrast with Semmouri et al. (2021), who found a significant positive correlation comparing the relative number of reads in a sample with the abundance of the corresponding taxa obtained through morphological identification ($R^2 = 0.37$, $p < 0.04$). Similarly, Serrana et al. (2019) found significant positive correlations between the total abundance of morphological taxa of macroinvertebrates and the read abundance of meta-taxa for all the examined sites ($R^2 = 0.18$, $p = 0.02$), while Yang et al. (2017) reported a significant positive correlation between the frequency of zooplankton species in metabarcoding and morphological identification ($R^2 = 0.43$, $p < 0.0001$). In these three studies however, DNA is used instead of eDNA, which can alter the results e.g., because the release, transport and degradation of eDNA is species-dependent (Deiner et al., 2017). Other differences are that Semmouri et al. (2021) used a different extraction protocol (CTAB) and amplified the 18S rRNA gene instead of the 18S rDNA gene in this thesis. Both Yang et al. (2017) and Serrana et al. (2019) amplified the COI (Cytochrome c Oxidase Subunit I)-gene, while the methods for sequencing were Ion Torrent and pyrosequencing, respectively.

Feng et al. (2022) conclude that eDNA metabarcoding revealed a higher richness at phylum, class and order level compared to morphological processing (based on net sampling). Djurhuus et al. (2018) detected all dominant copepod taxa with both eDNA and morphological assessments, demonstrating that eDNA metabarcoding is a promising technique for future biodiversity assessments of pelagic zooplankton. These findings are affirmed by Deiner et al. (2017) who state that eDNA metabarcoding leads to a greater diversity and an increased resolution of taxonomic identifications compared to conventional methods. Similarly, Semmouri et al. (2021) state that taxa were detected with a higher resolution when using DNA metabarcoding instead of morphological observations (10 – 33 taxa versus 8 – 14 taxa, respectively). In this thesis however, it was not possible to compare different taxa (i.e., phylum, class, order, family, genus and species) between eDNA metabarcoding and morphology, as the latter gave information only to the level of phylum. We did however see that both phyla (Cnidaria and Ctenophora) were detected more frequently when using eDNA compared to morphology (detection in 63.0% and 20.4% of the samples for eDNA and morphology, respectively). Additionally, in 44.4% of the samples, reads were detected while morphological counts were absent. This might be due to the fact that eDNA is still present from earlier deceased species, originates from another location where the species did occur physically or that the WP2 net was situated just outside the bloom and accidentally did not catch any gelatinous zooplankton. At one sampling event (station W10 in October), Ctenophora was morphologically present while no eDNA was found. Possible causes for this are e.g., that the species did not release a substantial amount of eDNA into the water, that the individual was accidentally caught in the water even though its presence was negligible or that false negatives in the laboratory caused the species not to be found.

In this thesis, five Cnidaria species (*Anthozoa* sp., *Gonothyraea loveni*, *Obelia bidentata*, *Rhizostoma pulmo* and *Sarsia tubulosa*) and two Ctenophora species (*Mnemiopsis leidyi* and *Pleurobrachia* sp.) were detected. *Mnemiopsis leidyi* and *Rhizostoma pulmo* were found throughout the whole sampling period (August 2022 – January 2023), except for December (**Figure 4-16A**). Similarly, Van Ginderdeuren, Hostens, et al. (2012) detected *M. leidyi* in the BPNS in all seasons, even in winter months when water temperatures were 2°C, while peaks were observed in October. Houghton et al. (2007) found that *Rhizostoma pulmo* stranded throughout the entire year in the Irish and Celtic Seas. Anthozoan species were detected from October until January (**Table 5**). No clear data indicating the presence of Anthozoa in winter in the North Sea has been found, while Krone et al. (2013) did demonstrate they occurred in spring, summer and fall. Ates et al. (1998) did conclude that *Sagartia elegans* (an anthozoan species) is sensitive to cold temperatures and can disappear during severe winters along the Dutch coast. The fact that *Anthozoa* sp. were still detected in December and January may thus be because eDNA is still present from earlier deceased individuals, or that it is originating from polyps. We detected both *Pleurobrachia* sp. and *Sarsia tubulosa* solely in January. This is contradicted by Vansteenbrugge et al. (2015), who retrieved *Pleurobrachia pileus* in all seasons in the BPNS, peaking in summer. Møller & Riisgård (2007b) detected *Sarsia tubulosa* amongst others in the beginning of February in Denmark (Limfjorden), suggesting that they can cope with lower water temperatures. Finally, we detected *Gonothyraea loveni* in November and *Obelia bidentata* in August and September. No temporal distribution is found for *G. loveni* in literature, but we do know the species has been registered in the BPNS already (WORMS, 2004). Vansteenbrugge et al. (2015) found *Obelia sp.* mainly in winter in the BPNS, contradicting our findings based on eDNA metabarcoding.

A possible explanation for the fact that some species were only detected in winter is that *M. leidyi* bloomed in summer, shedding substantial amounts of eDNA into the water which led to an underestimation of the other occurring species. In reality, it is thus possible that the other species also occurred in summer, but were not detected due to the unbalanced proportions in eDNA. This might also explain the discrepancy between the amount of reads: in August, September and October, 99.2%, 99.5% and 98.2% of all reads were assigned to *Mnemiopsis leidyi*, respectively (**Table 5**). This hypothesis is confirmed by Deiner et al. (2017), who state that the rate at which eDNA is produced, transported and degraded is species-dependent. Another explanation can be that PCR bias occurred, resulting in the preferential amplification of certain taxa (Gold et al., 2021). The SILVA eukaryote reference database (Quast et al., 2013) also has its limitations, possibly affecting distinctions between species and thus the accuracy of taxonomic assignment from eDNA (Gold et al., 2021).

eDNA metabarcoding has several advantages: it is cost- and time efficient, less laborious and causes less disturbance to the marine environment compared to morphological sampling (Ames et al., 2021; Miya, 2022; Takasu et al., 2019). Several studies indicate that higher levels of richness can be found at different levels of taxonomy, increasing the resolution and thus accuracy of taxonomic identifications (Deiner et al., 2017; Feng et al., 2022). Based on our data however, no significantly higher accuracy could be proven compared to morphological sampling, which is primarily the result of a lack of data.

5.3 Future challenges and opportunities

No significant trends were discovered based on eDNA metabarcoding. The insignificant results in both spatial and temporal trends are primarily attributed to a lack of data. Two main problems are present. Firstly, samples were taken in a time period of only half a year, in which the spring season and part of summer and winter were left out. By sampling over a bigger time frame (each month for one or more years), both temporal and spatial trends can be examined in more detail. Secondly, sampling was performed once per month. However, as jellyfish blooms appear rapid and sudden, blooms can be present on a certain day and be gone again one week later (Lucas et al., 2012; West et al., 2009). Increasing the sampling frequency is thus necessary in order to obtain clearer, more thrust-worthy results. When comparing the results with morphological catches, it might also be interesting to take multiple samples with the WP2 net at each sampling location, as blooms are not evenly distributed in the water.

One could also increase the efficiency of the annotation process of the sequences of interest and their accuracy by performing a cluster analysis prior to BLAST, simplifying the output (Mier & Andrade-Navarro, 2016). Additionally, an alternative to nanopore sequencing is Illumina sequencing, which has the benefits of having a higher accuracy (99% versus 92-97% for nanopore sequencing, a higher Phred score is used) and can thus potentially lead to an improved sequencing yield (Samanthi, 2021).

Instead of demultiplexing using the Guppy software, one could choose to use Porechop for adapter removal and demultiplexing of the reads. This might lead to improved results as Porechop is also specifically developed for Oxford Nanopore reads. The usage of the Kraken2 software for taxonomic sequencing classification may also positively influence the output and number of reads that remain for analysis, possibly ensuring better results compared to the BLAST that was performed. In future studies, the accuracy and efficiency of these tools should be evaluated and compared to the workflow that we have employed in this thesis.

6 Conclusion

We investigated whether it was possible to predict jellyfish blooms in the BPNS on the basis of eDNA metabarcoding. This technique was compared to morphological data, obtained by physically catching Cnidaria and Ctenophora using a WP2 net. Our results confirm that both Cnidaria and Ctenophora can be detected on the basis of eDNA: five Cnidaria species and two Ctenophora species were found. However, through the eDNA workflow, no significant spatial and/or temporal patterns were observed. Nevertheless, it was clear that a relatively high percentage of the reads originated from constructed harbor sections, while warmer months incorporated more reads than colder ones.

As is the case with eDNA, no significant spatial trends were observed based on morphology. Looking at temporal trends however, we did find significantly higher bloom concentrations in summer months for both phyla. Based on morphology, strong correlations between blooms and environmental parameters such as temperature, salinity and different pigments were observed. For eDNA metabarcoding, only correlations with temperature, conductivity, salinity and OBS could be explored, but none of these were significant. Additionally, no significant relation was found between eDNA metabarcoding reads and morphological counts, indicating that both methods did not cohere well.

In summary, our results suggest that eDNA metabarcoding can be a valuable approach to detect Cnidaria and Ctenophora species but does not suffice to predict the occurrence of jellyfish blooms. Although other studies indicated the promise of eDNA metabarcoding in acquiring an improved understanding for global patterns in zooplankton diversity, additional effort is needed to increase sampling frequency and sampling period to enable a comprehensive exploration of gelatinous zooplankton and the occurrence of jellyfish blooms in the BPNS.

Bibliography

Abato, J., Asselman, J., & Janssen, C. (2017). *Monitoring Chrysaora hysoscella (Cnidaria, Scyphozoa) in the Belgian part of the North Sea using Environmental DNA (eDNA).* [Ghent University]. https://libstore.ugent.be/fulltxt/RUG01/002/352/302/RUG01-002352302_2017_0001_AC.pdf

AKlompen. (2019). *Man-of-War venom, and the discovery of anaphylaxis*. Gelatinous Sting. https://gelatinoussting.com/2019/01/14/man-of-war-venom-and-the-discovery-of-anaphylaxis/

Alberto Bezares-Calderón, L., Jékely, G., & Berger, J. (2019). *Diversity of cilia-based mechanosensory systems and their functions in marine animal behaviour*. https://doi.org/10.1098/rstb.2019.0376

Ames, C. L., Ohdera, A. H., Colston, S. M., Collins, A. G., Fitt, W. K., Morandini, A. C., Erickson, J. S., & Vora, G. J. (2021). Fieldable Environmental DNA Sequencing to Assess Jellyfish Biodiversity in Nearshore Waters of the Florida Keys, United States. *Frontiers in Marine Science*, *8*. https://doi.org/10.3389/fmars.2021.640527

AMNH. (2017). *What Are Jellies_ Cnidarians and Ctenophores _ AMNH*. https://www.amnh.org/explore/news-blogs/news-posts/cnidarians-ctenophores-jellies

Amy Williams, E., Plachetzki, D., Zandawala, M., P Grimmelikhuijzen, C. J., & Koch, T. L. (2019). Global Neuropeptide Annotations From the Genomes and Transcriptomes of Cubozoa, Scyphozoa, Staurozoa (Cnidaria: Medusozoa), and Octocorallia (Cnidaria: Anthozoa). *Frontiers in Endocrinology | Www.Frontiersin.Org*, *10*, 831. https://doi.org/10.3389/fendo.2019.00831

Anderson, P. A. V., & Schwab, W. E. (1981). The organization and structure of nerve and muscle in the jellyfishCyanea capillata (coelenterata; scyphozoa). *Journal of Morphology*, *170*(3), 383–399. https://doi.org/10.1002/jmor.1051700309

Arai, M. N. (1996). *A Functional Biology of Scyphozoa*. Springer Netherlands. https://doi.org/10.1007/978-94-009-1497-1

Ates, R. M. L., Dekker, R., Faasse, M. A., & den Hartog, J. C. (1998). The occurrence of Sagartia elegans (Dalyell, 1848) (Anthozoa: Actiniaria) in the Netherlands. *Zoologische Verhandelingen*, *323*(31).

Attrill, M. J., Wright, J., & Edwards, M. (2007). Climate-related increases in jellyfish frequency suggest a more gelatinous future for the North Sea. *Limnology and Oceanography*, *52*(1). https://doi.org/10.4319/lo.2007.52.1.0480

Avian, M., Motta, G., Prodan, M., Tordoni, E., Macaluso, V., Beran, A., Goruppi, A., Bacaro, G., & Tirelli, V. (2021). *Asexual Reproduction and Strobilation of Sanderia malayensis (Scyphozoa, Pelagiidae) in Relation to Temperature: Experimental Evidence and Implications*. https://doi.org/10.3390/d13020037

Babcock, R. (1990). Reproduction and development of the blue coral Heliopora coerulea (Alcyonaria: Coenothecalia). *Marine Biology*, *104*(3). https://doi.org/10.1007/BF01314352

Baliarsingh, S. K., Lotliker, A. A., Srichandan, S., Samanta, A., Kumar, N., & Nair, T. M. B. (2020). A review of jellyfish aggregations, focusing on India's coastal waters. In *Ecological Processes* (Vol. 9, Issue 1). https://doi.org/10.1186/s13717-020-00268-z

Båmstedt, U., Kaartvedt, S., & Youngbluth, M. (2003). An evaluation of acoustic and video methods to estimate the abundance and vertical distribution of jellyfish. *Journal of Plankton Research*, *25*(11). https://doi.org/10.1093/plankt/fbg084

Bandara, K., Varpe, Ø., Wijewardene, L., Tverberg, V., & Eiane, K. (2021). *Two hundred years of zooplankton vertical migration research*. https://doi.org/10.1111/brv.12715

Barz, K., & Hirche, H. J. (2007). Abundance, distribution and prey composition of scyphomedusae in the southern North Sea. *Marine Biology*, *151*(3). https://doi.org/10.1007/s00227-006-0545-4

Beckmann, A., & Özbek, S. (2012). The nematocyst: A molecular map of the cnidarian stinging organelle. *International Journal of Developmental Biology*, *56*(6–8). https://doi.org/10.1387/ijdb.113472ab

Bennett, C. L., Nicholson, M. D., & Erdman, R. B. (2011). First Record of Copula sivickisi (Cnidaria: Cubozoa) in the Tropical Western Atlantic Ocean: An Enigmatic Occurrence from San Salvador Island, Bahamas. *The 14th Symposium on the Natural History of the Bahamas*, *June*.

Bocharova, E. S., & Kozevich, I. A. (2011). Modes of reproduction in sea anemones (Cnidaria, Anthozoa). *Biology Bulletin*, *38*(9), 849–860. https://doi.org/10.1134/S1062359011090020

Bosch-Belmar, M., Milisenda, G., Basso, L., Doyle, T. K., Leone, A., & Piraino, S. (2020). Jellyfish Impacts on Marine Aquaculture and Fisheries. In *Reviews in Fisheries Science and Aquaculture* (Vol. 29, Issue 2). https://doi.org/10.1080/23308249.2020.1806201

Bouillon, J., Medel, M. D., Pagès, F., Gili, J. M., Boero, F., & Gravili, C. (2004). Fauna of the Mediterranean Hydrozoa. In *Scientia Marina* (Vol. 68, Issue SUPPL. 2). https://doi.org/10.3989/scimar.2004.68s25

Brierley, A. S. (2017). Plankton. *Current Biology*, *27*(11), R478–R483. https://doi.org/10.1016/J.CUB.2017.02.045

Brodeur, R. D., Sugisaki, H., & Hunt, G. L. (2002). Increases in jellyfish biomass in the Bering Sea: Implications for the ecosystem. *Marine Ecology Progress Series*, *233*. https://doi.org/10.3354/meps233089

Bucklin, A., Lindeque, P. K., Rodriguez-Ezpeleta, N., Albaina, A., & Lehtiniemi, M. (2016). Metabarcoding of marine zooplankton: Prospects, progress and pitfalls. *Journal of Plankton Research*, *38*(3). https://doi.org/10.1093/plankt/fbw023

Buecher, E. (1999). Appearance of Chelophyes appendiculata and Abylopsis tetragona (Cnidaria, Siphonophora) in the Bay of Villefranche, northwestern Mediterranean. *Journal of Sea Research*, *41*(4). https://doi.org/10.1016/S1385-1101(99)00005-2

Buecher, E., Jacqueline, G. O. Y., Planque, B., Etienne, M., & Dallot, S. (1997). Long-term fluctuations of Liriope tetraphylla in Villefranche bay between 1966 and 1993 compared to Pelagia noctiluca pullulations. *Oceanologica Acta*, *20*(1).

Capel, K. C. C., Toonen, R. J., Rachid, C. T. C. C., Creed, J. C., Kitahara, M. V., Forsman, Z., & Zilberberg, C. (2017). Clone wars: Asexual reproduction dominates in the invasive range of Tubastraea spp. (Anthozoa: Scleractinia) in the South-Atlantic Ocean. *PeerJ*, *2017*(10). https://doi.org/10.7717/peerj.3873

Cartwright, P., & Nawrocki, A. M. (2010). Character Evolution in Hydrozoa (phylum Cnidaria). *Integrative and Comparative Biology*, *50*(3), 456–472. https://doi.org/10.1093/icb/icq089

Cegolon, L., Heymann, W. C., Lange, J. H., & Mastrangelo, G. (2013). Jellyfish stings and their management: A review. In *Marine Drugs* (Vol. 11, Issue 2). https://doi.org/10.3390/md11020523

Chen, Y. N., & Wang, H. (2015). Jellyfish mesoglea as a matrix for the synthesis of extremely high content silver dendrites. *Journal of Colloid and Interface Science*, *454*. https://doi.org/10.1016/j.jcis.2015.04.052

Chi, X., Dierking, J., Hoving, H.-J., Lüskow, F., Denda, A., Christiansen, B., Sommer, U., Hansen, T., & Javidpour, J. (2021). Tackling the jelly web: Trophic ecology of gelatinous zooplanktonin oceanic food webs of the eastern tropical Atlantic assessed by stableisotope analysis. *Limnol. Oceanogr*, *66*, 289–305. https://doi.org/10.1002/lno.11605

Çinar, M. E., Yokeş, M. B., Açik, Ş., & Bakir, A. K. (2014). Checklist of Cnidaria and Ctenophora from the coasts of Turkey. In *Turkish Journal of Zoology* (Vol. 38, Issue 6). https://doi.org/10.3906/zoo-1405-68

Clarke, A., Holmes, L. J., & Gore, D. J. (1992). Proximate and elemental composition of gelatinous zooplankton from the Southern Ocean. *Journal of Experimental Marine Biology and Ecology*, *155*(1). https://doi.org/10.1016/0022-0981(92)90027-8

Coates, M. M. (2003). Visual ecology and functional morphology of Cubozoa (Cnidaria). *Integrative and Comparative Biology*, *43*(4). https://doi.org/10.1093/icb/43.4.542

Collins, A. G., & Daly, M. (2005). A new deepwater species of stauromedusae, Lucernaria janetae (Cnidaria, Staurozoa, Lucernariidae), and a preliminary investigation of stauromedusan phylogeny based on nuclear and mitochondrial rDNA data. *Biological Bulletin*, *208*(3). https://doi.org/10.2307/3593154

Condon, R. H., Graham, W. M., Duarte, C. M., Pitt, K. A., Lucas, C. H., Haddock, S. H. D., Sutherland, K. R., Robinson, K. L., Dawson, M. N., Decker, M. B., Mills, C. E., Purcell, J. E., Malej, A., Mianzan, H., Uye, S., Gelcich, S., & Madin, L. P. (2012). Questioning the Rise of Gelatinous Zooplankton in the World's Oceans. *BioScience*, *62*(2), 160–169. https://doi.org/10.1525/bio.2012.62.2.9

Courtney, R., & Seymour, J. (2013). Seasonality in Polyps of a Tropical Cubozoan: A latina nr mordens. *PLoS ONE*, *8*(7), 69369. https://doi.org/10.1371/journal.pone.0069369

D. Cairns, S., & Gail Fautin, D. (2009). Cnidaria: Introduction. In D. L.Felder & D. K. Camp (Eds.), *Gulf of Mexico Origin, Waters, and Biota: Volume 1, Biodiversity*. Texas A & M University Press.

D'Ambra, I., & Lauritano, C. (2020). A Review of Toxins from Cnidaria. *Marine Drugs*, *18*(10), 507. https://doi.org/10.3390/md18100507

Daskalov, G. M., Grishin, A. N., Rodionov, S., & Mihneva, V. (2007). Trophic cascades triggered by overfishing reveal possible mechanisms of ecosystem regime shifts. *Proceedings of the National Academy of Sciences of the United States of America*, *104*(25). https://doi.org/10.1073/pnas.0701100104

Dawson, M. N., & Martin, L. E. (2001). Geographic variation and ecological adaptation in Aurelia (Scyphozoa, Semaeostomeae): Some implications from molecular phylogenetics. *Hydrobiologia*, *451*. https://doi.org/10.1023/A:1011869215330

Dawson, M. N., Martin, L. E., & Penland, L. K. (2001). Jellyfish swarms, tourists, and the Christ-child. *Hydrobiologia*, *451*. https://doi.org/10.1023/A:1011868925383

Deiner, K., Bik, H. M., Mächler, E., Seymour, M., Lacoursière-Roussel, A., Altermatt, F., Creer, S., Bista, I., Lodge, D. M., Vere, N., Pfrender, M. E., & Bernatchez, L. (2017). Environmental DNA metabarcoding: Transforming how we survey animal

and plant communities. *Molecular Ecology*, *26*(21), 5872–5895. https://doi.org/10.1111/mec.14350

Dekker, E., Dulière, V., & Lacroix, G. (2016). How vertical swimming behaviour affects jellyfish journey? *North Sea Open Science Conference*. https://odnature.naturalsciences.be/downloads/publications/dekker_etal_amemr2017_poster_a4.pdf

Diel, P., Kiene, M., Martin-Creuzburg, D., & Laforsch, C. (2020). *diversity Knowing the Enemy: Inducible Defences in Freshwater Zooplankton*. https://doi.org/10.3390/d12040147

Djurhuus, A., Pitz, K., Sawaya, N. A., Rojas-Márquez, J., Michaud, B., Montes, E., Muller-Karger, F., & Breitbart, M. (2018). Evaluation of marine zooplankton community structure through environmental DNA metabarcoding. *Limnology and Oceanography: Methods*, *16*(4). https://doi.org/10.1002/lom3.10237

Djurhuus, A., Port, J., Closek, C. J., Yamahara, K. M., Romero-Maraccini, O., Walz, K. R., Goldsmith, D. B., Michisaki, R., Breitbart, M., Boehm, A. B., & Chavez, F. P. (2017). Evaluation of filtration and DNA extraction methods for environmental DNA biodiversity assessments across multiple trophic levels. *Frontiers in Marine Science*, *4*(OCT). https://doi.org/10.3389/fmars.2017.00314

Dong, Z., Liu, D., & Keesing, J. K. (2010). Jellyfish blooms in China: Dominant species, causes and consequences. *Marine Pollution Bulletin*, *60*(7). https://doi.org/10.1016/j.marpolbul.2010.04.022

Doyle, T. K., Houghton, J. D. R., Buckley, S. M., Hays, G. C., & Davenport, J. (2007). The broad-scale distribution of five jellyfish species across a temperate coastal environment. *Hydrobiologia*, *579*(1). https://doi.org/10.1007/s10750-006-0362-2

Drew, E. A. (1972). The biology and physiology of alga-invertebrates symbioses. II. The density of symbiotic algal cells in a number of hermatypic hard corals and alcyonarians from various depths. *Journal of Experimental Marine Biology and Ecology*, *9*(1). https://doi.org/10.1016/0022-0981(72)90008-1

Duarte, C. M., Pitt, K. A., Lucas, C. H., Purcell, J. E., Uye, S. I., Robinson, K., Brotz, L., Decker, M. B., Sutherland, K. R., Malej, A., Madin, L., Mianzan, H., Gili, J. M., Fuentes, V., Atienza, D., Pages, F., Breitburg, D., Malek, J., Graham, W. M., & Condon, R. H. (2013). Is global ocean sprawl a cause of jellyfish blooms? *Frontiers in Ecology and the Environment*, *11*(2). https://doi.org/10.1890/110246

Dulière, V., Kerckhof, F., & Lacroix, G. (2014). Where is my jelly. *De Strandvlo*, *34(2)*, 48–56. https://odnature.naturalsciences.be/downloads/publications/dulieereetal_2014_whereismyjelly.strandvlo34(2).pdf

Eveland, L. L., Bohenek, J. R., Silberbush, A., & Resetarits, W. J. (2016). Detection of Fish and Newt Kairomones by Ovipositing Mosquitoes. In *Chemical Signals in Vertebrates 13* (pp. 247–259). Springer International Publishing. https://doi.org/10.1007/978-3-319-22026-0_18

Faasse, M., & Waajen, S. (2011). De steelkwallen van Nederland (Cnidaria: Staurozoa). *Nederlandse Faunistische Mededelingen*, *35*, 61–67. https://natuurtijdschriften.nl/pub/1002077

Fahlke, C., Santos, M. I. B., Neely, A., Senatore, A., Raiss, H., & Le, P. (2016). Physiology and Evolution of Voltage-Gated Calcium Channels in Early Diverging Animal Phyla: Cnidaria, Placozoa, Porifera and Ctenophora. *HYPOTHESIS AND THEORY Frontiers in Physiology | Www.Frontiersin.Org*, *1*, 481. https://doi.org/10.3389/fphys.2016.00481

Falkenhaug, T. (2014). Review of Jellyfish Blooms in the Mediterranean and Black Sea. *Marine Biology Research*, *10*(10). https://doi.org/10.1080/17451000.2014.880790

Feng, Y., Sun, D., Shao, Q., Fang, C., & Wang, C. (2022). Mesozooplankton biodiversity, vertical assemblages, and diel migration in the western tropical Pacific Ocean revealed by eDNA metabarcoding and morphological methods. *Frontiers in Marine Science*, *9*. https://doi.org/10.3389/fmars.2022.1004410

Fenner, P. J. (2005). Venomous jellyfish of the world. In *South Pacific Underwater Medicine Society Journal* (Vol. 35, Issue 3).

Flanders Marine Institute (VLIZ). (2023). *Exploring station data*. https://rshiny.lifewatch.be/station-data/

Fleming, N. E. C., Harrod, C., & Houghton, J. D. R. (2013). Identifying potentially harmful jellyfish blooms using shoreline surveys. *Aquaculture Environment Interactions*, *4*(3). https://doi.org/10.3354/aei00086

Frazão, B., Vasconcelos, V., & Antunes, A. (2012). Sea Anemone (Cnidaria, Anthozoa, Actiniaria) Toxins: An Overview. *Mar. Drugs*, *10*, 1812–1851. https://doi.org/10.3390/md10081812

Fukushi, K., Ishio, N., Tsujimoto, J., Yokota, K., Hamatake, T., Sogabe, H., Toriya, K., & Ninomiya, T. (2003). Preliminary Study on the Potential Usefulness of Jellyfish as Fertilizer. *Bulletin of the Society of Sea Water Science, Japan*. https://www.jstage.jst.go.jp/article/swsj1965/58/2/58_209/_pdf/-char/ja

Gadelha, J. R., Morgado, F., & Soares, A. M. V. M. (2012). Histological and Structural Analysis of Actinia equina L. (Cnidaria: Anthozoa) . *Microscopy and Microanalysis*, *18*(S5). https://doi.org/10.1017/s1431927612012962

Gambill, M., McNaughton, S. L., Kreus, M., & Peck, M. A. (2018). Temperature-dependent settlement of planula larvae of two scyphozoan jellyfish from the North Sea. *Estuarine, Coastal and Shelf Science*, *201*.

https://doi.org/10.1016/j.ecss.2016.08.042
Gershwin, L. (2005). *Taxonomy and phylogeny of Australian Cubozoa* [James Cook University]. https://researchonline.jcu.edu.au/27395/1/27395_Gershwin_2005_thesis.pdf
Gershwin, L. A. (2006). Nematocysts of the Cubozoa. In *Zootaxa* (Issue 1232). https://doi.org/10.11646/zootaxa.1232.1.1
Gershwin, L., Lewis, M., Gowlett-Holmes, K., & Kloser, R. (2014). The Ctenophores. In *Pelagic Invertebrates of South-Eastern Australia: A field reference guide*. CSIRO Marine and Atmospheric Research. https://publications.csiro.au/rpr/download?pid=csiro:EP1312314&dsid=DS2
Goffredo, S., & Dubinsky, Z. (2016). The cnidaria, past, present and future: The world of Medusa and her sisters. In *The Cnidaria, past, present and Future: The World of Medusa and her Sisters*. https://doi.org/10.1007/978-3-319-31305-4
Gold, Z., Sprague, J., Kushner, D. J., Marin, E. Z., & Barber, P. H. (2021). eDNA metabarcoding as a biomonitoring tool for marine protected areas. *PLoS ONE*, *16*(2 February 2021). https://doi.org/10.1371/journal.pone.0238557
Govindarajan, A. F., Carman, M. R., Khaidarov, M. R., Semenchenko, A., & Wares, J. P. (2017). Mitochondrial diversity in Gonionemus (Trachylina: Hydrozoa) and its implications for understanding the origins of clinging jellyfish in the Northwest Atlantic Ocean. *PeerJ*, *2017*(4). https://doi.org/10.7717/peerj.3205
Goy, J., Morand, P., & Etienne, M. (1989). Long-term fluctuations of Pelagia noctiluca (Cnidaria, Scyphomedusa) in the western Mediterranean Sea. Prediction by climatic variables. *Deep Sea Research Part A, Oceanographic Research Papers*, *36*(2). https://doi.org/10.1016/0198-0149(89)90138-6
Graham, W. M., Gelcich, S., Robinson, K. L., Duarte, C. M., Brotz, L., Purcell, J. E., Madin, L. P., Mianzan, H., Sutherland, K. R., Uye, S. I., Pitt, K. A., Lucas, C. H., Bøgeberg, M., Brodeur, R. D., & Condon, R. H. (2014). Linking human well-being and jellyfish: Ecosystem services, impacts, and societal responses. In *Frontiers in Ecology and the Environment* (Vol. 12, Issue 9). https://doi.org/10.1890/130298
Graham, W. M., Pagès, F., & Hamner, W. M. (2001). A physical context for gelatinous zooplankton aggregations: A review. *Hydrobiologia*, *451*. https://doi.org/10.1023/A:1011876004427
Greve, W., Lange, U., Reiners, F., & Nast, J. (2001). Predicting the seasonality of North Sea zooplankton. *Senckenbergiana Maritima*, *31*(2). https://doi.org/10.1007/BF03043035
Grohmann, P. A., Magalhaes, M. P., & Hirano, Y. M. (1999). First Record of the Order Stauromedusae (Cnidaria, Scyphozoa) from the Tropical Southwestern Atlantic, with a Review of the Distribution of Stauromedusae in the Southern Hemisphere. *Species Diversity*, *4*(2). https://doi.org/10.12782/specdiv.4.381
Gueroun, S. K. M., Javidpour, J., Andrade, C., Nogueira, N., Freitas, M., & Canning-Clode, J. (2021). Pelagic Cnidaria and Ctenophora diversity patterns and trends in Macaronesia insular systems (NE Atlantic). *Marine Biodiversity*, *51*(2). https://doi.org/10.1007/s12526-021-01174-z
Haddock, S. H. D. (2007). *Comparative feeding behavior of planktonic ctenophores*. https://doi.org/10.1093/icb/icm088
Hadziavdic, K., Lekang, K., Lanzen, A., Jonassen, I., Thompson, E. M., & Troedsson, C. (2014). Characterization of the 18s rRNA gene for designing universal eukaryote specific primers. *PLoS ONE*, *9*(2). https://doi.org/10.1371/journal.pone.0087624
Hale, G. (1999). The classification and distribution of the class Scyphozoa. In *pH thesis*.
Hamner, W. M., & Dawson, M. N. (2009). A review and synthesis on the systematics and evolution of jellyfish blooms: Advantageous aggregations and adaptive assemblages. *Hydrobiologia*, *616*(1). https://doi.org/10.1007/s10750-008-9620-9
He, S. (2004). *Generalized additive models for data with concurvity: Statistical issues and a novel model fitting approach* [University of Pittsburgh]. https://www.proquest.com/openview/4adbf2566796ec4f0b2b503245280628/1?pq-origsite=gscholar&cbl=18750&diss=y
Heimbichner Goebel, W. L., Colin, S. P., Costello, J. H., Gemmell, B. J., & Sutherland, K. R. (2020). Scaling of ctenes and consequences for swimming performance in the ctenophore Pleurobrachia bachei. *Invertebrate Biology*, *139*(3). https://doi.org/10.1111/ivb.12297
Helm, R. R. (2018). Evolution and development of scyphozoan jellyfish. *Biol. Rev*, *93*, 1228–1250. https://doi.org/10.1111/brv.12393
Holland, B. S., Dawson, M. N., Crow, G. L., & Hofmann, D. K. (2004). Global phylogeography of Cassiopea (Scyphozoa: Rhizostomeae): Molecular evidence for cryptic species and multiple invasions of the Hawaiian Islands. *Marine Biology*, *145*(6). https://doi.org/10.1007/s00227-004-1409-4
Holst, S. (2012a). Effects of climate warming on strobilation and ephyra production of North Sea scyphozoan jellyfish. *Hydrobiologia*, *690*(1). https://doi.org/10.1007/s10750-012-1043-y
Holst, S. (2012b). Morphology and development of benthic and pelagic life stages of North Sea jellyfish (Scyphozoa,

Cnidaria) with special emphasis on the identification of ephyra stages. *Marine Biology*, *159*(12), 2707–2722. https://doi.org/10.1007/s00227-012-2028-0

Holst, S., Heins, A., & Laakmann, S. (2019). Morphological and molecular diagnostic species characters of Staurozoa (Cnidaria) collected on the coast of Helgoland (German Bight, North Sea). *Marine Biodiversity*, *49*(4). https://doi.org/10.1007/s12526-019-00943-1

Holst, S., & Laakmann, S. (2019). First record of the stalked jellyfish Haliclystus tenuis Kishinouye, 1910 (Cnidaria: Staurozoa) in Atlantic waters. *Marine Biodiversity*, *49*(2). https://doi.org/10.1007/s12526-018-0888-3

Hori, H., Ohama, T., Kumazaki, T., & Osawa, S. (1982). Nucleotide Sequences of 5S rRNAs from four jellyfishes. *Nucleic Acids Research*, *10*(22), 7405–7408. https://doi.org/10.1093/nar/10.22.7405

Hosia, A., & Titelman, J. (2011). Intraguild predation between the native North Sea jellyfish Cyanea capillata and the invasive ctenophore Mnemiopsis leidyi. *Journal of Plankton Research*, *33*(3), 535–540. https://doi.org/10.1093/plankt/fbq106

Houghton, J. D. R., Doyle, T. K., Davenport, J., & Hays, G. C. (2006). Developing a simple, rapid method for identifying and monitoring jellyfish aggregations from the air. *Marine Ecology Progress Series*, *314*. https://doi.org/10.3354/meps314159

Houghton, J. D. R., Doyle, T. K., Davenport, J., Lilley, M. K. S., Wilson, R. P., & Hays, G. C. (2007). Stranding events provide indirect insights into the seasonality and persistence of jellyfish medusae (Cnidaria: Scyphozoa). *Hydrobiologia*, *589*(1). https://doi.org/10.1007/s10750-007-0572-2

Hsieh, Y.-H. P., & Rudloe, J. (1994). Potential of utilizing jellyfish as food in Western countries. *Trends in Food Science & Technology*, *5*(7), 225–229. https://doi.org/10.1016/0924-2244(94)90253-4

Hunt, L. J. H., & Denny, M. W. (2008). DESICCATION PROTECTION AND DISRUPTION: A TRADE-OFF FOR AN INTERTIDAL MARINE ALGA 1. *Journal of Phycology*, *44*(5), 1164–1170. https://doi.org/10.1111/j.1529-8817.2008.00578.x

Janßen, H., Augustin, C. B., Hinrichsen, H. H., & Kube, S. (2013). Impact of secondary hard substrate on the distribution and abundance of Aurelia aurita in the western Baltic Sea. *Marine Pollution Bulletin*, *75*(1–2). https://doi.org/10.1016/j.marpolbul.2013.07.027

Jaspers, C., Acuña, J. L., & Brodeur, R. D. (2015). Interactions of gelatinous zooplankton within marine food webs. *Journal of Plankton Research*, *37*(5), 985–988. https://doi.org/10.1093/plankt/fbv068

Jelly Fish Nets. (2014). *SOME ANTI-JELLYFISH NETS' IMAGES*. http://www.jellyfishnets.com/gallery.php

Johnsen, S., & Widder, E. A. (2000). *Ultraviolet absorption in transparent zooplankton and its implications for depth distribution and visual predation*.

Kennedy, J. (2019). What Is Zooplankton, or Animal Plankton? *ThoughtCo.Com*. https://www.thoughtco.com/zooplankton-definition-2291632

Kingsford, M. J., & Mooney, C. J. (2014). The ecology of box jellyfishes (Cubozoa). In *Jellyfish Blooms* (Vol. 9789400770157). https://doi.org/10.1007/978-94-007-7015-7_12

Krone, R., Gutow, L., Joschko, T. J., & Schröder, A. (2013). Epifauna dynamics at an offshore foundation - Implications of future wind power farming in the North Sea. *Marine Environmental Research*, *85*. https://doi.org/10.1016/j.marenvres.2012.12.004

Kuijlen, K. (2014). *ANATOMIE EN FYSIOLOGIE VAN SCYPHOZOA in relatie tot het ontstaan van een bloei van kwallen* [Universiteit Gent]. https://libstore.ugent.be/fulltxt/RUG01/002/165/632/RUG01-002165632_2014_0001_AC.pdf

Laffoley, D., & Baxter, J. M. (2016). Explaining Ocean Warming: Causes, scale, effects and consequences. In D. Laffoley & J. M. Baxter (Eds.), *Explaining Ocean Warming: Causes, scale, effects and consequences*. IUCN, International Union for Conservation of Nature. https://doi.org/10.2305/IUCN.CH.2016.08.en

Lakkis, N. A., Maalouf, G. J., & Mahmassani, D. M. (2015). Jellyfish Stings: A Practical Approach. In *Wilderness and Environmental Medicine* (Vol. 26, Issue 3). https://doi.org/10.1016/j.wem.2015.01.003

Lakna. (2017). *Difference Between Cnidaria and Ctenophora | Definition, Characteristics, Similarities and Differences*. https://pediaa.com/difference-between-cnidaria-and-ctenophora/

Lewis, C., Bentlage, B., Yanagihara, A., Gillan, W., Blerk, J. Van, Keil, D. P., Bely, A. E., & Collins, A. G. (2013). Redescription of Alatina alata (Reynaud, 1830) (Cnidaria: Cubozoa) from Bonaire, Dutch Caribbean. *Zootaxa*, *3737*(4). https://doi.org/10.11646/zootaxa.3737.4.8

Li, L., Mcgee, R. G., Isbister, G. K., & Webster, A. C. (2013). Interventions for the symptoms and signs resulting from jellyfish stings. In *Cochrane Database of Systematic Reviews* (Vol. 2013, Issue 12). https://doi.org/10.1002/14651858.CD009688.pub2

Lucas, C. H., Graham, W. M., & Widmer, C. (2012). Chapter Three - Jellyfish Life Histories: Role of Polyps in Forming and

Maintaining Scyphomedusa Populations. In M. Lesser (Ed.), *Advances in Marine Biology* (Vol. 63, pp. 133–196). https://doi.org/10.1016/B978-0-12-394282-1.00003-X

Lumini, A., & Nanni, L. (2019). *Ocean Ecosystems Plankton Classification* (pp. 261–280). https://doi.org/10.1007/978-3-030-03000-1_11

Lynam, C. P., & Brierley, A. S. (2007). Enhanced survival of 0-group gadoid fish under jellyfish umbrellas. *Marine Biology*, *150*(6). https://doi.org/10.1007/s00227-006-0429-7

Lynam, C. P., Hay, S. J., & Brierley, A. S. (2004). Interannual variability in abundance of North Sea jellyfish and links to the North Atlantic Oscillation. *Limnol. Oceanogr*, *49*(3), 637–643. https://doi.org/10.4319/lo.2004.49.3.0637

Lynam, C. P., Heath, M. R., Hay, S. J., & Brierley, A. S. (2005). Evidence for impacts by jellyfish on North Sea herring recruitment. *Marine Ecology Progress Series*, *298*. https://doi.org/10.3354/meps298157

Lynam, C. P., Lilley, M. K. S., Bastian, T., Doyle, T. K., Beggs, S. E., & Hays, G. C. (2011). Have jellyfish in the Irish Sea benefited from climate change and overfishing? *Global Change Biology*, *17*(2). https://doi.org/10.1111/j.1365-2486.2010.02352.x

Mapstone, G. M. (2014). Global diversity and review of Siphonophorae (Cnidaria: Hydrozoa). In *PLoS ONE* (Vol. 9, Issue 2). https://doi.org/10.1371/journal.pone.0087737

MarineBio. (2019). Zooplankton ~ MarineBio Conservation Society. In *Marinebio.org*. https://marinebio.org/creatures/zooplankton/

Martin-Abadal, M., Ruiz-Frau, A., Hinz, H., & Gonzalez-Cid, Y. (2020). Jellytoring: Real-time jellyfish monitoring based on deep learning object detection. *Sensors (Switzerland)*, *20*(6). https://doi.org/10.3390/s20061708

McFadden, C. S., Quattrini, A. M., Brugler, M. R., Cowman, P. F., Dueñas, L. F., Kitahara, M. V., Paz-García, D. A., Reimer, J. D., & Rodríguez, E. (2021). Phylogenomics, Origin, and Diversification of Anthozoans (Phylum Cnidaria). *Systematic Biology*, *70*(4). https://doi.org/10.1093/sysbio/syaa103

Mcilwaine, B., & Rivas Casado, M. (2021). JellyNet: The convolutional neural network jellyfish bloom detector. *International Journal of Applied Earth Observation and Geoinformation*, *97*, 102279. https://doi.org/10.1016/J.JAG.2020.102279

Megill, W. M., Gosline, J. M., & Blake, R. W. (2005). The modulus of elasticity of fibrillin-containing elastic fibres in the mesoglea of the hydromedusa Polyorchis penicillatus. *Journal of Experimental Biology*, *208*(20). https://doi.org/10.1242/jeb.01765

Mier, P., & Andrade-Navarro, M. A. (2016). CABRA: Cluster and Annotate Blast Results Algorithm. *BMC Research Notes*, *9*(1). https://doi.org/10.1186/s13104-016-2062-y

Miller, B. J., von der Heyden, S., & Gibbons, M. J. (2012). Significant population genetic structuring of the holoplanktic scyphozoan Pelagia noctiluca in the Atlantic Ocean. *African Journal of Marine Science*, *34*(3). https://doi.org/10.2989/1814232X.2012.726646

Mills, C. E. (2001). Jellyfish blooms: Are populations increasing globally in response to changing ocean conditions? *Hydrobiologia*, *451*. https://doi.org/10.1023/A:1011888006302

Miranda, L. S., Hirano, Y. M., Mills, C. E., Falconer, A., Fenwick, D., Marques, A. C., & Collins, A. G. (2016). Systematics of stalked jellyfishes (Cnidaria: Staurozoa). *PeerJ*, *2016*(5). https://doi.org/10.7717/peerj.1951

Miranda, L. S., Mills, C. E., Hirano, Y. M., Collins, A. G., & Marques, A. C. (2017). *A review of the global diversity and natural history of stalked jellyfishes (Cnidaria, Staurozoa)*. https://doi.org/10.1007/s12526-017-0721-4

Miranda, L. S., Morandini, A. C., & Marques, A. C. (2009). Taxonomic review of Haliclystus antarcticus Pfeffer, 1889 (Stauromedusae, Staurozoa, Cnidaria), with remarks on the genus Haliclystus Clark, 1863. *Polar Biology*, *32*(10). https://doi.org/10.1007/s00300-009-0648-8

Miura, S., & Kimura, S. (1985). Jellyfish mesogloea collagen. Characterization of molecules as alpha 1 alpha 2 alpha 3 heterotrimers. *Journal of Biological Chemistry*, *260*(28), 15352–15356. https://doi.org/10.1016/S0021-9258(18)95743-1

Miya, M. (2022). Environmental DNA Metabarcoding: A Novel Method for Biodiversity Monitoring of Marine Fish Communities. In *Annual Review of Marine Science* (Vol. 14). https://doi.org/10.1146/annurev-marine-041421-082251

Miyake, H., Terazaki, M., & Kakinuma, Y. (2002). On the polyps of the common jellyfish Aurelia aurita in Kagoshima Bay. *Journal of Oceanography*, *58*(3). https://doi.org/10.1023/A:1021628314041

Molinero, J. C., Ibanez, F., Nival, P., Buecher, E., & Souissi, S. (2005). The North Atlantic climate and the northwestern Mediterranean plankton variability. Limnol. Oceanogr., 50(4), 2005, 1213–1220. In *Limnol. Oceanogr* (Vol. 50, Issue 4). https://aslopubs.onlinelibrary.wiley.com/doi/abs/10.4319/lo.2005.50.4.1213

Møller, L. F., & Riisgård, H. U. (2007a). Impact of jellyfish and mussels on algal blooms caused by seasonal oxygen depletion and nutrient release from the sediment in a Danish fjord. *Journal of Experimental Marine Biology and Ecology*, *351*(1–2). https://doi.org/10.1016/j.jembe.2007.06.026

Møller, L. F., & Riisgård, H. U. (2007b). Population dynamics, growth and predation impact of the common jellyfish Aurelia aurita and two hydromedusae, Sarsia tubulosa, and Aequorea vitrina in Limfjorden (Denmark). *Marine Ecology Progress Series*, *346*. https://doi.org/10.3354/meps06960

Montgomery, L., Seys, J., & Mees, J. (2016). To pee, or not to pee: A review on envenomation and treatment in European jellyfish species. In *Marine Drugs* (Vol. 14, Issue 7). https://doi.org/10.3390/md14070127

Mortelmans, J., Goossens, J., Amadei Martínez, L., Deneudt, K., Cattrijsse, A., & Hernandez, F. (2019). LifeWatch observatory data: Zooplankton observations in the Belgian part of the North Sea. *Geoscience Data Journal*, *6*(2). https://doi.org/10.1002/gdj3.68

Motivans, E. (2017). Surprise! Albatrosses eat quite a lot of jellyfish. *ZME Science*. https://www.zmescience.com/ecology/animals-ecology/surprise-albatrosses-eat-quite-lot-jellyfish/

Ne'eman, I., Fishelson, L., & Kashman, Y. (1974). Sarcophine-a new toxin from the soft coral Sarcophyton glaucum (Alcyonaria). *Toxicon*, *12*(6). https://doi.org/10.1016/0041-0101(74)90192-5

Ortman, B. D. (2008). DNA Barcoding the Medusozoa and Ctenophora. *Dissertation*.

Oxford Nanopore Technologies. (2023a). *Ligation sequencing amplicons - PCR barcoding (SQK-LSK110 with EXP-PBC096)*. https://community.nanoporetech.com/docs/prepare/library_prep_protocols/pcr-barcoding-96-amplicons-sqk-lsk110/v/pbac96_9114_v110_revl_10nov2020

Oxford Nanopore Technologies. (2023b). *Release notes for Guppy*. https://community.nanoporetech.com/downloads/guppy/release_notes

Pagès, F., Gili, J., & Bouillon, J. (1992). Medusae (Hydrozoa, Scyphozoa, Cubozoa) of the Benguela Current (southeastern Atlantic). *Scientia Marina*, *56*(1).

Pauly, D., & Palomares, M. L. (2005). Fishing down marine food web: It is far more pervasive than we thought. *Bulletin of Marine Science*, *76*(2).

Pisani, D., Pett, W., Dohrmann, M., Feuda, R., Rota-Stabelli, O., Philippe, H., Lartillot, N., & Wörheide, G. (2015). Genomic data do not support comb jellies as the sister group to all other animals. *Proceedings of the National Academy of Sciences of the United States of America*, *112*(50). https://doi.org/10.1073/pnas.1518127112

Pohnert, G. (2019). Finding the fish factor. *ELife*, *8*. https://doi.org/10.7554/eLife.48459

Purcell, J. E. (2005). Climate effects on formation of jellyfish and ctenophore blooms: A review. In *Journal of the Marine Biological Association of the United Kingdom* (Vol. 85, Issue 3). https://doi.org/10.1017/S0025315405011409

Purcell, J. E., Uye, S. I., & Lo, W. T. (2007). Anthropogenic causes of jellyfish blooms and their direct consequences for humans: A review. In *Marine Ecology Progress Series* (Vol. 350). https://doi.org/10.3354/meps07093

Purcell, J. E., White, J. R., Nemazie, D. A., & Wright, D. A. (1999). Temperature, salinity and food effects on asexual reproduction and abundance of the scyphozoan Chrysaora quinquecirrha. *Marine Ecology Progress Series*, *180*. https://doi.org/10.3354/meps180187

Quast, C., Pruesse, E., Yilmaz, P., Gerken, J., Schweer, T., Yarza, P., Peplies, J., & Glöckner, F. O. (2013). The SILVA ribosomal RNA gene database project: Improved data processing and web-based tools. *Nucleic Acids Research*, *41*(D1). https://doi.org/10.1093/nar/gks1219

Quiñones, J., Chiaverano, L. M., Ayón, P., Adams, G. D., Mianzan, H. W., & Marcelo Acha, E. (2018). Spatial patterns of large jellyfish Chrysaora plocamia blooms in the Northern Humboldt Upwelling System in relation to biological drivers and climate. *ICES Journal of Marine Science*, *75*(4). https://doi.org/10.1093/icesjms/fsy004

R. Calder, D., & D. Cairns, S. (2009). Hydriods (Cnidaria: Hydrozoa) of the Gulf of Mexico. In *Gulf of Mexico Origin, Waters, and Biota: Volume 1, Biodiversity*.

Richardson, A. J., Bakun, A., Hays, G. C., & Gibbons, M. J. (2009). The jellyfish joyride: causes, consequences and management responses to a more gelatinous future. In *Trends in Ecology and Evolution* (Vol. 24, Issue 6). https://doi.org/10.1016/j.tree.2009.01.010

Samanta, S., Chakraborty, S., Bhattacharya, S., & Chattopadhyay, J. (2011). Fish kairomones, its benefits and detriments: A model based study both from releaser and acceptor perspective. *Ecological Complexity*, *8*(3). https://doi.org/10.1016/j.ecocom.2011.05.001

Samanthi, U. (2021). Difference Between Nanopore and Illumina Sequencing. *DifferenceBetween*. https://www.differencebetween.com/difference-between-nanopore-and-illumina-sequencing/

Santhanam, P., Begum, A., & Pachiappan, P. (Eds.). (2019). *Basic and Applied Zooplankton Biology*. Springer Singapore. https://doi.org/10.1007/978-981-10-7953-5

Sato, N. N., Kokubun, N., Yamamoto, T., Watanuki, Y., Kitaysky, A. S., & Takahashi, A. (2015). The jellyfish buffet: Jellyfish enhance seabird foraging opportunities by concentrating prey. *Biology Letters*, *11*(8).

https://doi.org/10.1098/rsbl.2015.0358

Schaub, J., Hunt, B. P. V., Pakhomov, E. A., Holmes, K., Lu, Y., & Quayle, L. (2018). Using unmanned aerial vehicles (UAVs) to measure jellyfish aggregations. *Marine Ecology Progress Series*, *591*. https://doi.org/10.3354/meps12414

Schiariti, A., Sofía Dutto, M., Oliveira, O. M., Faillia Siquier, G., Puente Tapia, F. A., & Chiaverano, L. (2021). Overview of the comb jellies (Ctenophora) from the South-western Atlantic and Sub Antarctic region (32–60°S; 34–70°W). In *New Zealand Journal of Marine and Freshwater Research* (Vol. 55, Issue 2). https://doi.org/10.1080/00288330.2020.1775660

Schnedler-Meyer, N. A., Kiørboe, T., & Mariani, P. (2018). Boom and Bust: Life History, Environmental Noise, and the (un)Predictability of Jellyfish Blooms. *Frontiers in Marine Science*, *5*. https://doi.org/10.3389/fmars.2018.00257

Seipel, K., & Schmid, V. (2005). Evolution of striated muscle: Jellyfish and the origin of triploblasty. In *Developmental Biology* (Vol. 282, Issue 1). https://doi.org/10.1016/j.ydbio.2005.03.032

Semmouri, I., De Schamphelaere, K. A. C., Willemse, S., Vandegehuchte, M. B., Janssen, C. R., & Asselman, J. (2021). Metabarcoding reveals hidden species and improves identification of marine zooplankton communities in the North Sea. *ICES Journal of Marine Science*, *78*(9). https://doi.org/10.1093/icesjms/fsaa256

Serrana, J. M., Miyake, Y., Gamboa, M., & Watanabe, K. (2019). Comparison of DNA metabarcoding and morphological identification for stream macroinvertebrate biodiversity assessment and monitoring. *Ecological Indicators*, *101*. https://doi.org/10.1016/j.ecolind.2019.02.008

Shearer, T. L., Van Oppen, M. J. H., Romano, S. L., & Wörheide, G. (2002). Slow mitochondrial DNA sequence evolution in the Anthozoa (Cnidaria). In *Molecular Ecology* (Vol. 11, Issue 12). https://doi.org/10.1046/j.1365-294X.2002.01652.x

Slobodkin, L. B., & Bossert, P. E. (2010). Cnidaria. In *Ecology and Classification of North American Freshwater Invertebrates* (pp. 125–142). Elsevier. https://doi.org/10.1016/B978-0-12-374855-3.00005-4

Smithsonian Ocean. (n.d.). *Extreme jellyfish*. https://ocean.si.edu/ocean-life/invertebrates/extreme-jellyfish#:~:text=The lion's mane jellyfish (Cyanea,the bottom of its tentacles.

Swain, T. D., Schellinger, J. L., Strimaitis, A. M., & Reuter, K. E. (2015). Evolution of anthozoan polyp retraction mechanisms: Convergent functional morphology and evolutionary allometry of the marginal musculature in order Zoanthidea (Cnidaria: Anthozoa: Hexacorallia). *BMC Evolutionary Biology*, *15*(1). https://doi.org/10.1186/s12862-015-0406-1

Takasu, H., Inomata, H., Uchino, K., Tahara, S., Mori, K., Hirano, Y., Harada, K., Yamaguchi, M., Nozoe, Y., & Akiyama, H. (2019). Spatio-temporal distribution of environmental dna derived from japanese sea nettle jellyfish chrysaora pacifica in Omura Bay, Kyushu, Japan. *Plankton and Benthos Research*, *14*(4). https://doi.org/10.3800/pbr.14.320

Tamm, S. L. (2014). Cilia and the life of ctenophores. *Invertebrate Biology*, *133*(1). https://doi.org/10.1111/ivb.12042

Tomlinson, B., Maynou, F., Sabatés, A., Fuentes, V., Canepa, A., & Sastre, S. (2018). Systems approach modelling of the interactive effects of fisheries, jellyfish and tourism in the Catalan coast. *Estuarine, Coastal and Shelf Science*, *201*. https://doi.org/10.1016/j.ecss.2015.11.012

Uye, S., & Ueta, U. (2004). Recent increase of jellyfish populations and their nuisance to fisheries in the Inland Sea of Japan. *Bulletin of the Japanese Society of Fisheries Oceanography*, *68*(1).

Van Ginderdeuren, K. (2013). *Zooplankton and its role in North Sea food webs : community structure and selective feeding by pelagic fish in Belgian marine waters* [Ghent University]. https://lib.ugent.be/catalog/rug01:001995215

Van Ginderdeuren, K., Fiers, F., De Backer, A., Vincx, M., & Hostens, K. (2012). Updating the zooplankton species list for the Belgian part of the North Sea. *BELGIAN JOURNAL OF ZOOLOGY*. https://lib.ugent.be/catalog/pug01:2997690

Van Ginderdeuren, K., Hostens, K., Hoffman, S., Vansteenbrugge, L., Soenen, K., De Blauwe, H., Robbens, J., & Vincx, M. (2012). Distribution of the invasive ctenophore Mnemiopsis leidyi in the Belgian part of the North Sea. *Aquatic Invasions*, *7*(2). https://doi.org/10.3391/ai.2012.7.2.002

Van Ginderdeuren, K., Van Hoey, G., Vincx, M., & Hostens, K. (2014). The mesozooplankton community of the Belgian shelf (North Sea). *Journal of Sea Research*, *85*. https://doi.org/10.1016/j.seares.2013.10.003

van Keeken, O. A., van Hoppe, M., Grift, R. E., & Rijnsdorp, A. D. (2007). Changes in the spatial distribution of North Sea plaice (Pleuronectes platessa) and implications for fisheries management. *Journal of Sea Research*, *57*(2-3 SPEC. ISS.). https://doi.org/10.1016/j.seares.2006.09.002

van Walraven, L., Driessen, F., van Bleijswijk, J., Bol, A., Luttikhuizen, P. C., Coolen, J. W. P., Bos, O. G., Gittenberger, A., Schrieken, N., Langenberg, V. T., & van der Veer, H. W. (2016). Where are the polyps? Molecular identification, distribution and population differentiation of Aurelia aurita jellyfish polyps in the southern North Sea area. *Marine Biology*, *163*(8). https://doi.org/10.1007/s00227-016-2945-4

Vandendriessche, S., Vansteenbrugge, L., Derweduwen, J., Maelfait, H., & Hostens, K. (2016). Jellyfish jelly press and jelly perception. *Journal of Coastal Conservation*, *20*(2). https://doi.org/10.1007/s11852-016-0423-2

Vansteenbrugge, L., Van Regenmortel, T., De Troch, M., Vincx, M., & Hostens, K. (2015). Gelatinous zooplankton in the Belgian part of the North Sea and the adjacent Schelde estuary: Spatio-temporal distribution patterns and population dynamics. *Journal of Sea Research*, *97*. https://doi.org/10.1016/j.seares.2014.12.008

Vasslides, J. M., Sassano, N. L., & Hales, L. S. (2018). Assessing the effects of a barrier net on jellyfish and other local fauna at estuarine bathing beaches. *Ocean and Coastal Management*, *163*. https://doi.org/10.1016/j.ocecoaman.2018.07.012

Waggett, R., & Costello, J. H. (1999). *Capture mechanisms used by the lobate ctenophore, Mnemiopsis leidyi, preying on the copepod Acartia tonsa*. https://academic.oup.com/plankt/article/21/11/2037/1499631

Waller, R. G., Tyler, P. A., & Gage, J. D. (2005). Sexual reproduction in three hermaphroditic deep-sea Caryophyllia species (Anthozoa: Scleractinia) from the NE Atlantic Ocean. *Coral Reefs*, *24*(4). https://doi.org/10.1007/s00338-005-0031-3

Welch, V., Vigneron, J. P., Lousse, V., & Parker, A. (2006). Optical properties of the iridescent organ of the comb-jellyfish Beroë cucumis (Ctenophora). *Physical Review E*, *73*(4), 041916. https://doi.org/10.1103/PhysRevE.73.041916

West, E. J., Welsh, D. T., & Pitt, K. A. (2009). Influence of decomposing jellyfish on the sediment oxygen demand and nutrient dynamics. *Hydrobiologia*, *616*(1). https://doi.org/10.1007/s10750-008-9586-7

Won, J. H., Rho, B. J., & Song, J. I. (2001). A phylogenetic study of the Anthozoa (phylum Cnidaria) based on morphological and molecular characters. *Coral Reefs*, *20*(1). https://doi.org/10.1007/s003380000132

Wood, S. (2006). *Generalized additive models: an introduction with R.* Chapman & Hall/CRC.

Work, T., & Meteyer, C. (2014). To Understand Coral Disease, Look at Coral Cells. *EcoHealth*, *11*(4), 610–618. https://doi.org/10.1007/s10393-014-0931-1

WORMS. (2004). *Gonothyraea loveni (Allman, 1859)*. World Register of Marine Species. https://www.marinespecies.org/aphia.php?p=taxdetails&id=117377#distributions

Wright, R. M., Le Quéré, C., Buitenhuis, E., Pitois, S., & Gibbons, M. J. (2021). Role of jellyfish in the plankton ecosystem revealed using a global ocean biogeochemical model. *Biogeosciences*, *18*(4). https://doi.org/10.5194/bg-18-1291-2021

Xing, Y., Liu, Q., Zhang, M., Zhen, Y., Mi, T., & Yu, Z. (2020). Effects of temperature and salinity on the asexual reproduction of Aurelia coerulea polyps. *Journal of Oceanology and Limnology*, *38*(1). https://doi.org/10.1007/s00343-019-8337-0

Xu, Y., Ishizaka, J., Yamaguchi, H., Siswanto, E., & Wang, S. (2013). Relationships of interannual variability in SST and phytoplankton blooms with giantjellyfish (Nemopilema nomurai) outbreaks in the Yellow Sea and East China Sea. *Journal of Oceanography*, *69*(5). https://doi.org/10.1007/s10872-013-0189-1

Yang, J., Zhang, X., Zhang, W., Sun, J., Xie, Y., Zhang, Y., Burton, G. A., & Yu, H. (2017). Indigenous species barcode database improves the identification of zooplankton. *PLoS ONE*, *12*(10). https://doi.org/10.1371/journal.pone.0185697

Zuur, A. F., Ieno, E. N., Walker, N., Saveliev, A. A., & Smith, G. M. (2009). *Mixed effects models and extensions in ecology with R*. Springer New York. https://doi.org/10.1007/978-0-387-87458-6

7 Appendix

7.1 Attachment 1: DNA Extraction of Seawater Samples protocol

Date (original version): 17/10/2022

Number of pages: 4

Date of last adjustment: 21/10/2022 (version: 3)

SP-XXX
DNA Extraction Of Seawater Samples

Author : Michiel De Cooman
Responsible : Ilias Semmouri

1 Goal / Doel

This protocol can be used to extract DNA from filtered seawater samples. A specialized kit is used for this: Qiagen DNeasy Blood & Tissue kit (Qagen cat 69504 or 69506). The protocol is adapted from Djurhuus et al. (2017).

2 Equipment / Benodigdheden

Machinery

- Shaking incubator at 56° type: Incubating minishaker, VWR
- Vortex (VWR)
- Centrifuge 2 mL type: Eppendorf Centrifuge 5425

Reagents

- Ethanol 98-100%
- 70% ethanol/Disolol
- Qiagen DNeasy Blood & Tissue Kit (cat 69504 or 69506) containing
  - ATL buffer
  - Proteinase K (2 mg/L final concentration) – additional proteinase K might be needed depending on the availability.
  - AL buffer
  - Spin columns
  - Collection tubes
  - AW1 buffer
  - AW2 buffer
  - AE buffer

Supplies

- Pipettes range 0.2µL-1000µL
- Centrifuge tube 1.5mL to 2mL
- Eppendorf tubes 2mL
- Tweezers
- Scissors
- Timer
- Lab coats, nitrile protection gloves

3 Preparations / Voorbereidingen

1. Check that all necessary reagents and supplies are available.
2. Switch on incubator to 56°, 350 rotations ***the night before*** the experiment.
3. Clean workspace with 70% ethanol, wash hands with soap and 70% ethanol.
4. Sterilize tweezers and scissors with 75% ethanol.
5. Take filtered seawater samples (i.e. the filters in Eppendorf tubes) out of -80° freezer, use insulation box to keep cold.

4 Methods / Methoden

4.1. Estimated duration

The protocol involves a waiting time of ***approximately 3.5 hours***.

4.2 Protocol steps

1. Carefully unfold the filter membranes and cut in 2 with scissors.
2. Place filter membranes in labelled 2mL Eppendorf tubes.
3. Add 165µL ATL buffer (Qiagen) to each tube. The same tip can be used if filter is not touched.
4. Vortex tubes for 50 s, then incubate the samples in the shaking incubator at 56° for 30 min.
5. Repeat step 3 and 4.
6. Add 20µL Proteinase K (Qiagen) to the samples, vortex for approximately 15 s, incubate 2h at 56°.
7. After incubation, vortex the Eppendorf tubes for 15 s and centrifuge 1 min (4,000 ***rcf***) at room temperature.
8. Transfer the resulting supernatant (+-350µL) into a ***new*** 2mL Eppendorf tube.
9. Centrifuge the tube containing the filter membrane a second time for 1 min (4,000 rcf).
10. Add the resulting rest of supernatant to the 2mL Eppendorf tube from step 8. Centrifuge this tube for 1 min (13,000 ***rcf***).
11. Perform an additional short centrifuge if necessary (in case no pallet is seen).
12. Transfer all the supernatant into a ***new*** 2mL Eppendorf tube. Take care not to touch the pallet.
13. Add 320 µL AL buffer (Qiagen) to the 2mL Eppendorf tube containing the supernatant, vortex for 20 s, incubate 10 min at 56°.

14. Add 320 µL ethanol (96-100%) to each sample, vortex for 20 s.
15. Pipet +-50% of the resulting volume of each sample into a DNeasy spin column (*note: label these beforehand!*), that is placed in a 2mL collection tube. Centrifuge these columns for 1 min (6,000 ***rcf***). Remove the liquid from the collection tube.
16. Add the remaining volume to the spin column. Centrifuge the samples again for 1 min (6,000 ***rcf***).
17. Place the centrifuged spin column into a ***new*** 2mL collection tube. Add 500 µL AW1 buffer (take the bottle where ethanol is added). Centrifuge 1 min (6,000 ***rcf***).
18. Place the spin column into a ***new*** 2mL collection tube. Add 500 µL AW2 buffer (take the bottle where ethanol is added). Centrifuge for 3 min (16,000 ***rcf***).
19. Empty the liquid of the collection tube in the organic waste bin. Put the spin column in the same collection tube again and centrifuge for 1 min (16,000 ***rcf***).
20. Check if the spin column is ***completely*** dry. If not, perform an additional short spin in the centrifuge.
21. Transfer the spin column to a ***new*** 1.5mL Eppendorf tube. Label each tube accordingly, and label these tubes as first elution series (e.g. "A").
22. Add 30µL AE buffer to the center of spin column membrane (***onto*** white filter). Incubate 1 min at room temperature, centrifuge 1 min (6,000 ***rcf***). Store tube.
23. Transfer the spin column to a ***new*** 1.5mL Eppendorf tube. Label each tube accordingly and label these tubes as second elution series (e.g. "B").
24. Repeat step 22.
25. The quality of the DNA extractions of elution series A and B can be done using Nanodrop (SP-036). *Note: if quality control is unsuccessful, making a third elution series might be helpful (repeat steps 18 and 19).*
26. Successful DNA samples can be stored in the -80° freezer.

5 References / Referenties

Djurhuus, A., Port, J., Closek, C. J., Yamahara, K. M., Romero-Maraccini, O., Walz, K. R., … Chavez, F. P. (2017). Evaluation of filtration and DNA extraction methods for environmental DNA biodiversity assessments across multiple trophic levels. Frontiers in Marine Science, 4(OCT), 314. https://doi.org/10.3389/fmars.2017.00314

7.2 Figures and tables

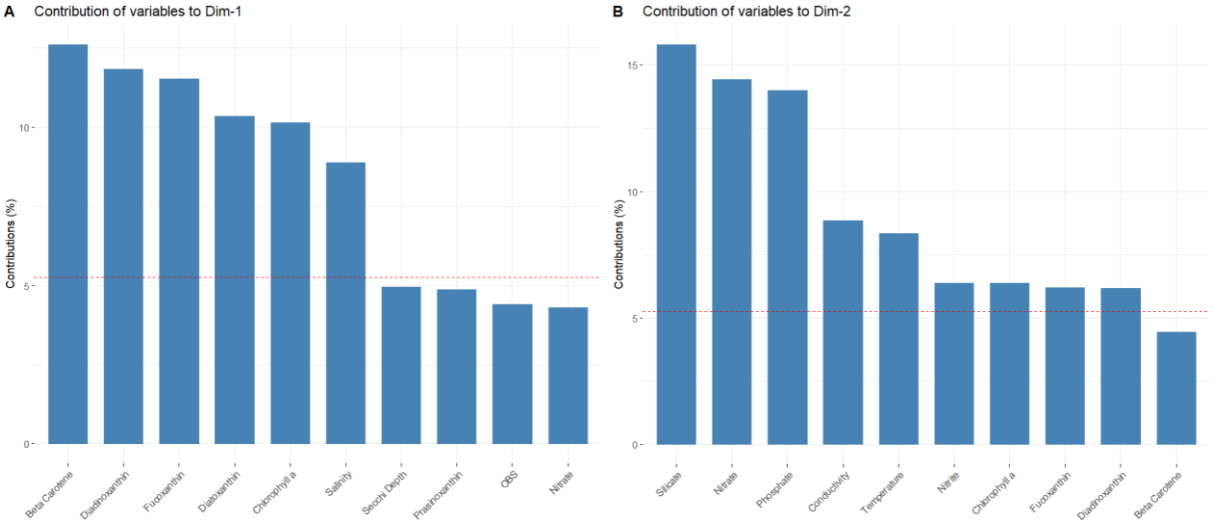

Figure A- 1 (A) Contribution of the top ten variables to the first dimension. (B) contribution of the top ten variables to the second dimension.

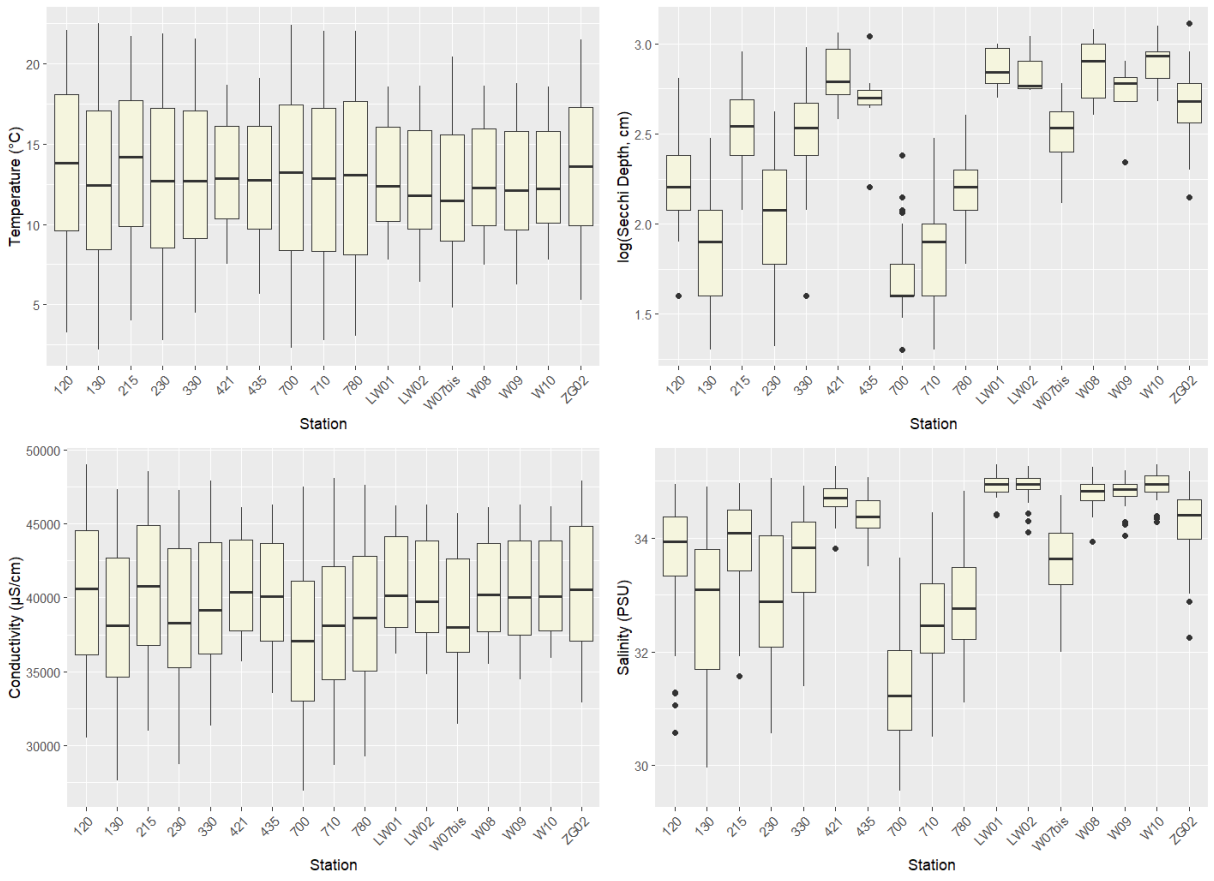

Figure A- 2 Boxplots showing spatial variation in a selection of measured abiotic parameters independently of time.

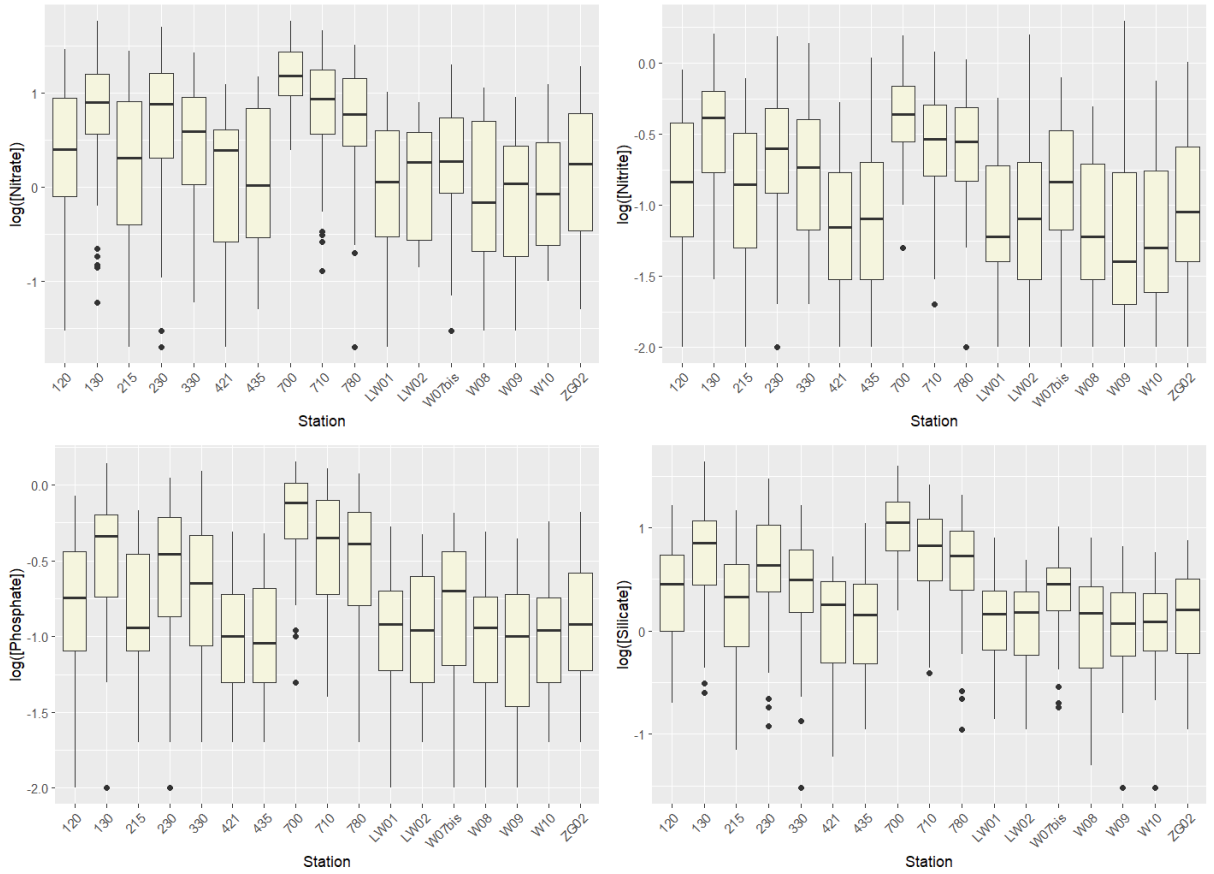

Figure A- 3 *Boxplots showing spatial variation in measured nutrient concentrations (all expressed in µmol/L and log transformed to account for outliers), independently of time.*

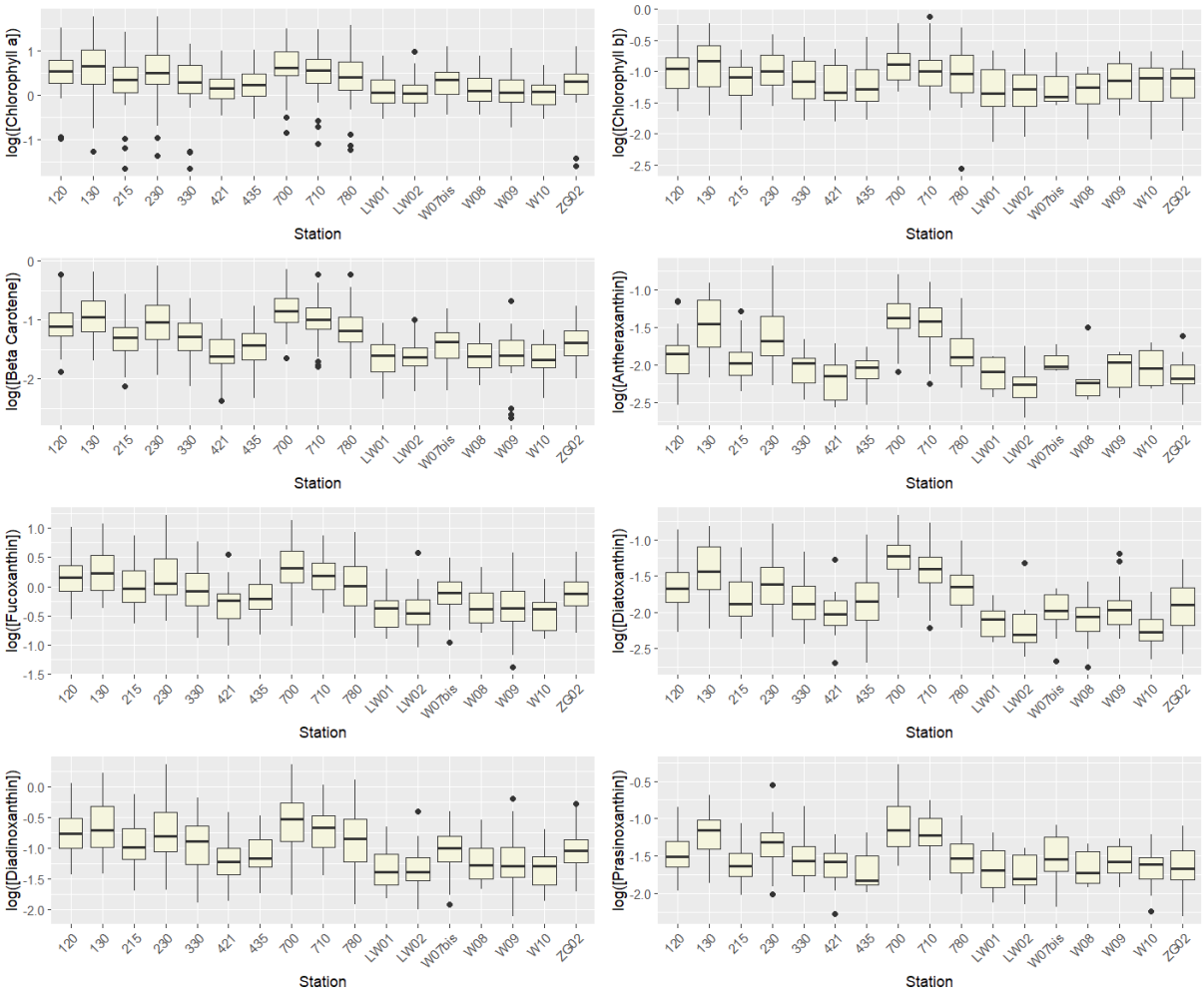

Figure A- 4 Boxplots showing spatial variation in measured pigment concentrations (all expressed in µg/L and log transformed to account for outliers) independently of time.

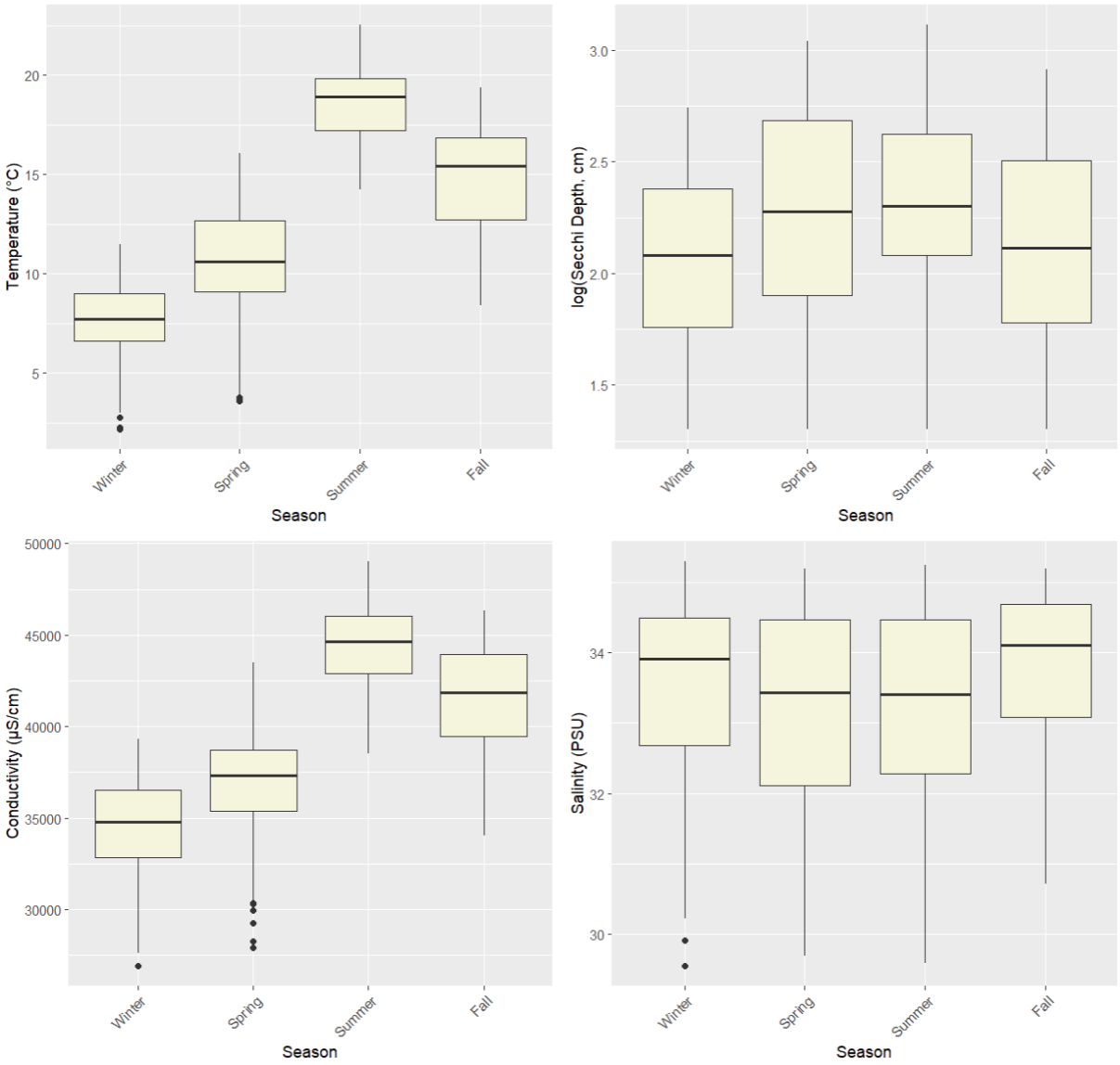

Figure A- 5 Boxplots showing seasonal variation in a selection of measured environmental parameters.

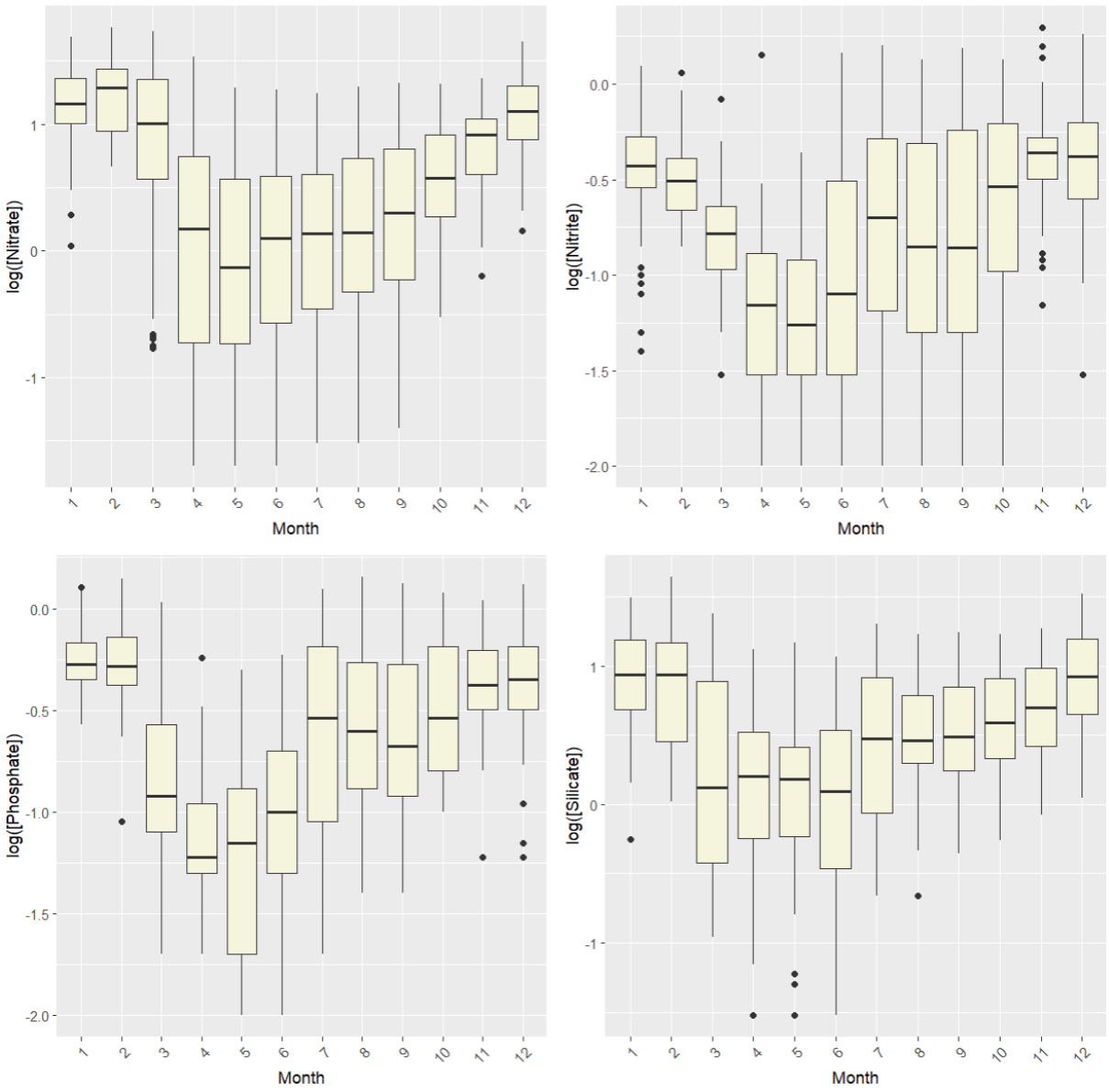

Figure A- 6 Boxplots showing temporal variation in measured nutrient concentrations (all expressed in µmol/L and log transformed to account for outliers).

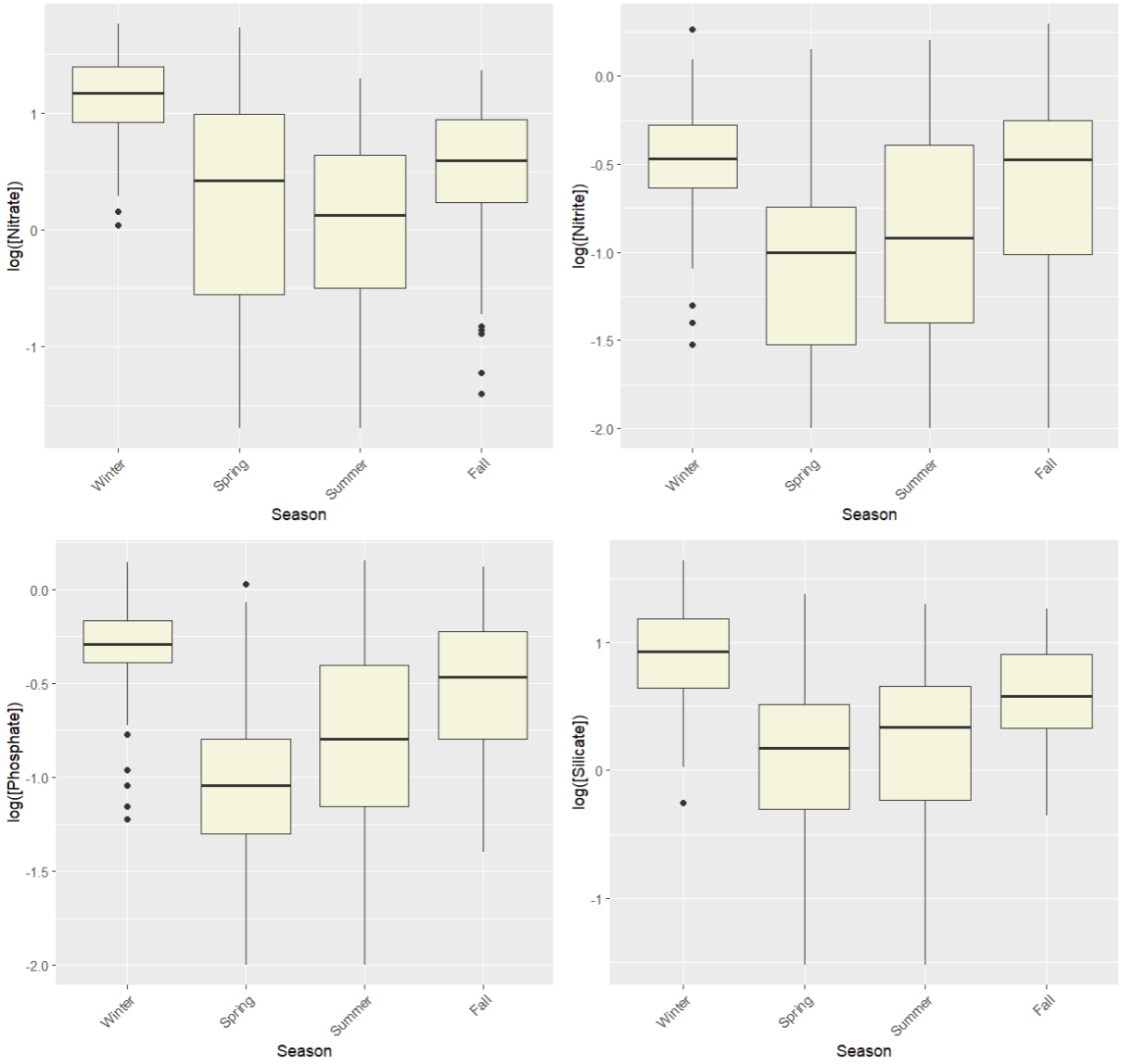

Figure A- 7 *Boxplots showing seasonal variation in measured nutrient concentrations (all expressed in µmol/L and log transformed to account for outliers).*

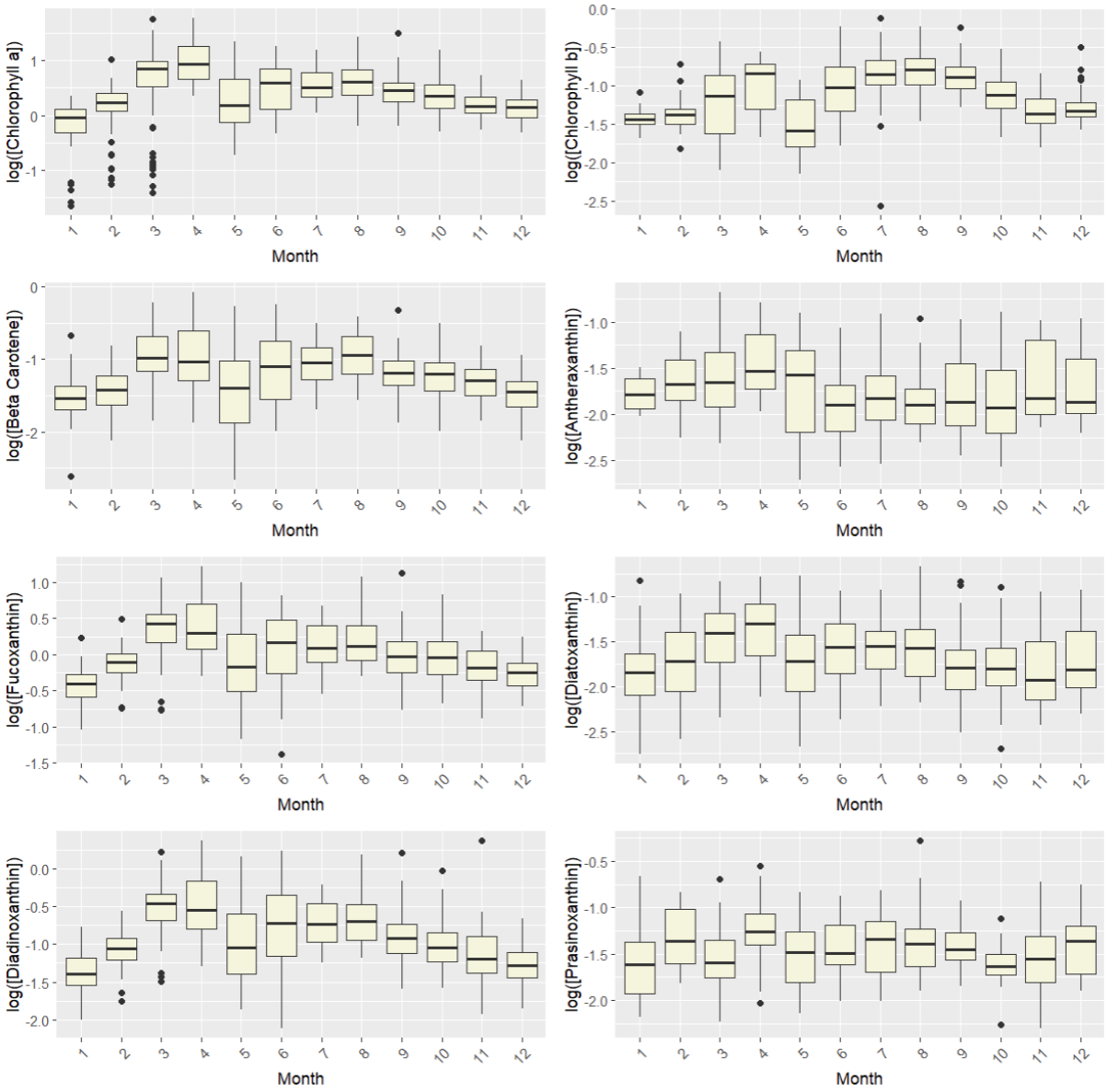

Figure A- 8 Boxplots showing temporal variation in measured pigment concentrations (all expressed in µg/L and log transformed to account for outliers).

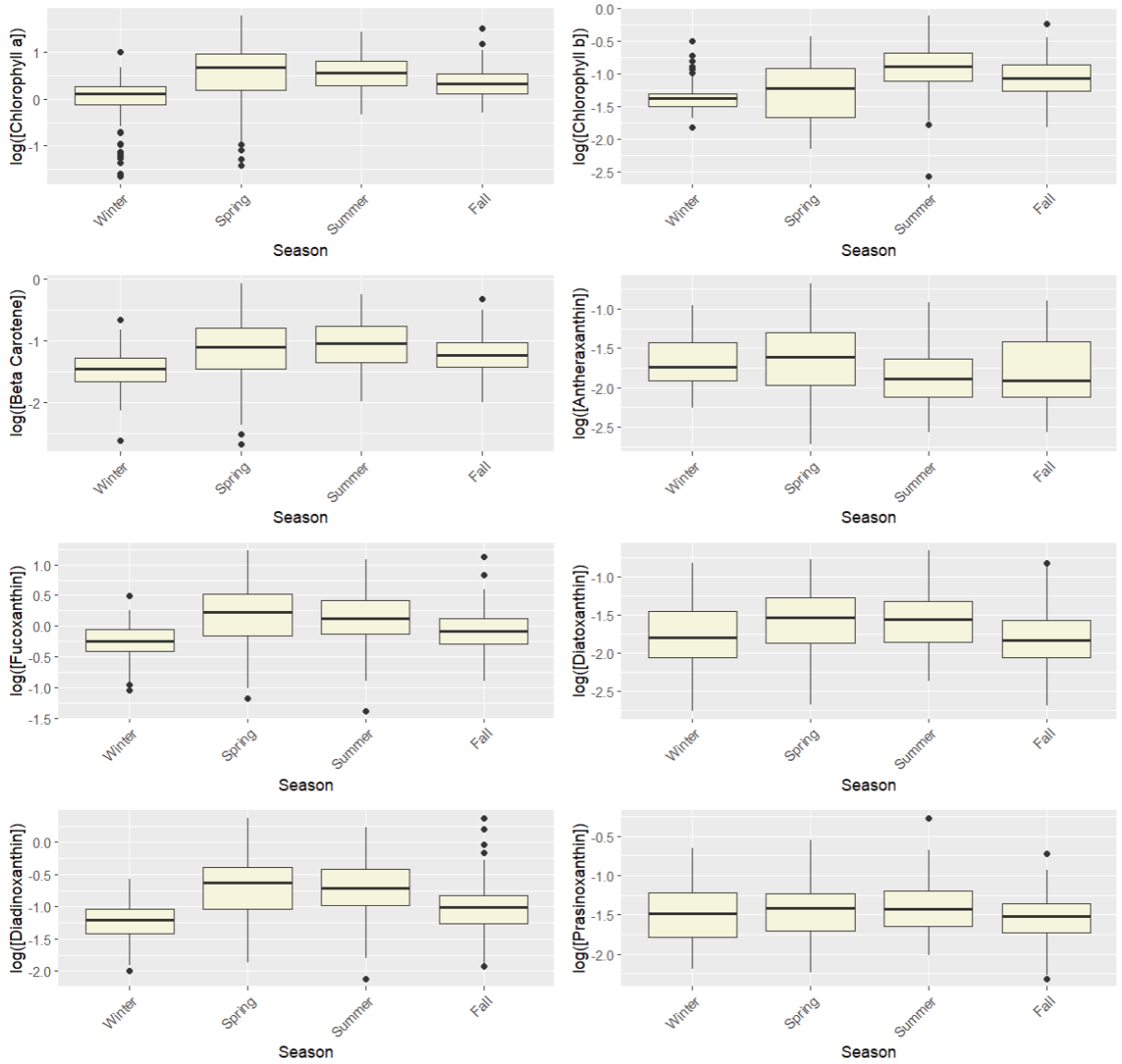

Figure A- 9 Boxplots showing seasonal variation in measured pigment concentrations (all expressed in µg/L and log transformed to account for outliers).

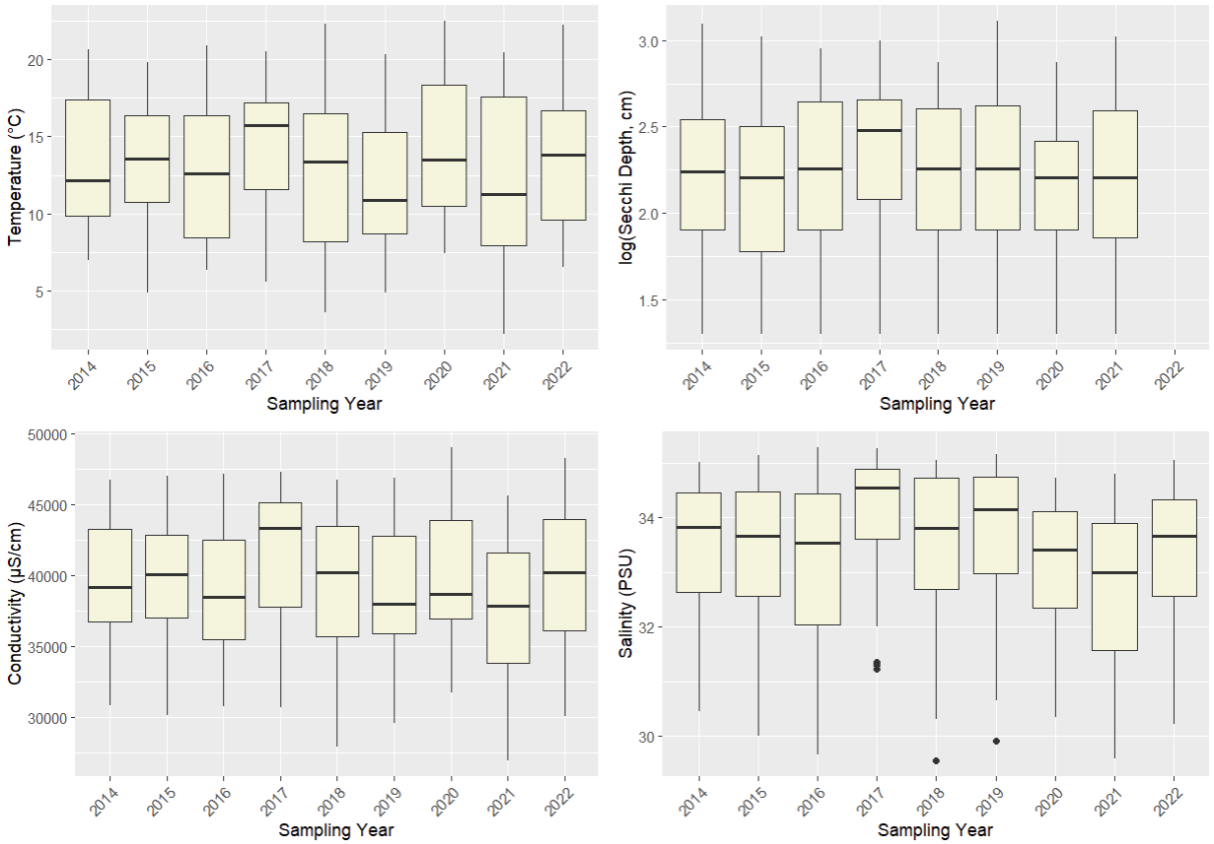

Figure A- 10 Boxplots showing temporal variation in a selection of measured environmental parameters.

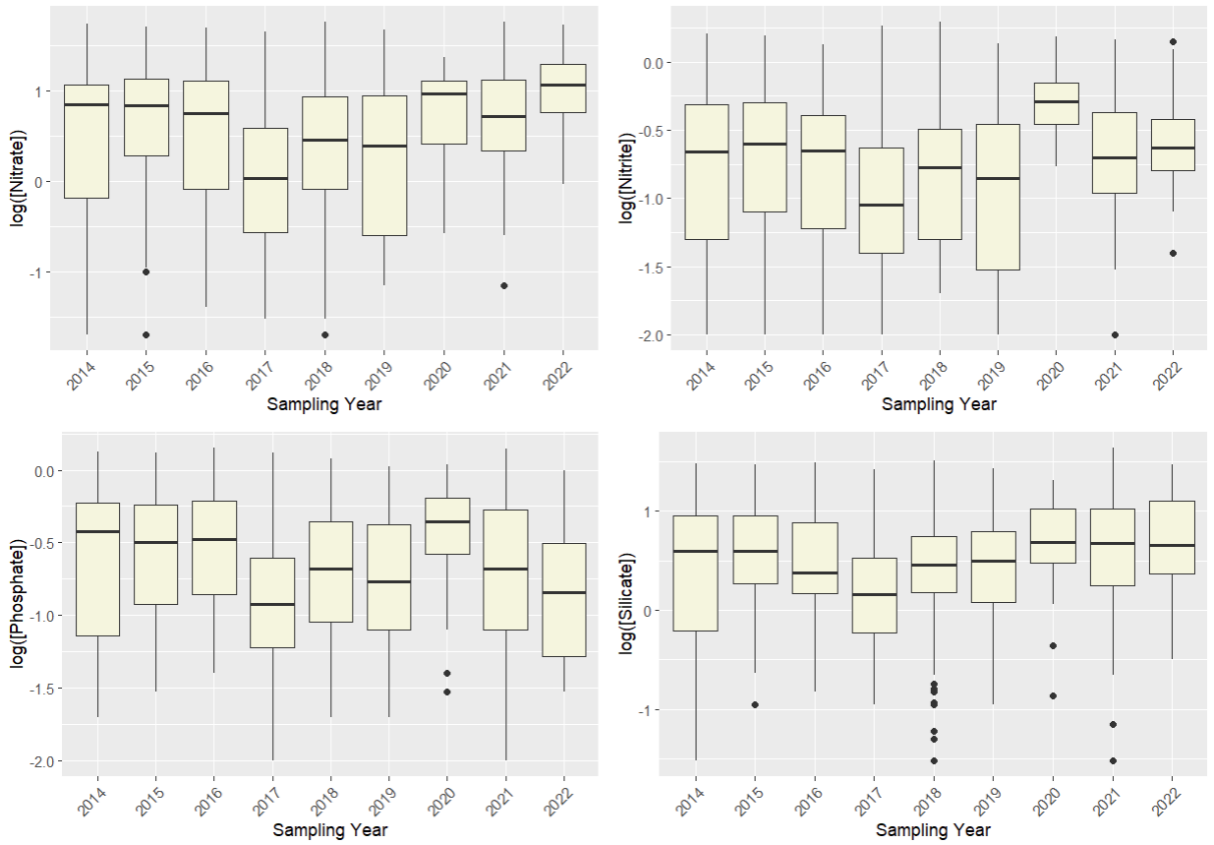

Figure A- 11 Boxplots showing temporal variation in measured nutrient concentrations (all expressed in µmol/L and log transformed to account for outliers).

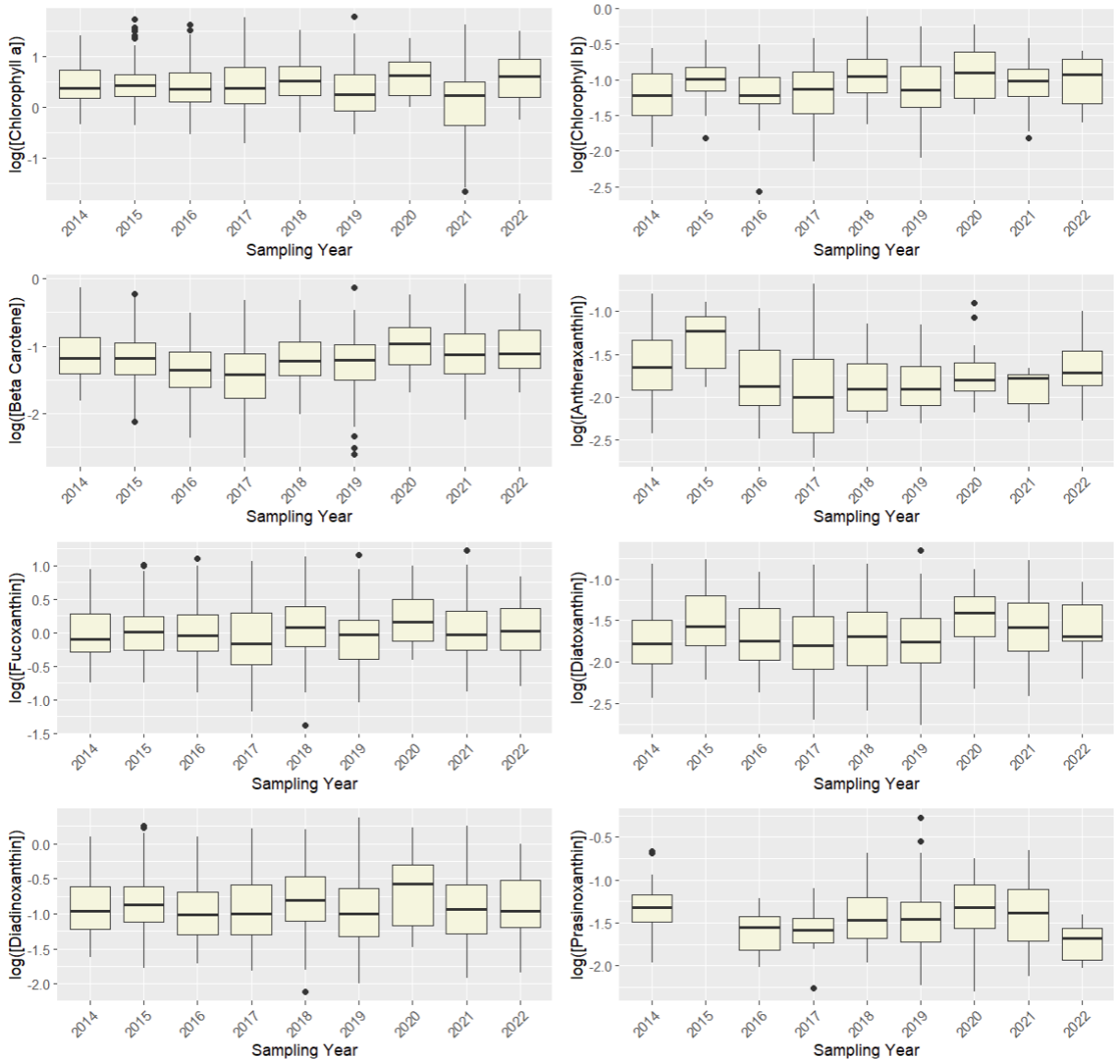

Figure A- 12 Boxplots showing temporal variation in measured pigment concentrations (all expressed in µg/L and log transformed to account for outliers).

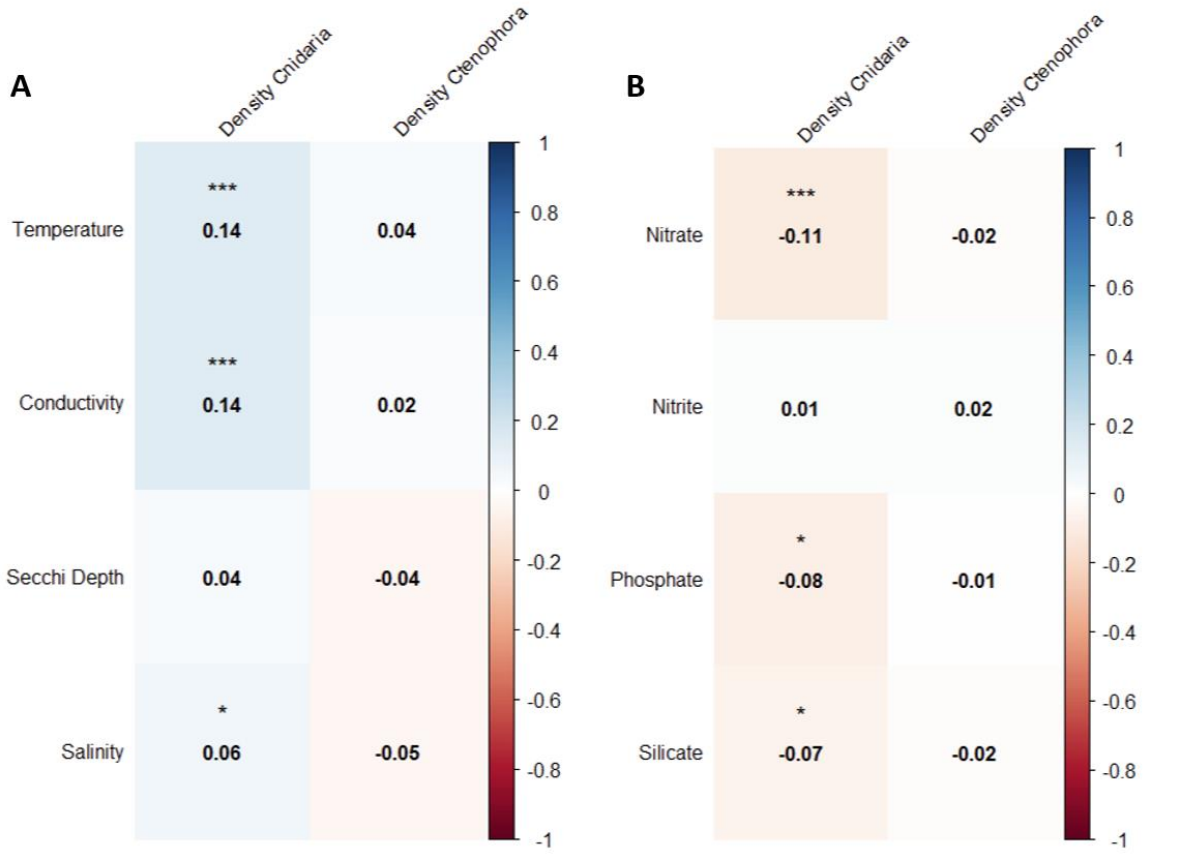

Figure A- 13 Correlation plot depicting the correlation (Spearman rank) between Cnidaria and Ctenophora densities (columns) and (A) a selection of measured environmental parameters (row) and (B) a selection of measured nutrients (row). The Spearman rho correlation coefficient is shown in each cell. The color of the cell indicates the strength and direction of the correlation, as depicted in the legend. Asterisks indicate correlations with a p-value smaller than 0.05 (*), 0.01 (**) and 0.001 (***).

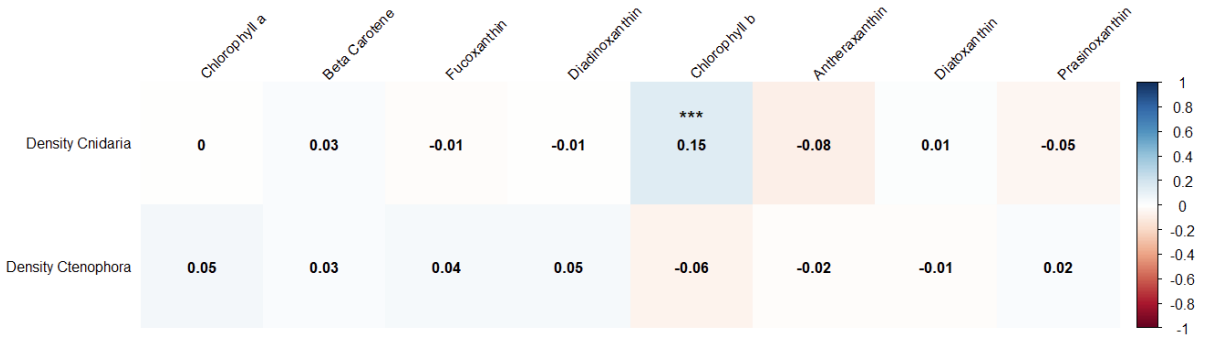

Figure A- 14 Correlation plot depicting the correlation (Spearman rank) between Cnidaria and Ctenophora densities (rows) and a selection of measured pigment concentrations (columns). The Spearman rho correlation coefficient is shown in each cell. The color of the cell indicates the strength and direction of the correlation, as depicted in the legend. Asterisks indicate correlations with a p-value smaller than 0.05 (*), 0.01 (**) and 0.001 (***).

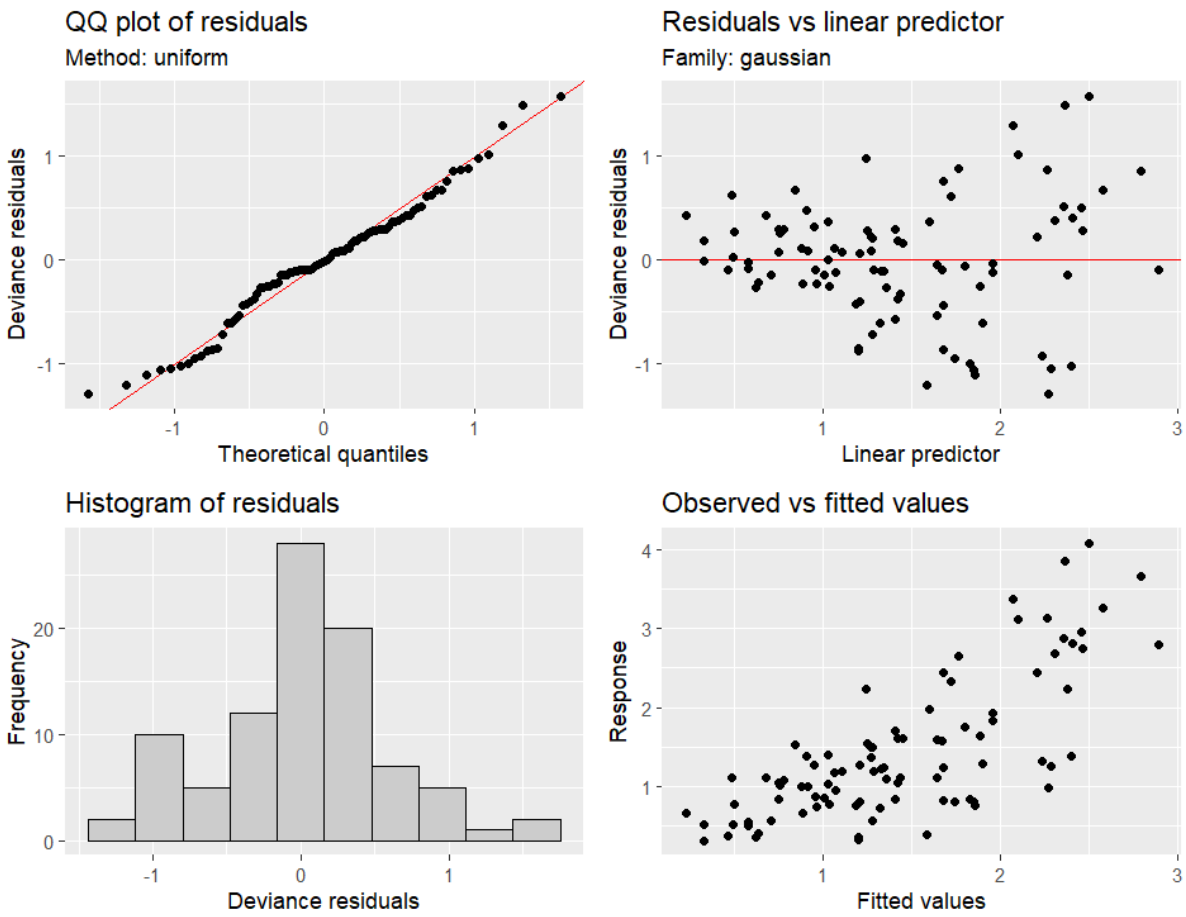

Figure A- 15 Diagnostic plots for the best fitted GAM model for Cnidaria bloom density estimations in the BPNS. The QQ-plot and the histogram of the residuals are used to verify normality. The plot of standardized residuals against fitted values assesses homogeneity.

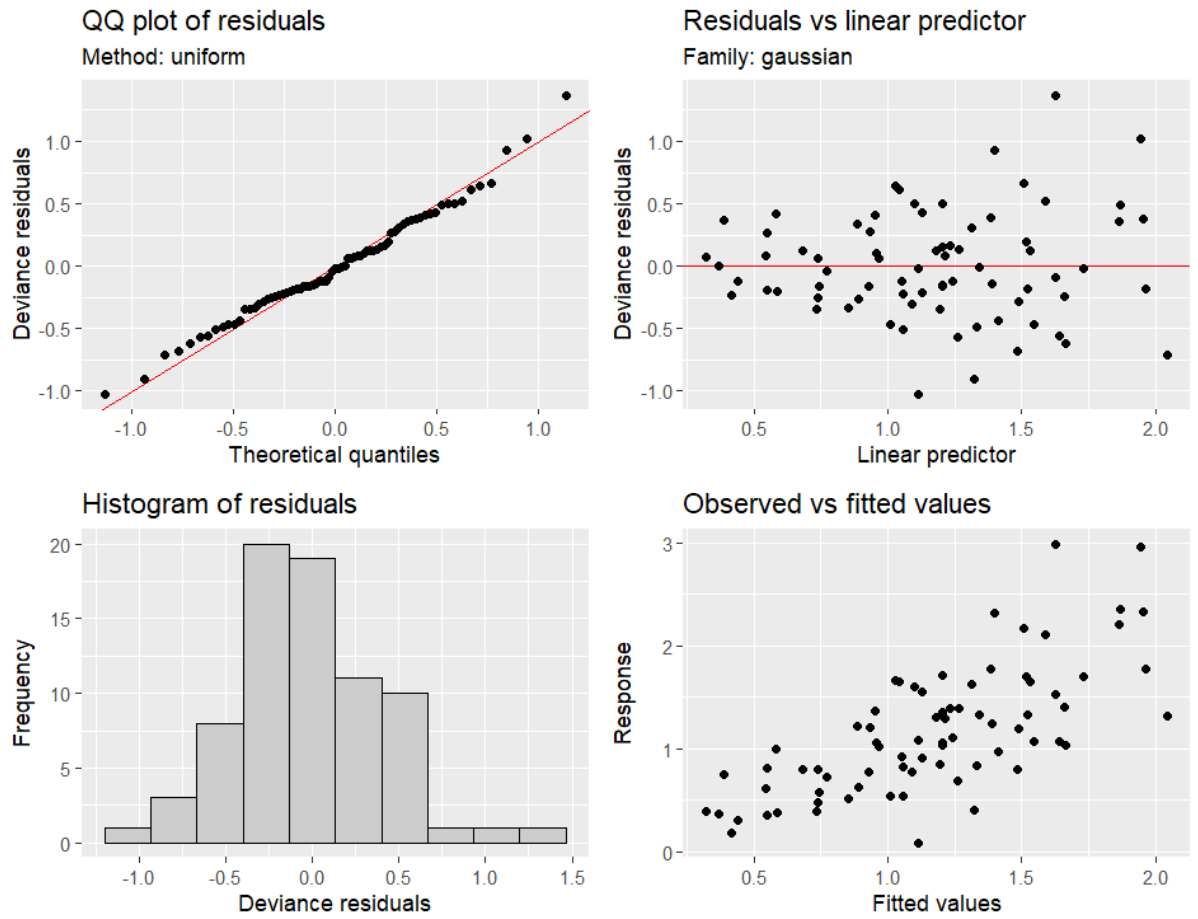

Figure A- 16 Diagnostic plots for the best fitted GAM model for Ctenophora bloom density estimations in the BPNS. The QQ-plot and the histogram of the residuals are used to verify normality. The plot of standardized residuals against fitted values assesses homogeneity.

Table A- 1 Results of 18S eDNA metabarcoding from all sampling locations. QF = Quality-filtered reads, BC = Base-called reads, A = Annotated reads.

Station	Sampling time	Base-called reads	Quality-filtered reads	QF/BC (%)	Annotated reads	A/QF (%)
120	17/08/2022	21 650	16 502	76.2	652	4.0
	28/09/2022	16 501	6669	40.4	181	2.7
	25/10/2022	24 132	7096	29.4	209	2.9
	14/12/2022	26 461	20 783	78.5	414	2.0
130	17/08/2022	33 168	24 103	72.7	404	1.7
	18/08/2022	24 888	16 309	65.5	160	1.0
	28/09/2022	24 207	16 772	69.3	309	1.8
	25/10/2022	25 672	10 876	42.4	373	3.4
	23/11/2022	28 547	8694	30.5	242	2.8
	19/01/2023	25 969	17 812	68.6	303	1.7
215	17/08/2022	24 698	10 783	43.7	326	3.0
	28/09/2022	17 245	7257	42.1	179	2.5
	25/10/2022	20 586	14 543	70.6	576	4.0
	14/12/2022	751	268	35.7	13	4.9
230	17/08/2022	25 243	18 843	74.6	168	0.9
	28/09/2022	23 786	14 813	62.3	407	2.7
	25/10/2022	17 934	11 914	66.4	241	2.0

	23/11/2022	24 926	7341	29.5	248	3.4
	2/12/2022	462	161	34.8	0	0.0
	19/01/2023	26 886	15 697	58.4	323	2.1
700	18/08/2022	22 562	15 274	67.7	250	1.6
	28/09/2022	21 693	9951	45.9	205	2.1
	25/10/2022	17 236	9397	54.5	268	2.9
	22/11/2022	21 557	13 562	62.9	457	3.4
	12/12/2022	3	2	66.7	0	0.0
	19/01/2023	21 754	13 131	60.4	330	2.5
710	18/08/2022	32 969	14 712	44.6	357	2.4
	28/09/2022	32 599	15 165	46.5	165	1.1
	25/10/2022	19 035	14 077	74.0	258	1.8
	22/11/2022	33 345	14 328	43.0	469	3.3
	12/12/2022	7	2	28.6	0	0.0
	19/01/2023	20 785	14 821	71.3	299	2.0
780	18/08/2022	23 990	10 387	43.3	359	3.5
	28/09/2022	19 857	4267	21.5	199	4.7
	25/10/2022	20 344	13 254	65.1	228	1.7
	22/11/2022	24 946	11 727	47.0	404	3.4
	12/12/2022	23 089	16 943	73.4	427	2.5
	19/01/2023	25 424	16 764	65.9	364	2.2
330	18/08/2022	23 205	14 742	63.5	388	2.6
	28/09/2022	23 256	10 243	44.0	221	2.2
	25/10/2022	32 447	12 195	37.6	352	2.9
	23/11/2022	21 028	9191	43.7	180	2.0
	12/12/2022	23 791	18 283	76.8	386	2.1
	19/01/2023	28 252	12 926	45.8	279	2.2
ZG02	17/08/2022	23 977	8204	34.2	247	3.0
	28/09/2022	16 462	7751	47.1	193	2.5
	25/10/2022	28 883	6657	23.0	224	3.4
	14/12/2022	25 602	19 511	76.2	369	1.9
ZG02b	14/12/2022	23 815	17 101	71.8	372	2.2
421	28/09/2022	24 161	5763	23.9	161	2.8
	25/10/2022	23 854	7889	33.1	265	3.4
435	28/09/2022	18 117	7058	39.0	144	2.0
	25/10/2022	21 926	16 121	73.5	540	3.3
W07bis	28/09/2022	22 079	4405	20.0	202	4.6
	25/10/2022	24 825	12 842	51.7	603	4.7
W08	28/09/2022	19 660	11 144	56.7	219	2.0
	25/10/2022	22 119	9647	43.6	351	3.6
W09	28/09/2022	16 134	8341	51.7	145	1.7
	25/10/2022	20 450	7257	35.5	140	1.9
W10	28/09/2022	17 766	9940	55.9	153	1.5
	25/10/2022	20 640	11 961	58.0	351	2.9
LW01	28/09/2022	24 270	4652	19.2	116	2.5
	25/10/2022	20 938	12 590	60.1	381	3.0

LW02	28/09/2022	19 643	6094	31.0	226	3.7
	25/10/2022	21 653	11 250	52.0	375	3.3
BA	17/08/2022	15 132	9888	65.3	291	2.9
	28/09/2022	26 961	8346	31.0	197	2.4
SP	29/08/2022	24 168	16 816	69.6	806	4.8
	5/09/2022	20 260	13 388	66.1	504	3.8
	29/11/2022	25 434	9393	36.9	559	6.0
	19/01/2023	24 675	18 820	76.3	490	2.6
Quay	17/08/2022	21 332	10 052	47.1	296	2.9
	18/08/2022	29 203	11 151	38.2	340	3.0
	5/09/2022	15 831	11 343	71.7	877	7.7
	2/12/2022	1138	627	55.1	14	2.2

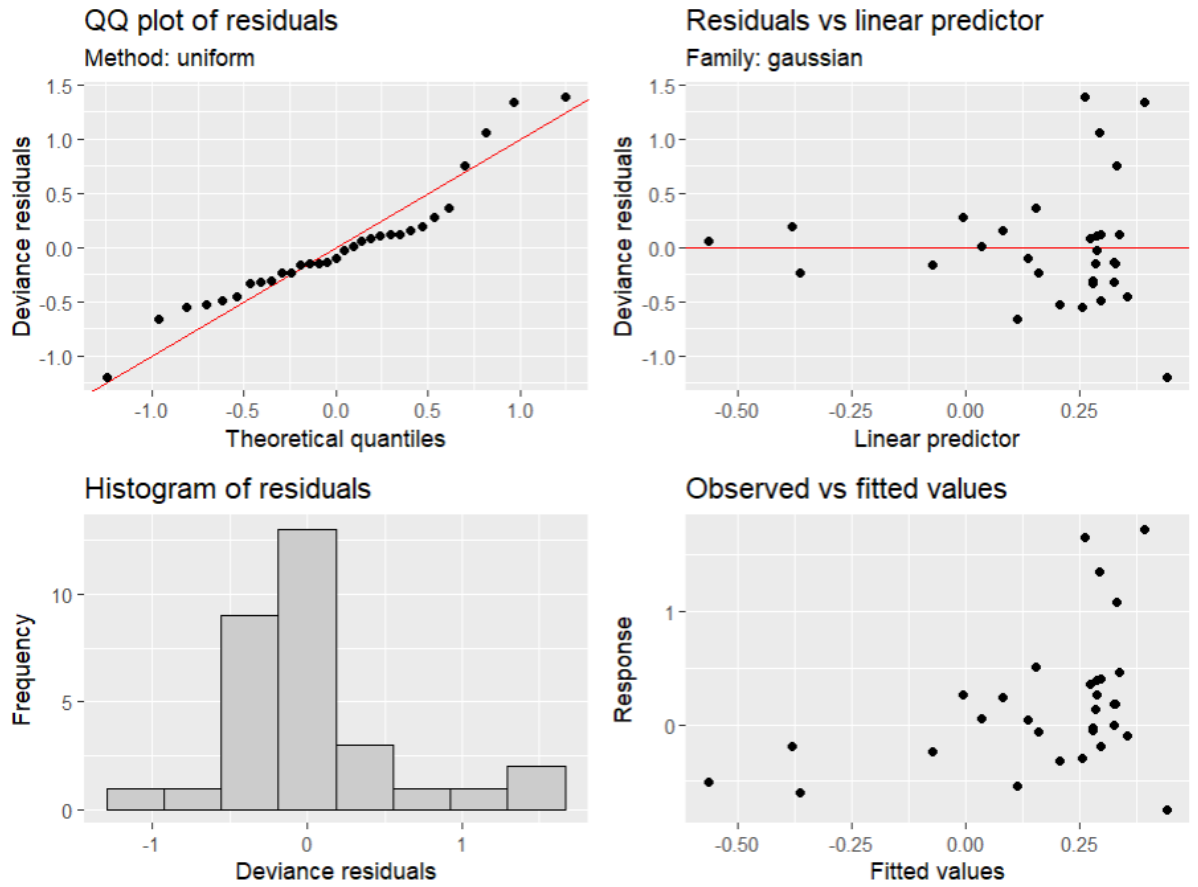

Figure A- 17 Diagnostic plots for the best fitted GAM model for Mnemiopsis leidyi reads in the BPNS. The QQ-plot and the histogram of the residuals are used to verify normality. The plot of standardized residuals against fitted values assesses homogeneity.

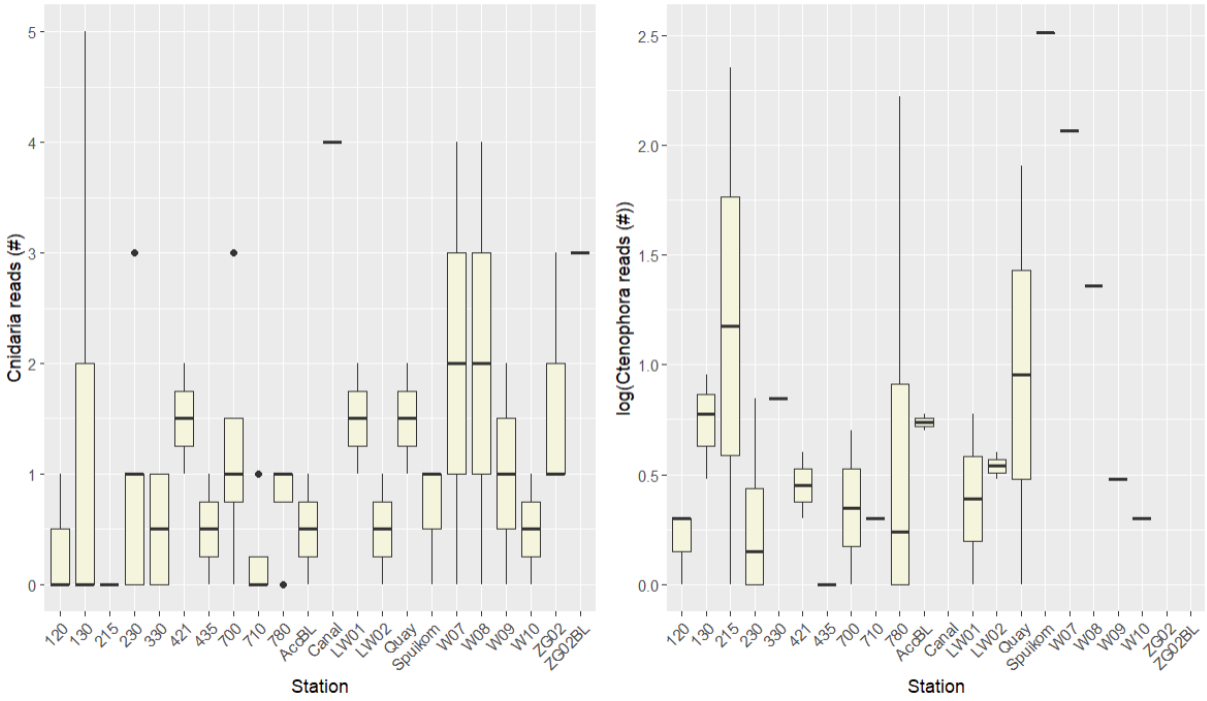

Figure A- 18 Boxplots showing spatial variation in number of retrieved eDNA metabarcoding reads independently of time. Reads of Ctenophora are log-transformed to cope better with outliers.

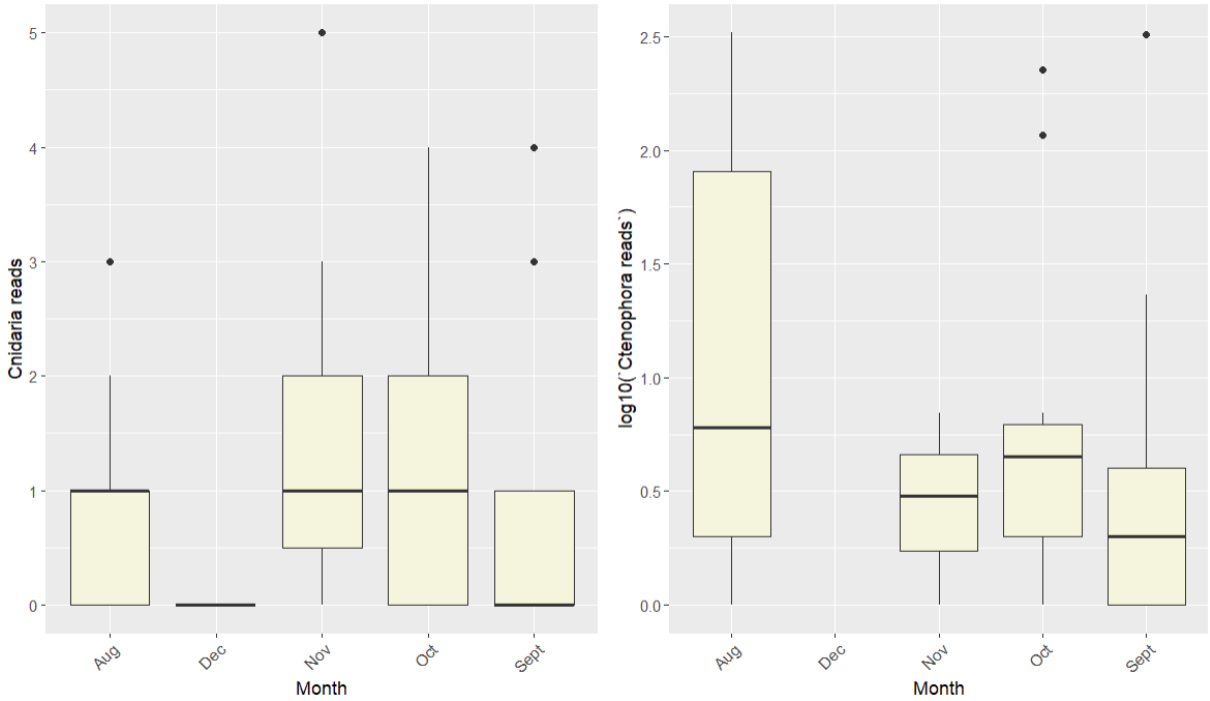

Figure A- 19 Boxplots showing temporal variation in number of retrieved eDNA metabarcoding reads. Reads of Ctenophora are log-transformed to cope better with outliers.